DURBAN UNIVERSITY OF TECHNOLOGY
INYUVESI YASETHEKWINI YEZOBUCHWEPHESHE

Investigation and Mitigation of Temporary Overvoltage caused by Harmonic Filters for Variable Speed Drives

By

Prenushka Ayar

Student Number: 21101718

A dissertation submitted in fulfilment of the requirements for the Master of Engineering Degree in the Department of Electrical Power Engineering, Faculty of Engineering and the Built Environment

Durban University of Technology

Supervisor: **Dr Evans Eshiemogie Ojo**

Co-supervisor: **Dr Ajibola O. Akinrinde**

October, 2021

Declaration

I hereby declare that this dissertation is my work, and each text has been correctly referenced or cited. Moreover, this work has not been previously published in portion or whole for another degree at any other University.

This research was duly supervised by Dr. Evans E. Ojo and Dr. Ajibola O. Akinrinde at the Durban University of Technology.

Submitted by:

28/10/2021

……. ……..……..

Prenushka Ayar Date

Student Number: 21101718

Approved for Final Submission by:

29/10/2021

……. …….

Supervisor: Dr Evans E. Ojo Date

30/10/2021

……. …….

Co-Supervisor: Dr Ajibola O. Akinrinde Date

ACKNOWLEDGEMENTS

My sincere gratitude and appreciation go to my supervisor and co-supervisor, Dr. Evans E. Ojo and Dr. A. Akinrinde for their invaluable support and guidance throughout this study. Without their guidance, help, knowledge, and encouragement, I would not have made headway in this project.

I am extremely grateful to Mr. Caleb Jordache Pillay for his support and assistance throughout this research. Without his constant support and motivation, it would not have been possible to complete this dissertation.

Lastly, I am immensely grateful to my parents for the love, prayers, and sacrifices they have made for my education over the years.

Abstract

The introduction of variable speed drives (VSD's) has become very popular in industrial operations, as it allows for smoother and more efficient operations of different processes. The installation of a VSD in an electrical system reduces the operational costs and if well implemented, it prolongs the life span of electrical equipment in the power system. Despite the fact that the use of VSD's offers these benefits, the main disadvantage is that its operations produce harmonics. However, the implementation of harmonic filters to eliminate these harmonics can cause temporary overvoltage during the filter switching which can negatively affect the systems operations. Temporary overvoltage and its mitigation are a matter of concern; thus, this study is aimed at investigating and mitigating the temporary overvoltage caused by the harmonic filters used to control the operations of variable speed drives.

The investigations conducted comprised of analytical modelling, computer simulations, and case studies. For all these aspects of the study, four harmonic filters were modelled, simulated, analysed, and were also implemented for the case studies. Firstly, was the analytical investigation where a network of VSDs of with and without filters was designed, modelled, and simulated to ascertain the harmonics produced. Secondly, was the computer simulation of the network in the ATP software. Thirdly, were the case studies, in which the harmonic analyser was installed for three different industries to measure the harmonic distortion and the power quality of the system. From the results, it is found that the 3^{rd} and 5^{th} harmonic orders were the highest in all three studies conducted. Harmonic filters may be used to reduce harmonic distortion to levels detailed in IEEE 519-1992 standards. The single-tuned, double-tuned, C-Type, and high pass filters were proposed for the purpose of mitigation. According to the results from the simulation, the double-tuned, and single-tuned filters were the most successful in mitigating the 3^{rd} and 5^{th} harmonics. Overvoltage's for both energization and de-energization of the harmonic filters were found to be greater than the power frequency withstand limit.

To avoid the undesirable effects that overvoltage has on the system, pre-insertion resistors, surge arresters, and controlled switching was considered for the mitigation of the overvoltages produced during the switching of the harmonic filters. Based on the simulation results, the surge arrester greatly mitigated the overvoltage caused by the energization, followed by the use of a pre-insertion resistor. Controlled switching was the least effective mitigation method in all three case studies and is therefore not the best choice to limit the temporary overvoltage.

Table of Contents

List of Figures

List of Tables

Nomenclature

A	Amps
C	Capacitor
C_f	Filter capacitance
ΔC	Change in capacitance
f_r	Resonant frequency
Δf	Change in frequency
μf	Micro farad
H_z	Hertz
mH	Millihenry
kV	Kilovolt
kW	Kilowatt
KVa	Kilovolt-ampere
$KVAr$	Kilo volt-ampere reactive
L	Inductor
L_f	Filter inductance
ΔL	Change in inductance
MVA	Mega volt amp
n	Drive efficiency
P_0	Power rating of the drive
Q	Quality factor
Q_f	Reactive power
R	Resistor
R_f	Filter resistance
$r.m.s$	Root mean square
rpm	Revolutions per minute
δ	Tuning factor
th	Holding time
V	Volts
V_p	Primary voltage
V_s	Secondary voltage
v_{rms}	Root mean square voltage
ω	Natural frequency
ω_h	Tuned harmonic h
W_p	Parallel resonant frequency
W_s	Series resonant frequency
X_c	Capacitive reactance
X_{eq}	Equivalent impedance
X_l	Inductive reactance
Ω	Ohm

Acronyms

AC	Alternating Current
ATP	Alternative Transient Program
CB	Circuit Breaker
CT	Current Transformer
DC	Direct Current
EMTP	Electromagnetic Transients Program
HVDC	High Voltage Direct Current
IEEE	Institute for Electrical and Electronic Engineers
IGBT	Insulated Gate Bipolar Transistor
LED	Light Emitting Diode
MOSA	Metal Oxide Surge Arrester
PC	Personal Computer
PCC	Point of Common Coupling
PWM	Pulse Width Modulation
THD	Total Harmonic Distortion
THDI	Total Harmonic Current Distortion
THDV	Total Harmonic Voltage Distortion
TOU	Time of Use
TRF	Transformer
VAR	Volt Ampere Reactive
VSD	Variable Speed Drive

Chapter 1
Introduction

1.1 Background

Variable frequency drives also known as variable speed drives offer the benefit of energy efficiency for motor-driven systems. Although there are many benefits of using VSD's, the main drawback is the harmonics created by the switching components found in these drives. The passive filters, which consist of multiple shunt branches, are tuned to certain frequencies to filter certain harmonics. The filter acts as a low impedance path at the harmonic frequency, which enables the filter to shunt most of these harmonics at their frequencies [1].

Harmonic filter design procedures and the mitigation process for harmonics have been documented in several publications and standards have been developed. Hence, due to the adverse effects of harmonics, the institute of electrical and electronic engineers (IEEE) has developed standards for harmonic distortion that a customer's load can inject back into the utility line [2]. The selection of tuning frequencies, damping factors, quality factors and interactions between harmonic filters and system impedance needs to be considered as documented in [3]. There are various types of filters that can be used to mitigate the harmonics in a system. Several combinations of filters have been used to carry out the filtering process and this process is dependent on the harmonics present as well as the industrial application.

There are many filters, single-tuned filters, which are mostly used in industries to reduce harmonics caused by variable speed drives. The single-tuned filter consists of a resistor, capacitor, and inductor. It provides a high-quality factor for maximum dissipation with negligible losses due to the absence of a damping resistor. High pass filters are used to suppress a wider range of frequencies compared to single-tuned filters, thereby reducing the size of the components, and avoiding capacitive power factor when the system is not loaded. Band pass filters are used to model high order filters or double-tuned filters. The filter is equivalent to two single-tuned filters connected in parallel. The quality factor is high and provides maximum attenuation for two harmonics. C-Type filters are a second-order filter, which is designed to have an impedance characteristic similar to the single-tuned filter with the advantage of having lower power losses [4].

The temporary overvoltage caused by the energizing and de-energizing of these filters has been investigated in various researches [5 19]. This temporary overvoltage can last for a significantly long period and has a frequency that is close to the system frequency. These overvoltages can

be damped or un-damped. During energization of the filter in the harmonic conditions, the peak currents in the filter are a few times higher than the steady state levels. It has also been established from field tests and computer simulations that the greater the harmonic content during de-energization, the higher the trapped residual filter voltage [6, 7].

Although the overvoltage only occurs for a short duration, it can cause heating and mechanical stress on the power equipment. Due to the adverse effects of overvoltage on power equipment, measures must be taken to prevent the failure of reactor insulation during switching activities. Some of the measures undertaken are the use of the pre-insertion resistors, the surge arrestors, and the control switching. Pre-insertion resistors act as a bypass across circuit breakers to close before energization of the filter [8]. This resistor provides damping to reduce the overvoltage and the possibility of circuit breaker re-strike. Surge arrestors are placed at specific locations in the circuit to limit surge energy. Controlled switching is another effective means of mitigating overvoltages. The magnitude of energization transient current is reduced which results in a longer life expectancy of the circuit breaker [9].

1.2 Motivation of Study

Harmonic filters are often used in industry to eliminate harmonics and correct power factor. However, the temporary overvoltage caused by the energizing and de-energizing of harmonic filters can cause a decrease in the lifespan of electronic components due to overheating. This increases the consumption of power and increases the amount of current harmonics in the system. To avoid the undesirable effects caused by temporary overvoltage on power systems, there is the need to develop mitigation techniques.

The various methods of mitigating overvoltage were highlighted in the previous section, a combination of either of these mitigation methods can yield positive results. To determine the possible positive outcomes of combining these mitigation methods, computer simulations were carried out. Based on the computer simulations results, a comparison was done to determine which of the combination will provide the best outcome. Thus, the use of pre-insertion resistors, surge arresters, and controlled switching was investigated through modelling and simulation to determine the best method of mitigating overvoltage and its harmful effects. These results were also validated in various case studies.

1.3 Context of this Study

Many industries use VSD's for a range of different applications due to their cost and energy-saving capabilities. VSD's can alter the speed of a motor by regulating the output voltage in proportion to the output frequency. The high-frequency switching operations of the drive produce harmonics that negatively affect the electrical system. Passive harmonic filters are commonly used to reduce harmonic distortion and its harmful effects. Three different case studies were considered in this research using experimental methods and simulation to determine the most effective harmonic filter, which would best limit the harmonics produced. Temporary overvoltage produced by the switching of the harmonic filters causes significant damage to the electrical equipment in the power system. An increase in power consumption, unnecessary tripping of circuit breakers, and stress on the electrical insulation are just some of the common symptoms of temporary overvoltage. Therefore, it is imperative to know the overvoltage caused by the energization and de-energization of the filter as well as possible solutions by which to mitigate the risk and consequences of these temporary overvoltages. Using ATP software, the mitigating effect of the pre-insertion resistor, surge arrester, and controlled switching were simulated, and the best solution was chosen.

1.4 Aims and Objectives

This research aims to investigate and mitigate the temporary overvoltage caused by harmonic filters installed to correct the harmonics produced by VSD's. This may be broken down as follows:

- To determine the level and order of harmonics produced by VSD's, using experimental methods and by simulation.
- To determine the type of harmonic filters which would best correct the harmonics.
- To investigate the temporary overvoltage caused by the switching operation of the harmonic filters.
- To determine the methods of mitigating the temporary overvoltage

To achieve these aims, the following objectives have been accomplished:

- The level and order of harmonics produced by VSD's, using experimental methods and by simulation have been determined.
- Harmonic filters which best correct these harmonics were identified.

- The temporary overvoltage caused by the switching operation of the harmonic filters was investigated.
- Measures that can be implemented to mitigate these overvoltages were established.

1.5 Significance of the Study

The rapid use of variable speed drives in various industries poses the problem of harmonic distortion. Harmonic filters can greatly reduce harmonic distortion, but their switching activities may cause temporary overvoltage to occur. The contribution of the study is as follows:

1. This study investigates the performance of different harmonic filters and their ability to reduce harmonic distortion. The implementation of harmonic filters would minimize disruptions during the production process and offer energy efficiency that can reduce operating costs.
2. This study was also used to identify the temporary overvoltage levels which could be caused by the switching of the harmonic filters and possible mitigating measures. The implementation of the mitigation measures would prevent electrical failures as well as comply with the SANS 10142.1 standard that stipulates the maximum overvoltage permitted for an electrical system.
3. Based on the successful completion of this project, implementation of the mitigation measures would also reduce the maintenance costs and prevent downtime which could be caused by temporary overvoltage

1.6 Thesis Outline

This dissertation consists of six chapters, brief description of the contents as contained in each chapter are discussed as follows:

Chapter one presents the introduction of the thesis. This includes the motivation, aims, and objectives, research questions, and significance of the study.

Chapter two presents the literature survey. It explains how the harmonics are produced by the operation of VSD's and the different types of harmonic filters that are available to filter these harmonics. It also elaborates on the temporary overvoltage caused by the switching activities of the filters as well as ways to mitigate the temporary overvoltage. Case studies based on similar research were compiled to review previous works done by other authors.

Chapter three presents the modelling and computer simulation using ATP software. This chapter presents the analytical analysis of the proposed model and the concept of the computer model formulation as well as its implementation and simulation.

Chapter four presents the simulation of different combinations of harmonic filters using ATP software and the analysis and discussion of the excerpted results.

Chapter five presents three different case studies. The case studies investigate the harmonics present in three different manufacturing industries. Using experimental methods and by simulation, the magnitude and order of harmonics produced by the operation of the VSD's were investigated. To reduce the harmonic distortion, harmonic filters were simulated, and the best filter was chosen. The temporary overvoltage caused by the energization and de-energization of the filter was found to cause adverse effects on the electrical system. Therefore, this chapter also focuses on the simulation of the pre-insertion resistor, surge arrester, and controlled switching to determine the best mitigation technique. The chapter concludes with the summary of results, which compares the findings obtained from the three case studies. The results present the best combination of harmonic filter and mitigation technique to reduce harmonic distortion and temporary overvoltage, respectively.

Chapter six presents the conclusion and recommendations of similar work for future research.

Chapter 2

Literature Survey

2.1 Background

The dramatic increase in the use of variable speed drives over the years has reduced the dependence on expensive mechanical systems. In developed countries, approximately two-thirds of power in the industry is consumed by VSD's [10]. The wide popularity of VSD's results from their robust nature as well as good control of frequency to regulate speed, high efficiency, and basic configuration [11]. The installation of VSD's can increase the energy efficiency and savings in energy consumption by approximately 50 % or more as compared to the direct online starter installation [12].

The VSD as a device can be divided into three basic sections, the rectifier, DC bus, and the inverter as shown in Figure 2.1. The rectifier in a VSD is used to convert the supply power from AC to DC, which feeds the motors. A VSD may have multiple rectifier sections and these sections could be the source of harmonic current. The harmonic current produced is determined by the pulse number of the drive [13]. After the power flows through the rectifier, it is stored on a DC bus, which may be subject to harmonics due to switching, which can cause damage to the system [14]. The final part of the drive is the inverter that generates a pulse width modulated waveform, which is generally used to run the three-phase induction motor mostly employed for industrial applications. The inverter is mostly the Insulated Gate Bipolar Transistors (IGBT) that can switch on and off multiple times to control the delivered power to the motor. The IGBT uses pulse width modulation (PWM) to generate a sine wave at the required frequency. VSD's can be used to control AC induction motors that may drive fans, pumps, and other industrial applications.

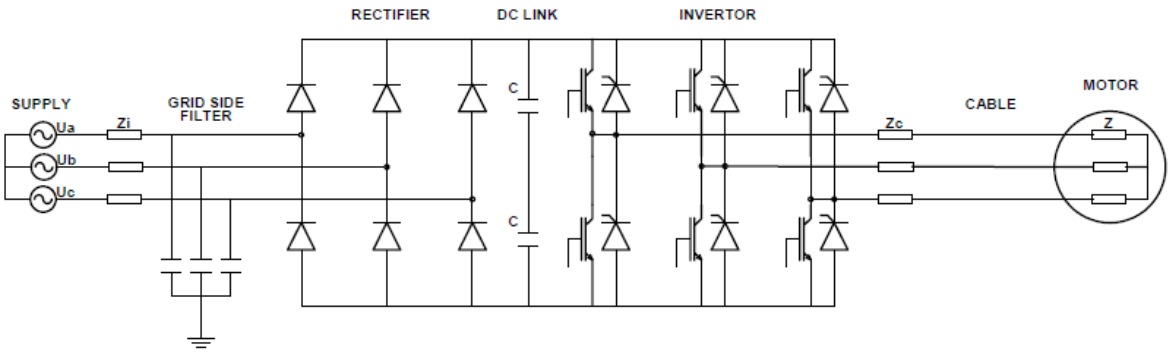

Figure 2.1: Schematic diagram of VSD

Although there are many benefits in using drives, the main drawback is the harmonics that are produced. Harmonics are the voltage or current frequencies that are a multiple of the fundamental frequency of the system, produced by the action of non-linear loads [15]. The operation of a drive produces harmonics that distort the fundamental voltage and current waveforms. This can cause voltage drops, a decrease in motor and transformer efficiency, and distortion to components in the electrical system. These can cause an increase in temperature and reduce the life expectancy of the motors. Another major concern is resonance, which is predominant when capacitor banks are installed for power factor correction. Resonance occurs when the harmonics generated by the VSD are the same frequency as that of the resonant frequency. This may lead to overheating, nuisance in tripping of circuit breakers, and equipment malfunction amongst others [16].

It is observed from previous studies that the PWM drives, produce harmonics mainly of the fifth and third-order. Field measurements show that voltage and current harmonics are time-variant due to the continuous changes in system load conditions. Furthermore, there is a greater number of harmonics produced when the motor is run at full load as when compared to start-up or partial loading. Even harmonics rarely occur because of the half-wave symmetric characteristic. Triplen harmonics, which are the odd multiples of the third harmonic, can be neglected when looking at the harmonic spectrum for VSD's. From studies, the third, fifth, and seventh harmonics are the most predominant when analysing the harmonic spectrum of motor drives [17, 18]. Because of the adverse effects that harmonics cause in the power system, harmonic analysis needs to be conducted and this can include the modelling of VSD's and the associated devices [19]. It also involves the analysis of the harmonic currents from the supply into the electrical network and determines the total harmonic distortion in the system.

2.2 Harmonic Filters

Harmonic filtering is one of the most common solutions to prevent harmonics from entering the system. The harmonic filter can compensate harmonics by generating the same harmonic component in the opposite phase. This application is used for several coupled motors working simultaneously for high-efficiency applications. The basic guideline for passive filter selection is determining the harmonics profile of the drive without passive filters. The fundamental reactive power is estimated and based on this value the size of the capacitor is calculated. The operation of the filter depends on factors such as its source impedance and quality factor. By using the values of the inductor, capacitor, and quality factor, the resistor value can be found.

The effectiveness of installing a harmonic filter is dependent on the decrease in harmonics it provides and must take into consideration the network system involved [20]. The switching operation of the harmonic filter causes temporary overvoltages to occur that negatively effects the electrical system and its operation.

Temporary overvoltages are lightly damped or slightly damped spike voltages that can occur for a short or a relatively long duration [21]. It usually occurs from a switching operation or fault clearing. Even though the overvoltage experienced may last for only a few seconds it may cause heating and stress on the electrical equipment. Overvoltages during switching are amplified by factors such as the size of the capacitor bank that is being switched, the type of load at the consumer's end, and the short circuit characteristics of the system [22]. Based on the harmonic analysis, a suitable filter can be chosen to attenuate the harmful harmonics together with appropriate mitigation techniques to minimize overvoltage occurring during switching.

2.3 Types of Harmonic Filters

The main function of a harmonic filter is to reduce harmonic distortion flowing in the power system. Three-phase filters are commonly used in industries as it is both cost-effective and easy to install. Four main types of harmonic filters are used to decrease harmonic distortion and improve the power factor of a power system. These are single-tuned, double-tuned, C-Type, and high pass filters.

2.3.1 Single-tuned Harmonic Filter

Single-tuned filters, as shown in Figure 2.2, are commonly used in many industries and serve as the foundation for more advanced filter configurations. It is composed of an inductor (L), a capacitor (C), and a resistor (R) connected in series. This configuration offers low impedance at the tuning frequency thus deflecting all currents of a certain frequency. The filter is used to attenuate lower order harmonics (3^{rd}, 5^{th}, and 7^{th}) at the resonance condition. The disadvantage of using the single-tuned filter is that it creates sharp parallel resonance. Therefore, the resonant frequency must be safely moved away from the concerned harmonic [23]. The factors that are important when considering the design of single-tuned filters are the harmonic order that needs to be filtered, the capacitive reactive power, and the quality factor. The equations (2.1) to (2.3), describe the values used to define the input parameters with regards to the single-tuned filter.

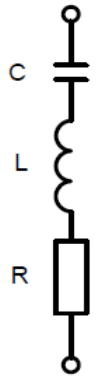

Figure 2.2: Single-tuned harmonic filter

$$C_1 = \frac{n^2 - 1}{n^2} \times \frac{Q_f}{\omega V^2} \tag{2.1}$$

$$L_f = \frac{1}{n^2 \omega^2 C_f} \tag{2.2}$$

$$R_f = \frac{2\pi f L_f}{Q} \tag{2.3}$$

Where Q_f is the reactive power of the filter, V is the nominal voltage, ω is the system frequency, Q is the quality factor, C_f is the filter capacitance, L_f is the filter inductance, R_f is the filter resistance and n is the harmonic order. The single-tuned filter is normally connected to a circuit breaker, which is used to switch the filter in and out. The passive filter is made up of a series RLC circuit connected in parallel to the converter [24]. The filter is connected in shunt with the system to provide a low impedance path for harmonic current tuned at a single frequency. The quality factor (Q) in equation (2.4) defines the bandwidth of the filter and is expressed as the ratio between the reactance (X) and the resistance (R) of the filter.

$$Q = \frac{X}{R} \tag{2.4}$$

The tuning factor (δ) is another important factor to consider. It is the detuning of the filter from the nominal tuned frequency. The tuning factor is expressed in equation (2.5) below. The tuning of the harmonic filter is important to reduce harmonic distortion and meet the required harmonic levels.

$$\delta = \frac{\Delta f}{f} + \frac{1}{2}\left(\frac{\Delta L}{L} + \frac{\Delta C}{C}\right) \tag{2.5}$$

Where Δf is the change in frequency, ΔL is the change in inductance and ΔC is the change in capacitance.

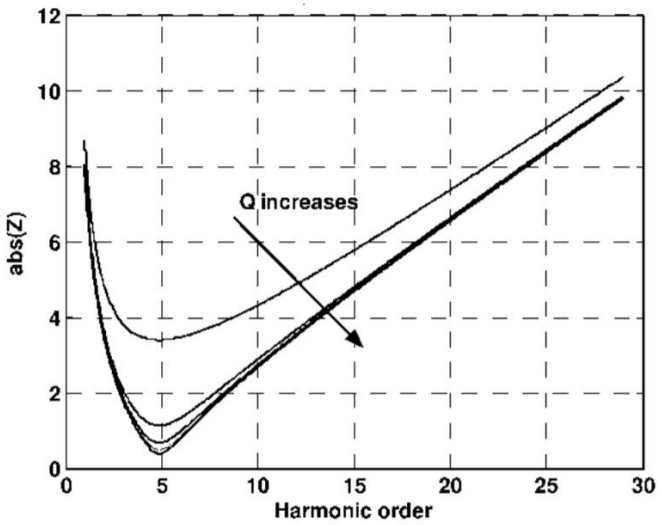

Figure 2.3: Single-tuned filter impedance curve [19]

Figure 2.3, the notch shows that this filter can eliminate a specific harmonic. The disadvantage of this design is that the single-tuned filters notch design is sensitive to parameter variations of inductance and capacitance and any shift can lead to amplification of the target harmonic [19].

2.3.2 Double-tuned Filters

The double-tuned filter is equivalent to two single-tuned filters connected in parallel. It is classified into two groups, the conventional double-tuned filter, and the damped double-tuned filter. Adding a resistor to a conventional double-tuned filter reduces the harmonic distortion experienced during resonance, this is known as a damped double-tuned filter. The filter is comprised of a series resonant circuit and a parallel resonant circuit connected in series [25]. Double-tuned filters can suppress the harmonics at two different frequencies simultaneously [26]. The series circuit gives series resonant frequency and the parallel circuit gives parallel resonant frequency. The two resonant frequencies can filter two lower-order current harmonics from the power system. The advantage of this filter over the single-tuned filter is that only one reactor is subjected to the full line voltage and it occupies a smaller space with only one circuit breaker being required for each phase. The configuration of the conventional double-tuned filter is shown in Figure 2.4, which is the combination of a series resonant circuit (L_1, C_1) and a parallel resonant circuit (L_2, C_2).

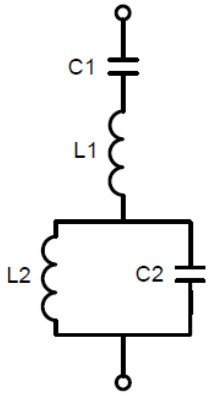

Figure 2.4: Double-tuned harmonic filter

The parameters of the double-tuned filter can be determined by considering two single-tuned filters connected in parallel. Two parallel single-tuned filters can be used to represent a double-tuned filter, therefore they have equal impedances. The resonant frequencies of the two single-tuned passive filters are given by equations (2.6) and (2.7).

$$W_a = \frac{1}{\sqrt{L_a C_a}} \tag{2.6}$$

$$W_b = \frac{1}{\sqrt{L_b C_b}} \tag{2.7}$$

Where W_a, W_b are the resonant frequencies of two single-tuned passive filters, L_a, C_a is the inductance and capacitance of the first equivalent single-tuned filter, and L_b, C_b is the inductance and capacitance of the second equivalent double-tuned filter

Comparing the coefficient of W, we find the equation of C_1 to be the sum of the capacitance of two equivalent single-tuned filters connected in parallel as shown in equation (2.8).

$$C_1 = C_a + C_b \tag{2.8}$$

The parameter L_1 is given by equation (2.9) below.

$$L_1 = \frac{1}{C_a W_a^2 + C_b W_b^2} \tag{2.9}$$

W_a and W_b are calculated in equations (2.6) and (2.7) respectively. L_1 is inversely proportional to the sum of the capacitance of the two equivalent single-tuned filters multiplied by the square of their respective resonant frequencies. Where L_1 is equal to the first inductance of the filter.

Using L_1 and C_1, we can calculate series resonance frequency W_s and parallel resonance frequency W_p of the double-tuned filter. Their frequencies can be determined by equations (2.10) and (2.11) respectively.

$$W_s = \frac{1}{\sqrt{L_1 C_1}} \tag{2.10}$$

$$W_p = \frac{W_a W_b}{W_s} \tag{2.11}$$

The value of L_2 can be obtained by equation (2.12) below.

$$L_2 = \frac{\left(1 - \frac{W_a^2}{W_s^2}\right)\left(1 - \frac{W_a^2}{W_p^2}\right)}{C_1 W_a^2} \tag{2.12}$$

The series resonant frequency (W_s) and parallel resonant frequency (W_p) of the double-tuned filter as well as the equivalent resonant frequencies of two single-tuned filters are considered.

The value of C_2 can be obtained from equations (2.13).

$$C_2 = \frac{1}{L_2 W_p^2} \tag{2.13}$$

Where C_2 is the value of the second capacitor in the double-tuned filter, whilst L_2 is the value of the second inductor of the double-tuned filter.

Hence all the parameters needed for the double-tuned filter can be obtained from the parameters of two parallel-connected single-tuned filters. The filter is widely used in HVDC projects not only to suppress the appointed harmonic current but also to provide the reactive power needed in the electrical system.

2.3.3 High Pass Filters

The high pass filter is categorised into first, second, and third-order high pass filters. The first-order filter is rarely used because of its large power losses and resonance problems. The second-order filter is easy to use and provides good filtering with fewer losses. The filter is represented in Figure 2.5 and is made up of a parallel combination of an inductor and resistor connected in series to a capacitor. This filter is commonly used to suppress 5^{th} harmonic order currents or higher current due to its flat impedance characteristics for high frequencies.

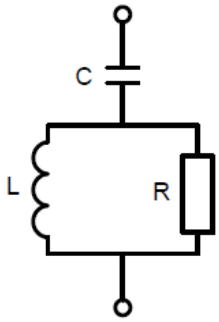

Figure 2.5: High pass harmonic filter

If power loss due to capacitor and reactor resistance is neglected, the equivalent impedance of filter at the fundamental frequency (ω) is given as (2.14).

$$X_{eq} = X_C - X_L = \frac{1}{\omega C} - \omega L \tag{2.14}$$

Where X_{eq} is the equivalent impedance, X_c is the capacitive reactance of the filter, X_L is the inductive reactance of the filter, C is the capacitance and L is the inductance.
The equivalent impedance becomes the ratio of the squared voltage (V) to the reactive power (Q) of the filter as shown in equation (2.15).

$$X_{eq} = \frac{V^2}{Q} \tag{2.15}$$

At the tuned frequency ωh (tuned harmonic h), the filter total reactance is given as (2.16).

$$X_h = \frac{1}{\omega h C} - \omega h L \tag{2.16}$$

Where X_h is the total reactance of the filter and ωh is the harmonic order at the tuned frequency. Filter total reactance should be zero at the tuned frequency as seen in equation (2.17).

$$X_h = \frac{1}{\omega h C} - \omega h L = 0 \tag{2.17}$$

Solving the above equation results in the equation (2.18) below.

$$X_C = h^2 X_L \tag{2.18}$$

The capacitive reactance of the filter (X_c) is equal to the harmonic order squared multiplied by the inductive reactance of the filter. From equation (2.18) into equation (2.14) results in equation (2.19).

$$X_C = \frac{h^2}{h^2 - 1} X_{eq} \tag{2.19}$$

Substituting equation (2.15) into equation (2.18) results in equation (2.20)

$$X_C = \frac{h^2}{h^2 - 1}\left(\frac{V^2}{Q}\right) \tag{2.20}$$

The capacitance (C) of the filter is equal to the inverse of the fundamental frequency (ω) multiplied by the capacitive reactance of the filter (X_C) as seen in equation (2.21).

$$C = \frac{1}{\omega X_C} \tag{2.21}$$

From equation (2.20), we can calculate parameter C of the filter as per equation (2.22)

$$C = \frac{h^2 - 1}{\omega h^2} - \left(\frac{Q}{V^2}\right) \tag{2.22}$$

The inductance (*L*) can be expressed as the capacitive reactance divided by the fundamental frequency multiplied by the square of the harmonic order, given by (2.23).

$$L = \frac{X_L}{\omega h^2} \tag{2.23}$$

From equation (2.19) into equation (2.23) results in an important equation for calculating parameter L of the filter and is given in equation (2.24).

$$L = \left(\frac{1}{h^2 - 1}\right)\left(\frac{V^2}{\omega Q}\right) \tag{2.24}$$

Where h is the harmonic order, V is the system voltage and *ω* is the system frequency.
The quality factor Q_f of the second-order high pass filter is defined as the ratio of resistance to the reactance of the parallel *RL* circuit at the tuned frequency. The quality factor defines the bandwidth that determines the sharpness of the tuning frequency and is shown in equation (2.25) below.

$$Q_f = \frac{R}{\omega h L} \tag{2.25}$$

Therefore, the value of the damping resistance (R) is calculated as:

$$R = Q_f \omega h L \tag{2.26}$$

The damping resistor seen in equation (2.26), reduces the quality factor of the filter thus increasing the bandwidth making it suitable for a range of harmonic frequencies to be filtered. The selectivity indicates that the harmonic frequency must be in the bandwidth with a smaller bandwidth providing a higher selectivity. The filter is designed to connect with a single-tuned filter to attenuate lower and higher-order harmonic frequencies. Because of its advantageous characteristics, the filter is used in industrial applications with high-powered VSD's. The third-order high pass is designed using the specifications of the first and second-order filters. It is formed by cascading in series the first and second-order filters. The third-order high pass filter gives improved performance compared to the second-order filter however due to the complex design and economic factors it is used in medium voltage applications only [27].

2.3.4 C-Type Filter

The C-Type filter is an efficient and economical passive harmonic filter that can be tuned for a range of harmonic frequencies. The filter works by providing a low impedance path to the ground for the harmonic currents tuned at harmonic frequency [28]. The C-Type filter is comprised of a high pass filter connected with a capacitor added in series with a reactor as shown in Figure 2.6. The significant feature of the filter is that the L and C components are resonant at the fundamental frequency, therefore the power loss experienced by the damping resistor R is lessened [29]. The filter can attenuate high-frequency harmonics due to its flat impedance characteristic above the tuned frequency [30].

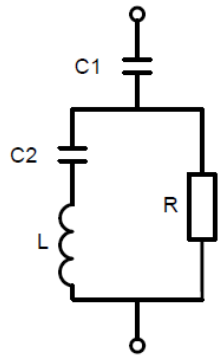

Figure 2.6: C-Type harmonic filter

Power loss due to capacitors and reactor resistance is neglected therefore equivalent impedance of filter at fundamental frequency *w* is given in equation (2.27).

$$Z_{eq} = -\frac{j}{\omega C_1} \tag{2.27}$$

Where Z_{eq} is the equivalent impedance, j is an imaginary number in mathematics and C_1 is the first capacitance of the filter. Also, the total capacitive reactance of C_1 is shown in equation (2.28).

$$X_{C_1} = -\frac{j}{\omega C_1} = -j\frac{V^2}{Q_1} \tag{2.28}$$

Where Q_1 is the reactive power capacity at the fundamental frequency. From equation (2.28) C_1 may be calculated using equation (2.29).

$$C_1 = \frac{Q_1}{\omega V^2} \tag{2.29}$$

Where C_1 is the first capacitance of the filter. The parameter for C_2 of the filter may be calculated using equation (2.30).

$$C_2 = \frac{\left(h^2 - 1\right)Q_1}{\omega V^2} \tag{2.30}$$

Where C_2 is the second capacitance of the filter. The parameter for L can be evaluated by equation (2.31).

$$L = \frac{V^2}{\left(h^2 - 1\right)\left(\omega Q_1\right)} \tag{2.31}$$

Where L is the inductance of the filter and V is the nominal voltage. The quality factor (Q_f) of the C-Type filter is defined as the ratio of resistance to the reactance of the parallel RL circuit at the tuned frequency. The quality factor determines the bandwidth and sharpness of the tuning frequency and it is obtained using equation (2.32).

$$Q_f = \frac{R}{\omega_h L} \tag{2.32}$$

The damping resistance (R) is calculated using equation (2.32). The resistor increases the damping of the system during energizing or de-energizing of the filter.

$$R = Q_f \omega_h L \tag{2.33}$$

The major disadvantage of this filter is that it is larger compared to the single branch filter therefore it is mainly used for a large 12-pulse drive with high order harmonics.

2.4 IEEE 519 Standards

2.4.1 Introduction

The distortion of a perfect sinewave is often referred to by the voltage and current harmonic distortion. The distortion is not a new occurrence and works to limit harmonics in the power system have always been a concern for engineers. Typically, the distortion is caused by non-linear loads such as VSD's, transformers, and rotating machines which are supplied from the utility power system. Using the IEEE 519-1992 standard, allows engineers to better understand the effects of this phenomenon and limit its presence in electrical networks.

2.4.2 Effects of Harmonics

Harmonics affect various types of equipment in the network and the effect of these harmonics are divided into four main categories. These are the effects on:

- The power system
- The consumer load
- Communication circuits
- Revenue billing

Harmonic currents in the electrical network cause equipment overheating which may affect rotating machineries such as motors and transformers. Harmonics can also cause false circuit breaker tripping, metering inaccuracies, and thyristor firing errors. In addition, harmonic currents can cause excessive noise on nearby communication lines. Harmonic distortion can affect a customer's billing by causing an error in the metering system, costing the customer more than he is using and liable for.

2.4.3 Harmonic Sources

Non-linear loads are the main contributors to harmonics in the electrical system. There are various types of electrical equipment which cause harmonics such as fluorescent lighting, arc furnaces, computers, and other items. The largest source comes from static converters in the form of VSD's. The VSD uses solid-state switching devices such as thyristors or diodes that convert power from one frequency to another. This switching operation produces current harmonics that are injected back into the supply network.

2.4.4 Voltage and Current Harmonic Limits

Electrical standards regarding harmonics have been stipulated in the IEEE 519 standard. This document contains recommendations, systems, and requirements for controlling harmonic current and voltage in electrical systems. The standards contain harmonic current limits which specify the maximum allowable harmonic current that the customer can inject into the utility system at the point of common coupling (PCC). These harmonic current limits vary based on the short circuit strength of the system it is being injected into. The current limits are based on the size of the customer relative to the size of the supply. The Short Circuit Ratio (SCR) is defined as the relative size of the load with respect to the supply.

The SCR is given by equation (2.34).

$$SCR = \frac{Shortcircuit(MVA)}{Load(MW)} = \frac{I_{sc}}{I_L} \tag{2.34}$$

Where I_L is the total current at fundamental frequency in the load and I_{sc} is the level of short circuit current at the PCC. Table 2.1 lists the recommended maximum current distortion levels as a function of SCR and harmonic order.

Table 2.1: Current harmonic distortion limits [31]

Maximum harmonic current distortion in percent of I_l						
Individual harmonic order (odd harmonics)						
I_{sc} / I_l	<11	$11 \le h <17$	$17 \le h <23$	$23 \le h <35$	$35 \le h$	TDD
<20	4.0	2.0	1.5	0.6	0.3	5.0
20<50	7.0	3.5	2.5	1.0	0.5	8.0
50<100	10.0	4.5	4.0	1.5	0.7	12.0
100<1000	12.0	5.5	5.0	2.0	1.0	15.0
>1000	15.0	7.0	6.0	2.5	1.4	20.0
Even harmonics are limited to 25 % of the odd harmonic limits above						
Current distortion that result in a DC offset, e.g. half-wave converters are not allowed						
*All power generation equipment is limited to these values of current distortion, regardless of actual I_{sc} / I_l						

IEEE 519 voltage distortion limits are the second set of recommendations for harmonics and establishing the acceptable amount of voltage distortion at the PCC. The allowable harmonic voltage prescribed is based on the lowest levels that allow for optimal operation of the customer's electrical equipment. The IEEE 519 limits for harmonic voltage distortion are shown in Table 2.2.

Table 2.2: Voltage harmonic distortion limits [31]

Bus voltage	Individual V_h (%)	THD (%)
V < 69Kv	3	5
69 ≤ kV < 161kV	1.5	2.5
V ≥ 161kV	1	1.5

According to Table 2.2, harmonic voltage distortion on a power system 69 kV and below is limited to 5 % total harmonic distortion (THD) with each harmonic limited to 3 %. Utilities often investigate or enforce current limits when voltage distortion limits have been exceeded. It is to the benefit of the customer to implement measures that limit harmonics in the system, this will improve operations and avoid equipment deterioration. One of these measures is using passive harmonic filters to reduce harmonic distortion to the levels detailed in IEEE 519.

2.5 Overvoltages in Power Systems

Overvoltage is defined as the increase in voltage in a power system that exceeds the maximum value of the operating voltage. When the supply voltage is larger than the rated voltage for a period longer than one minute it is considered as an overvoltage. There are two types of causes of overvoltage.

1. Overvoltage due to external causes
2. Overvoltage due to internal causes

Overvoltage due to external causes may occur because of lightning strikes which result in the breakdown of electrical equipment insulation. This type of overvoltage is considered a natural phenomenon, while internal overvoltage is also known as temporary or switching overvoltage is due to switching operations in the power system. There are three main classes of internal overvoltage that occur in an electrical system.

2.5.1 Types and Causes of Internal Overvoltage

2.5.1.1 Temporary Overvoltage

Temporary overvoltage occurs for a relatively long duration and is caused by faults, switching operations, or nonlinearities. Temporary overvoltage differs from other overvoltages by the duration, frequencies of oscillation, amplitude, or fall time [32].

2.5.1.2 Slow Front Overvoltage

Slow front or switching overvoltages are common in power systems due to the switching operations. When an unloaded electrical line is charged, the voltage at the receiving end will increase to a high amount that causes overvoltage to occur, this is due to the Ferranti Effect [33].

2.5.1.3 Very-Fast Overvoltage

Arc interruption or circuit breaker restrike, due to switching operations, causes very fast overvoltage to occur. The overvoltage can also be caused by a fault in a gas-insulated substation (GIS) or certain lighting conditions. Equipment located close to the interruption point is at a high risk of damage.

2.5.2 Temporary Overvoltage Caused by Switching Operations

Overvoltage produced by the switching operations in a power system during routine operations occurs often and may cause severe stress on the power system. The operation of switching devices such as circuit breakers can join or separate parts of a power system. Capacitor banks used for power factor correction or as part of harmonic filters, cause the circuit breaker to interrupt a mainly capacitive load when operating under normal load conditions. Closing a switch in a capacitive network will result in inrush current which can lead to damage to the protection system. It is important to quantify the amplitude, frequency, and shape of the voltage oscillations caused by the opening and closing operations. The amplitude, frequency, and shape of the current and voltage oscillations will be determined by the rest of the network configuration as seen from the circuit breaker terminals. Switching overvoltages do not cause flashovers like lightning, however switching surges gain importance as they occur more often and are sustained for longer periods.

2.5.3 Circuit Breaker Operation during Current Interruption: The Electric Arc

A circuit breaker is a mechanical switching device, capable of making, carrying, and breaking currents under normal conditions and specified abnormal circuit conditions [33]. During

normal operation, the circuit breaker contacts are closed and only open once a tripping signal is received. Circuit breakers are selected according to their current carrying capabilities, insulating capacity, switching performance, and mechanical functions. For the analysis of switching operations, the circuit breaker may be modelled as an ideal switch. The models presented by Cassie (1939) and Mayr (1943) proposed a clear understanding of circuit breaker modelling and arc-circuit interaction.

Current interruption is achieved by mechanically separating the metallic contacts of the circuit breaker so that the gap formed is filled by a liquid, a gas, or a vacuum. During the current interruption, an electric arc is formed when the contacts of a circuit breaker are opened. The arc is extinguished by drawing the arc out and increasing its resistance. This results in the current being reduced to such a value that the heat formed is not sufficient to maintain the arc and thus the arc is extinguished.

2.5.4 Overvoltage Standards

2.5.4.1 The SANS 10142.1 Standard

Electrical equipment in a power system will be suitable for operation on the maximum steady (r. m. s) voltage and overvoltage to which it is likely to be subjected [34]. Equipment shall be rated in accordance with the intended application for use on the following voltages used in South Africa:

Standard voltages

1. 230 V single-phase
2. 230/400 V three-phase four-wire, and the tolerance of +/- 10 % of the voltages.

2.5.4.2 The IEEE 1159 Standards

The IEEE approved the IEEE 1159 standard in 1995, which evaluates the power quality and recommended practice for monitoring an electrical system [35]. The IEEE standard states the limits or values within which any customer can expect the voltage characteristics to remain under normal operating conditions. Table 2.3 illustrates the requirements regarding power quality in voltage supply variations.

Table 2.3: IEEE 1159 standards [35]

	Duration for a week period	Duration for every 10 min period
Voltage variations	95 % of r.m.s. values (averaged in 10 min intervals) in the interval U_n +/- 10 %	Average r.m.s. values must be in the interval U_n +10 % -15 % (for LV networks)

In the area of voltage variations, both standards have a case where the voltage supply exceeds up to 10 % the level of the nominal voltage supply. This denotes the importance of investigating overvoltage in a power system when the voltage is higher than +10 % of the nominal voltage.

2.6 Harmonic Filter Switching

The switching in and out of harmonic filters may cause overvoltage problems. The switching operations of capacitors and reactors used in filter circuits may experience insulation failures during switching operations. IEEE standard 1313.1.1996 defines temporary overvoltage's as an oscillatory phase to ground or phase to phase over voltage that is at a given location of relatively long duration and that is un-damped or only weakly damped [36].

In many applications, the filter is switched daily which can cause over voltages that may exceed the power frequency withstand voltage at the bus. An increase in the harmonic content in the filter circuit leads to higher overvoltage magnitudes. If the overvoltage is large enough it may cause mechanical stress on the electrical equipment. Large amounts of harmonic content may also lead to higher over voltage levels and can affect the possibility of circuit breaker re-strike. Temporary over voltages are typically caused by harmonic resonant conditions, load rejections, and fault clearing. When the filter is switched off in the current zero position the capacitor remains charged at the voltage peak. If continuous switching occurs after a period of approximately 10ms, it can cause high switching over voltages. If repeated re-strikes occur, the switching over voltages can become so high that the system insulation becomes stressed which may lead to arcing at the circuit breaker.

2.6.1 Energization of Harmonic Filter

During energization, discharging of a capacitor leads to short circuits known as capacitor switching transients. This short circuit creates high inrush currents and voltage dips on the source [37]. During energization of the filter in harmonic conditions, the peak currents in the filters are a little higher than the steady-state current. The energizing of the filter generates steep fronted voltage waves on the filter's reactor, which may result in high over voltages. The surge of inrush current from the source causes a transient overvoltage on the bus [38]. When the circuit breaker closes inrush current will flow and this inrush current could be limited by surge impedance of the cable depending on the cable's length [39]. The magnitude and shape of the temporary overvoltage can also vary with system parameters but are dependent on the circuit breaker switching and the point on the wave where this switching occurs [40, 41]. Thus, circuit breakers play a major role in influencing the operating conditions of a power system.

When a circuit breaker closes, the three poles of the breaker may not close symmetrically, therefore, increasing the magnitude of the temporary overvoltage. The main contributing event in this phenomenon is the overvoltage produced by energizing the filter due to the charging and discharging of the filter capacitors [6]. The nominal voltage across a filter capacitor without harmonics being considered is greater than the bus voltage by a factor of k seen in equation (2.35).

$$k = \frac{f^2}{f_r^2 - 1} \tag{2.35}$$

Where f is the system frequency and f_r is the resonant frequency. Consequently, based on equation (2.35), the effect of filter switching will increase the amplitude of voltage on the filter capacitor to twice the nominal power [5]. The harmonic filter energization causes high voltage and current distortion in the filter circuit. According to SANS 10142.1, the allowable tolerance for a 400 V system is ± 10% [34]. If the voltage after energization is above the allowable tolerance specified by SANS 10142.1, appropriate measures of mitigation must be taken.
When a filter is switched off and then re-energized after a short while, the capacitors of the filter remain charged causing another severe case of overvoltage across the filter reactor [42]. Energization of the filter with a source voltage of the opposite polarity can cause a high voltage to drop across the reactor of the filter.

2.6.2 De-Energization of Harmonic Filter

The opening of the harmonic filter using a circuit breaker can cause high over voltages. When the breaker contacts are opened the fault current is not interrupted immediately, an arc forms between the breaker contacts and may be sustained provided there is enough current flowing [43]. The presence of harmonic content in the interrupting filter can increase the recovery voltage across the circuit breaker causing re-strikes between the breaker contacts. If the circuit breaker is de-energized after zero crossing, the voltage will be at its maximum since there is a 90° phase difference between voltage and current. Circuit breaker re-strikes may occur when there is a charge of the filter capacitor bank. Therefore, re-strikes can generate over voltages higher in magnitude than on closing [44]. The over voltage magnitude depends on the order of the switching filter and harmonic current phase shift. Due to the constant switching of the harmonic filter over voltages occur across the filter that may exceed the nominal voltage. This may prove dangerous to equipment such as circuit breakers and transformers.

2.7 Effects of Overvoltage on Power Systems

Electrical equipment cannot perform effectively during overvoltage. The higher the overvoltage experienced, the shorter the lifespan of the components will be [45]. Overvoltage leads to stress on the insulation of the electrical equipment and causes damage to them when it frequently occurs. Also, in the case of overvoltage, electrical equipment used for domestic or office use does not perform adequately and safely in the presence of this disturbance. Some of the more common symptoms of overvoltage stress include:

- Power consumption increases
- Low operation efficiency
- Malfunction and probably shut down
- Unnecessary tripping of circuit breakers in the circuitry
- Increase in power consumption

2.8 Mitigation Measures

Mitigation measures are to be considered if the overvoltage caused by the switching operations is greater than the allowable tolerances defined in SANS 10142.1. This overvoltage could cause damage to the filters and system equipment. For this reason, mitigation measures using surge arresters, controlled switching, and pre-insertion resistors are investigated below.

2.8.1 Controlled Switching

Controlled switching allows for precise switching of the circuit breaker upon opening or closing minimizing over voltage. The combination of circuit breakers and digital technology has allowed for intelligent controlled switching devices [46]. Controlled switching allows for the individual operation of each circuit breaker pole. The primary purpose of controlled switching is to reduce inrush current which can contribute to an extended lifetime of system components. The operation includes triggering the electrical contact of the circuit breaker at the desired voltage waveform. The optimal closing of the circuit breaker is at the zero point on the waveform, at this point, there is minimal stress on the system. The controller determines a reference time related to the phase angle of the supply voltage. Thereafter, a waiting time is created to give an output closing command to the breaker.

The closing or opening command of the circuit breaker is delayed to the optimal time related to the phase angle of the voltage or current. Each breaker pole is expected to close at zero crossing to minimise over voltage. The zero-crossing time of one of the phases is needed while the others can be calculated from the reference phase. Suppose phase A is closed at the optimal point, the remaining two phases B and C will be expected to close at 120 and 60 degrees respectively [6]. The operation is usually extended by 120ms compared to direct tripping of the circuit breaker [47]. Therefore, the circuit breaker will close at the correct time instant to reduce voltage and current transients. This method has been used to reduce temporary over voltages in offshore wind farms utilizing synchronised switching controllers.

The results show that the temporary over voltages caused by the switching operations decreases with the use of a controlled switching device [48]. This method has also been used to mitigate power system switching transients in sensitive loads such as automated industrial production lines i.e. microprocessors. The controlled switching device reduces voltage oscillations and temporary over voltages caused by capacitor bank switching [49]. The use of controlled switching to reduce overvoltage has had many economic benefits such as longer maintenance intervals and eliminating the need for closing resistors [50].

2.8.2 Surge Arresters

The over voltage on a filter and recovery voltage across the switching device may be reduced by the installation of surge arresters on the filter side of the switching device [51]. Surge arresters operate when their predetermined threshold value is over its limit. The surge is diverted to the ground, and the current is reduced to a negligible value. This is due to the composition of the metal oxide surge arrester (MOSA) that is comprised of zinc oxide that is pulverised into fine grains. A potential barrier at the boundary of each zinc oxide grain controls the flow of current from one grain to another [52].

There are various existing models for surge arresters however, the MOSA is used in this application and was modelled after the IEEE surge arrestor model. In the event of over-voltage, the surge arrester has high resistance and sufficient energy discharge to dissipate the over voltage without losing thermal stability. The location of the surge arrester is important in its ability to limit the surge. The ideal position is placing the arrester between the circuit breaker and the supply cable [53]. The MOSA operates from high impedance to low impedance as transient voltage exceeds the threshold value. The protection level must be set lower than the withstanding voltage of the equipment being protected [54]. MOSA has a high non-linear

voltage-current characteristic for switching studies, according to IEEEANSI C62.1993 standards [6].

The surge arrester can withstand increased operating voltage for a period making it ideal to use in situations where temporary over voltages occur. Some of the advantages of using MOSA are that it has a high energy absorption capability and the zinc oxide dividers possess high stability during and after discharge [54]. This method has been used to reduce switching over voltages in transmission lines. The surge arrester is installed in suitable locations along the transmission line to help reduce switching over voltages to an acceptable level [55].

2.8.3 Pre-Insertion Resistors

Pre-Insertion resistors are an effective means to mitigate transient over voltage caused by capacitors during energization. There are two pre-insertion resistor configurations, these are parallel and series pre-insertion resistors. The selection of the required configuration depends on the space requirements, the stress imposed, and the cost [56]. It is inserted between the circuit breaker contacts and acts as a by-pass, which closes before filter energization.

The resistor provides damping and reduces system transients. While opening the breaker the resistor is disconnected before, the contacts are opened. The resistor provides damping and reduces the over voltage. It operates such that the pre-insertion resistor is electrically connected at one end and the other end of the resistor carries a stationary electrode. The pre-insertion resistor is placed in the circuit for a few milliseconds before energization. The resistor provides damping thereby providing the mitigating effect.

Due to the use of a pre-insertion resistor, the overall losses in the circuit are increased which decreases the value of the peak voltage and current transients [57]. This method is used to reduce temporary over voltages produced by filter banks at onshore wind farm substations. The pre-insertion resistor is used across the circuit breaker to provide damping which reduces the surge energy [6].

2.9 Previous Case Studies

Fahmi, et al., [58], studied the harmonic distortion in the plastic processing industry. The use of electronic switching devices in the plastic industry causes an increase in non-linear loads [59]. It was found that the problem may be resolved by reducing harmonics with the installation of a harmonic filter. The system was first modelled by using MATLAB simulation. To perform the harmonic measurements, a portable measuring analyser was installed at the PCC. From the measured results it was found that the total harmonic current distortion (THDi) was

approximately 15.5 %. This is higher than the IEEE 519-1992 standard. A single-tuned passive filter was chosen to reduce the current harmonics from 15.55 % to 4.77 %. The filter was found to have the ability to attenuate the desired harmonic and only limit other harmonic orders.

Soomro and Almelian, [60] researched the excessive use of power electronic devices and their effects on power quality problems due to the generation of harmonics. The effects of harmonics include overheating of electrical cables and equipment, lower efficiency in electric machines, nuisance tripping of thermal protections amongst others. The use of passive filters is a common method to mitigate harmonics.

This paper describes the optimal design of a single-tuned passive filter by using Matlab simulation which shows the effectiveness of the filter. The authors first simulated the non-linear load with and without single-tuned filters. The harmonic value is seen to have decreased, improving the THD from 28.8 % to 4.87 % by using the single-tuned harmonic filter. The filter is a simple yet effective method in reducing harmonics as well as improving the power factor and efficiency of the system.

Cheepati, et al., [25] used Matlab simulation to show the elimination of current harmonics with the use of a double-tuned filter to improve the power quality of HVDC converter stations. The conventional doubled tuned filter can be designed either by equivalent method or parametric method. By using two single-tuned filters connected in parallel the filter parameters are calculated using the equivalent method. The values of the double-tuned filter can be determined using the parametric method, where known data such as reactive power demand of the non-linear load is used. The double-tuned filter improves power factor, reduces harmonics, and compensates for reactive power demand.

In [61] Othman, et al., compared two case studies with different harmonic orders in the system. The first case study was to suppress the 3^{rd} and 5^{th} order harmonics, whereas the second case was to suppress harmonics up to the 15^{th} order. The system was simulated using Matlab software. The double-tuned filter has the advantage of cancelling harmonics at two different frequencies. The filter was able to reduce harmonic distortion with a noticeable decrease in THD. The lower percentage of THD enables the operation of the unbalanced system. The results show that the filter reduced the two highest harmonic orders whilst the harmonic orders outside the range of the filter were not noticeably suppressed due to the filter's design parameters.

Joseph, et al., [62] studied the harmonics injected by major household appliances and analysed a filter to mitigate these harmonics. Investigation into these types of loads showed that appliances used in households inject odd harmonics, unlike industries that inject even

harmonics. The common household appliances involve switching components that disrupt the sinusoidal waveform of the supply current. The system is simulated using Matlab simulation to compare the level and order of harmonics before and after the filter is installed. A C-Type filter is a good option as it avoids resonance problems, and it can suppress a wider range of harmonic frequencies. Compared to the notch filters the C-Type filter reduces THD to 4 % from 21 % within the limit specified by IEEE-519 standard. The filter is durable with a high tolerance level and the problem of parallel resonance is eliminated using C-Type filters in a domestic environment.

In [63] Klempka studied large non-linear loads such as arc furnaces that cause high levels of voltage and current distortion. He found that the simplest method to improve power quality was the installation of passive power filters [64]. The voltage harmonics in the system at the PCC during the operation of the furnace were obtained utilizing a harmonic analyser. Based on the results the parameters of the C-Type filter were determined. The measurements carried out after the installation of the C-Type filter showed that the filter ensured second-order harmonic reduction in the power system. This resulted in lower production costs due to lower electrical power costs. Also, the improvement in power quality reduces the possibility of electrical failures which causes an interruption in production in the plant. The filter was able to reduce the harmful harmonics and reduce voltage and current distortion in the power system.

The design and application of a second-order high pass filter to reduce harmonic distortion at PCC were studied by Das [65]. The distribution system was modelled accordingly with two id fan motors being the major non-linear loads. The power system component modelling was an important factor for harmonic analysis. The system showed a decrease in harmonic distortion from 42.41 % to 1.32 %, within IEEE 519 limits after the installation of the harmonic filter. The current distortion was around 10 % whilst the voltage distortion was approximately 26 %. The second-order high pass filter was able to suppress several harmonics ranging from lower-order to higher-order harmonics. This effectively decreased both voltage and current distortion to an acceptable level.

Chapter 3

Modelling and Computer Simulations

3.1 Variable Speed Drive

A variable speed drive is an integral part of an AC rotating machine normally used for power conversion and control. As shown in Figure 3.1, the input AC line power from the grid is received by the drive and this AC power supply is usually supplied at constant voltages (400 V or 230 V) and constant frequency (usually 60 Hz or 50 Hz). The VSD converts the constant supply voltage and frequency to a variable voltage and frequency used by the motor. Thus, for the VSD to have this ability, consequently, the drive will be able to change the motor speed and control its torque. Therefore, optimal performance and efficiency of the electrical rotating machine can be gained by using variable speed drives.

Figure 3.1: AC drive

In recent times, there are numerous industrial applications of variable speed drives and this is due to recent advances in solid-state electronics which decreased the cost of AC drives. In industry, variable speed electrical drives are systems with an induction motor as shown in Figure 3.1. As shown in Figure 3.2, the VSD consists of the rectifier, filter, and inverter. The conversion of AC power to Direct Current (DC) power is achieved through the rectifier in a VSD. After the power flows through the rectifiers, it is stored on a DC bus. The DC bus consists of capacitors that store power from the rectifier and later deliver it via the inverter section. The last portion of the VSD is known as an “inverter.” This contains transistors that deliver power to the motor.

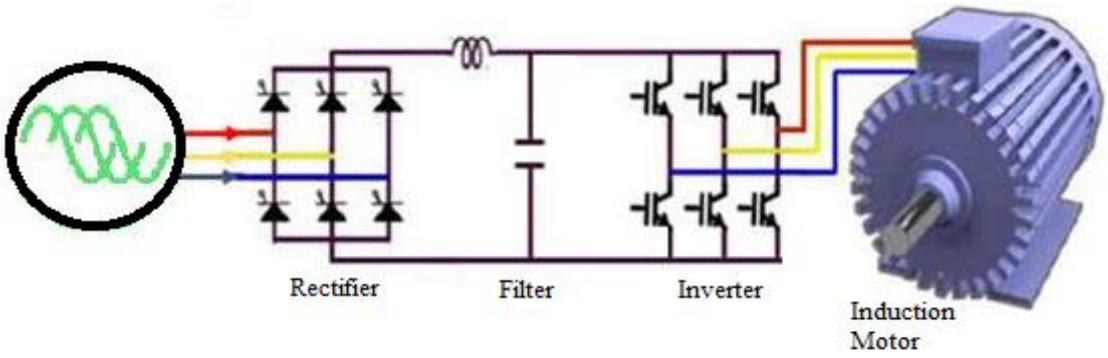

Figure 3.2: Diagram of VSD for an induction motor

The fact that the popular use of VSD in the industries has increased these days, due to the application of power-electronic converters which has improved the reliability and efficiency of the system. But the applications of VSD come with their disadvantages (undesirable phenomena) and the effect it has on operation has prompted the need for investigations. This is necessary because of the serious effects of current and voltage distortion which is the main cause of harmonic distortion. The increasing popularity of VSD's has brought into focus the harmonic effects created by drives. This has made it known that the drive without any harmonic mitigation technology may interfere with neighbouring equipment, reduce equipment life, and negatively impact the utility power quality. Under some circumstances, the total harmonic current distortion (THDi) may approach the level of the fundamental current. Thus, there is a need to combat these effects.

To combat these effects is the use of a traditional filter coupled with a passive harmonic filter. This chapter focuses on the modelling of the main components that make up the electrical network such as the BCTRAN transformer, circuit breaker, motor, and VSD. To observe the overvoltage that occurs when the harmonic filter is switched, the filter together with the existing network is simulated using the Alternative Transients Program (ATP) simulation software. Due to the adverse effect of the problem, the components mentioned above were used to model and simulate filters and then arrived at the optimal design that can be used to mitigate the problem of overvoltages caused by the operations of VSDs.

3.2 The Operation of Variable Speed Drive

Variable speed drives are versatile and can be used in applications that involve pumps, fans, compressors, and other equipment. The drive operates by varying the speed of an AC motor by changing the supply frequency. The VSD converts the AC supply voltage into DC by using a rectifier. The voltage is then smoothed using DC-link capacitors which provide a more stable

DC voltage. The inverter then converts the DC voltage back to AC by using a technique called PWM. This process involves using transistors to switch the DC voltage on and off to produce the AC output voltage and frequency. By modulating the pulse width over each half wave, the R.M.S. voltage across the motor phases can be controlled. This allows the VSD to vary the amount of current flowing between motor phases [66].

PWM drive technology is still considered new and is continuously being improved with new power switching devices [67]. The operation of a VSD is managed by a control unit that monitors the rectifier, DC-link, and inverter circuit to deliver the desired output signal. The drive is equipped with a control panel that may be used to disconnect power during motor maintenance. VSD's are easily retrofitted to existing AC motors making the performance of the motor match the performance of a DC system. This means there will be significantly lower maintenance costs and downtime during production compared to a DC system. VSD technology with the use of AC motors is now widely used and is extremely useful in improving the efficiency of a system.

3.3 Harmonic Analysis

The power quality of an electrical network is defined by the voltage, current, frequency, and power balance of the system. The distortion of any of these is defined as harmonics [68]. Harmonic analysis or study plays a vital role in understanding and characterizing the extent of harmonic problems [69]. It is used when finding a solution for an existing harmonic problem such as designing a harmonic filter. In this study, the mitigation technique used to reduce the harmonic is the installation of a single-tuned harmonic filter. To execute harmonic analysis, first, we must perform Fourier analysis [23].

$$f(t) = \frac{a_0}{2} \sum_{n=1}^{\infty} a_n \cos nt + \sum_{n=1}^{\infty} b_n \sin nt \tag{3.1}$$

$$f(t) = \frac{a_0}{2} + (a_1 \cos t + b_1 \sin t) + (a_2 \cos 2t ...) \tag{3.2}$$

The term $(a_1 \cos t + b_1 \sin t)$ in equation (3.2) is known as the fundamental harmonic and $(a_2 \cos 2t + b_2 \sin 2t)$ is the second harmonic, etc. The limits for the individual harmonic distortion can be evaluated as defined in equation (3.3).

$$IHD_{V_d}^{(h)}(\%) = \frac{\left|V_i^{(h)}\right|}{\left|V_i^1\right|} \times 100 \leq IHD_V^{MAX} \tag{3.3}$$

Where the h_{th} harmonic order, $|V|$ is the voltage magnitude at the bus "i" and IHD^{MAX} is the maximum allowable voltage harmonic distortion level. The total harmonic distortion factor is given in equation (3.4).

$$V_{THD} = \frac{\sqrt{\sum_{h=2}^{h} V_h^2}}{V_i} \tag{3.4}$$

There are three methods for analysing harmonics: time domain, direct frequency harmonic analysis, and iterative techniques.

For the time domain methods, this method involves the numerical integration of system differential equations. Time-domain representation is the most widely used method for power system modelling. Harmonic analysis using the time domain method involves simulating the system in the steady-state and then using the Fourier transform. This method has the advantage that it provides an accurate representation of the control system [70].

Direct frequency domain harmonic analysis consists of performing a load flow to determine the operating conditions of the system and then calculating harmonic injections using simplified non-linear models. The disadvantage of this system is that it does not take into consideration the effect of harmonic voltages on non-linear devices.

In the iterative harmonic analysis, when a non-linear device injects harmonic current into an AC system, harmonic voltage is produced. If the non-linear device is sensitive to harmonic voltages, the injected harmonic current will change [70]. This then requires an iterative solution for harmonic analysis of the system. These methods use Gauss-Seidel and Newton Raphson methods. This method is not commonly used for a system that has a high harmonic distortion.

3.4 Analysis of Network with VSDs

Harmonics are generated by non-linear devices such as static power converters, VSD's, switched-mode suppliers, cyclo converters, etc. A sample industrial power system with VSD's as the main harmonic source is depicted in Figure 3.3. Since VSD's have become a common device that is used in power systems, harmonic studies become integral when designing systems and their operation.

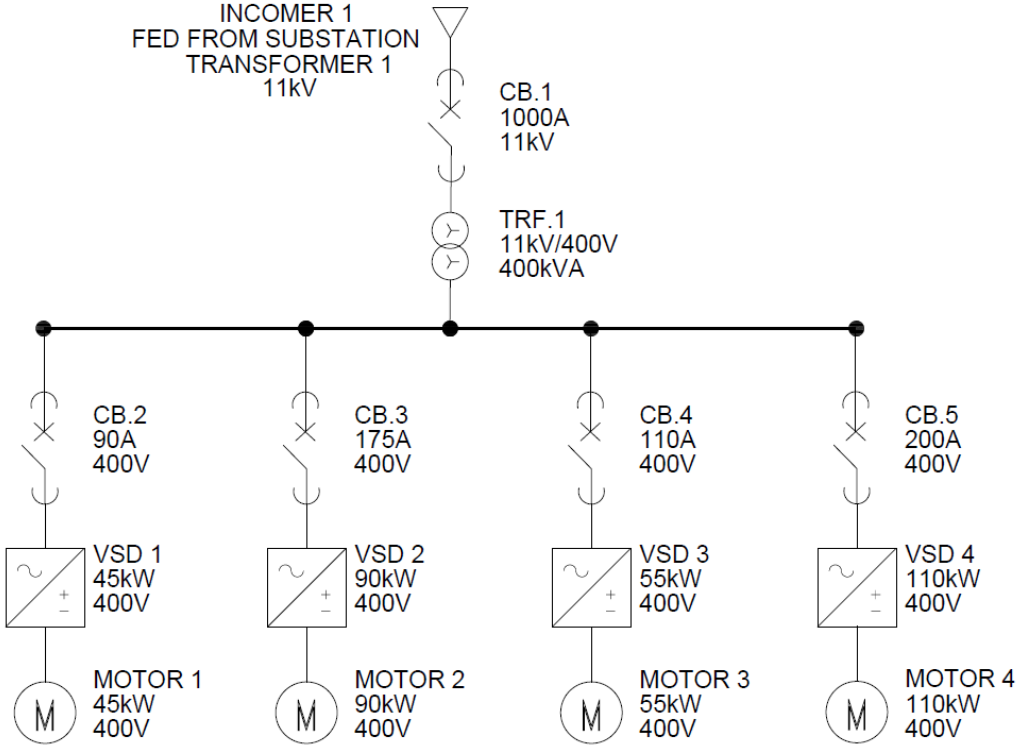

Figure 3.3: Network single line diagram without filters

Figure 3.3 displays the single line diagram of a single bus system without filters. The four VSD's represent the non-linear loads which are the main cause for the harmonics in the system. It also contains four induction motors connected to each VSD. For the above system, load flow analysis is performed to determine the active power, reactive power, bus voltages, and powers. Thereafter harmonic analysis is performed which determines the individual and total harmonic distortion factors at the bus [49, 71]. The ratings of each component in the electrical system are shown in Table 3.1.

Table 3.1: System ratings

Components	Ratings
Incomer supply	11 kV
TRF 1	11 kV/400 V
VSD 1 & Motor 1	45 kW
VSD 2 & Motor 2	90 kW
VSD 3 & Motor 3	55 kW
VSD 4 & Motor 4	110 kW

3.5 Harmonic Filtering Using Single-tuned Harmonic Filter

Based on the study performed, the implementation of a harmonic filter is the best solution to mitigate the harmonics produced by the operation of the VSD's. The single-tuned filter was found to be the best filter to suppress a specific harmonic at the tuned frequency. The harmonic orders that are to be reduced in this study are of the 3rd and 5th order. Equations (3.5) to (3.10), define the parameters used to design a single-tuned filter which involves the calculation of the resonant frequency, capacitor, inductor, and resistor values that enable the mitigation of harmonics in the power frequency [60].

$$f_r = \frac{1}{2\pi\sqrt{LC}} \tag{3.5}$$

Where f_r is the resonant frequency in Hertz, L is the filter inductance in Henry and C is the filter capacitance in Farad.

The capacitive reactance (X_C), and capacitance (C) at the fundamental frequency (f) are given by equations (3.6) and (3.7).

$$X_C = \frac{V^2}{Q_c} \tag{3.6}$$

$$C = \frac{1}{2\pi f X_C} \tag{3.7}$$

Where V is the (r.m.s) nominal line to line voltage (in kV).

The inductive reactance (X_L), and inductance (L) at the fundamental frequency (f) are given by equations (3.8) and (3.9).

$$X_L = \frac{X_c}{h_n^2} \tag{3.8}$$

$$L = \frac{X_L}{2\pi f} \tag{3.9}$$

Where h_n is the harmonic order.

The resistance (R) for a specific quality factor (Q) and the characteristic reactance (X_n) is given in equations (3.10) and (3.11).

$$R = \frac{X_n}{Q} \tag{3.10}$$

$$X_n = \sqrt{X_L X_C} \tag{3.11}$$

3.6 Mitigating of Harmonics Using Single-tuned Filter

The operation of VSD's produces harmonic currents and absorption of reactive power. To control the effects that harmonics have on the electrical system, single-tuned filters are shunt connected to the electrical network. The effectiveness of this mitigation technique can be expressed analytically. The %THD change determines how effective the filter is in mitigating the harmonics. Thereafter these results are compared to IEEE 519 standard to analyse the effectiveness of this mitigation technique. To demonstrate this Figure 3.4 shows the harmonics present in an electrical system with the absence of a harmonic filter.

The 3rd and 5th harmonics are the highest and produce voltage distortions of 16.725 V and 11.081 V respectively. The THD of the system was found to be 5.32 %. The addition of a single-tuned harmonic filter limits the 3rd harmonic to 0.13998 V and the 5th harmonic to 0.0774 V with the THD dropping to 0.1381 % as seen in Figure 3.5. Comparing these results to the IEEE 519-1992 standard filter limits both the 3rd and 5th harmonics to ≤ 3 % and the THD to ≤ 5 %. This proves that using a single-tuned filter is an effective means of mitigating harmonics in this system.

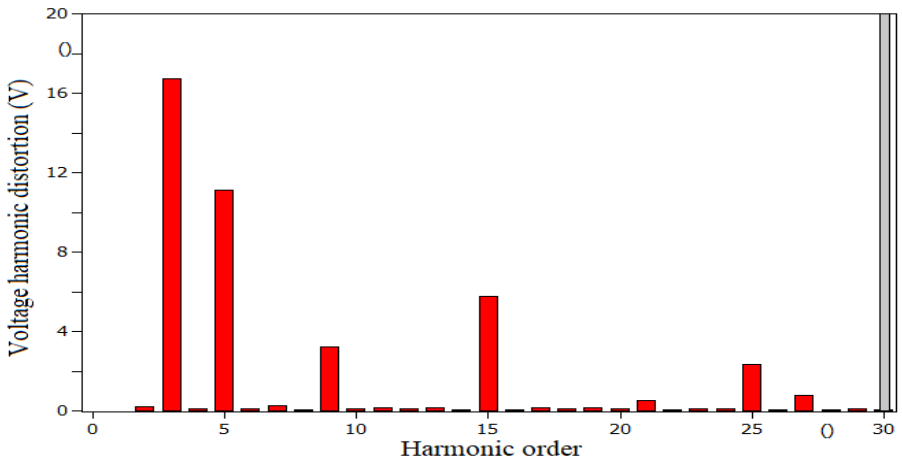

Figure 3.4: Harmonics before using filter

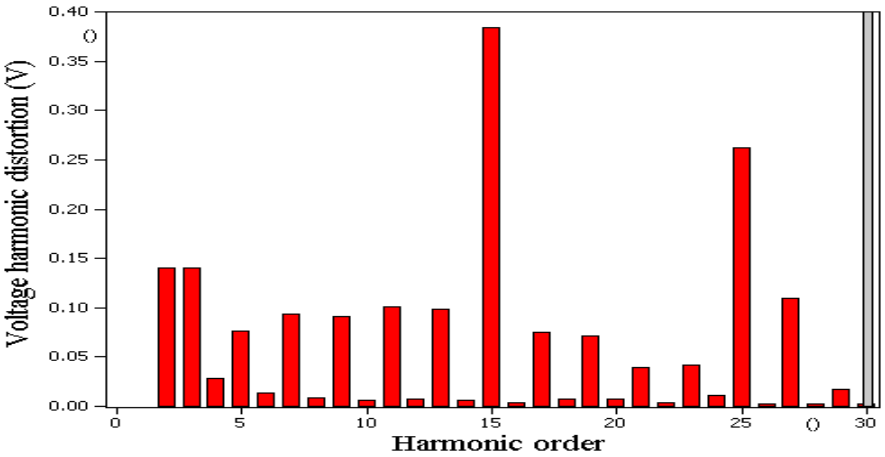

Figure 3. 5 Harmonics after using single-tuned filter

3.7 The Analysis of Single-tuned Filter

The harmonic filter attenuates all harmonic voltages at the voltage bus [72]. To mathematically express how harmonic voltages are affected; the attenuation factor is shown in equation (3.20). Figure 3.6 shows the basic circuit used to calculate the h-th harmonic attenuation factor produced by the n-th harmonic filter. In this diagram, I(h) represent the h-th harmonic injected by the VSD, $Z_s(h)$ accounts for the system impedance and $Z_n(h)$ represents the n-th harmonic filter impedance at the h-th harmonic.

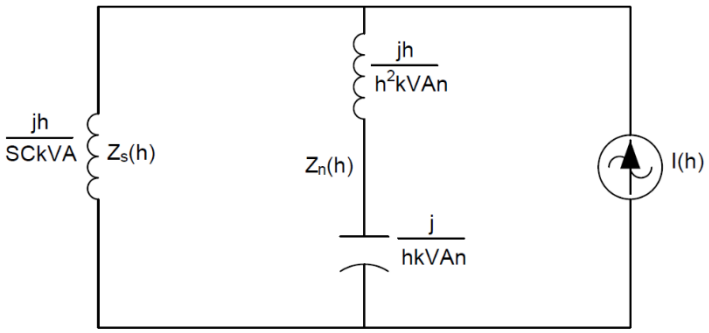

Figure 3.6: Equivalent circuit for attenuation factor

The n-th harmonic filter impedance at the harmonic frequency (h) can be expressed in terms of the filter kVAr, (kVAn) and its tuning frequency (h_n) as shown in equation (3.12).

$$Z_n(h) = \frac{j}{kVAn}\left(\frac{h}{h_n^2} - \frac{1}{h}\right) = \frac{j}{kVAn}\left(\frac{h^2 - h_n^2}{h_n^2}\right) \tag{3.12}$$

The distribution system impedance seen by the low voltage bus at the harmonic frequency (h) is related to the low voltage bus short circuit kVA as shown in (3.13).

$$Z_s(h) = \frac{jh}{SCkVA} \tag{3.13}$$

To simplify the calculation, the filter and the system are represented by their admittance values.

$$Y_n(h) = \frac{kVAn}{j}\left(\frac{h_n^2}{h^2 - h_n^2}\right) \tag{3.14}$$

$$Y_s(h) = \frac{SCkVAn}{jh} \tag{3.15}$$

The equivalent admittance seen by the VSD is calculated by adding $Y_n(h)$ and $Y_s(h)$.

$$Y_{eq}(h) = \frac{kVAn}{jh}\left(\frac{h^2 h_n^2}{h^2 - h_n^2}\right) + \frac{SCkVA}{jh} \tag{3.16}$$

$$Y_{eq}(h) = \frac{1}{jh}\left[dkVAn + SCkVA\right] \tag{3.17}$$

Where,

$$d = \left(\frac{h^2 h_n^2}{h^2 - h_n^2}\right) \tag{3.18}$$

The attenuation factor $a_n(h)$ is then obtained using equation (3.20).

$$a_n(h) = \frac{V(h)}{Vf(h)} = \frac{Y_{eq}(h)}{Y_s(h)} = \frac{\frac{1}{jh}\left[dkVAn + SCkVA\right]}{\frac{SCkVA}{jh}} \tag{3.19}$$

$$a_n(h) = 1 + \frac{dkVAn}{SCkVA} \tag{3.20}$$

When more than one filter is connected, the attenuation factor of the h-th harmonic voltage is given by equation (3.21).

$$a_n(h) = 1 + \frac{d_1 kVAn(1)}{SCkVA} + \frac{d_n kVAn(N)}{SCkVA} \tag{3.21}$$

Where,

$$d_k = \left(\frac{h^2\left(h_n(k)\right)^2}{h^2 - \left(h_n(k)\right)^2}\right) \tag{3.22}$$

Using the proposed methodology discussed in this chapter, it is possible to determine the ratings of the filter to keep the harmonic distortion within acceptable standards and to define filter requirements. One of the methods to accomplish this is using the attenuation factor. The attenuation factor is used to analyse the effect of connecting harmonic filters to the system to reduce a specific harmonic. Using this factor, the filter ratings may be adjusted to allow for maximum mitigation of the targeted harmonics produced by the operation of the VSD's.

3.8 Network with Harmonic Filters

Figure 3.7 shows the single line diagram of the system with two single-tuned filters connected to the main bus. The filter was designed with the help of harmonic order (here we are considering the 3rd and 5th harmonics), voltages at the bus, frequency, reactive power values of the system, and resistance, inductance, and capacitance parameters. By installing the filter to attenuate the 3rd and 5th harmonics, we can observe a decrease in the level of harmonics.

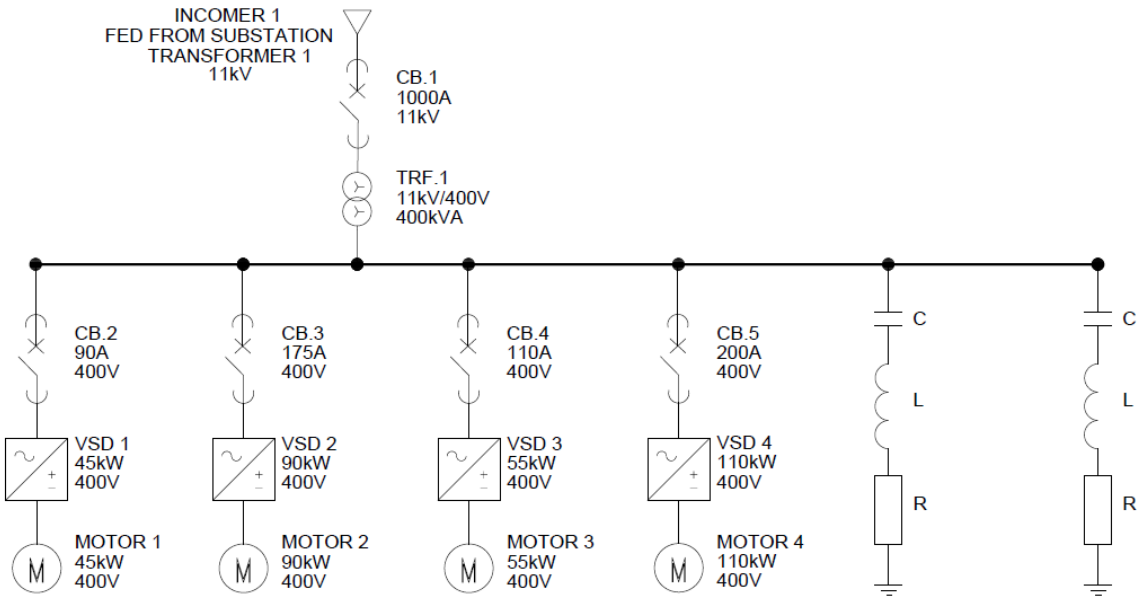

Figure 3.7: Single line diagram with filters

3.9 ATP Software

ATP is one of the most widely used programs for digital simulation of transient phenomena of electromagnetic as well as electromechanical nature in electric power systems [73]. The software allows for intricate electrical network structures to be simulated. The program can predict variables within electric power networks as a function of time. The software incorporates equivalent networks for all the components in the power system. ATP contains

models of transformers, surge arresters, transmission lines, and rotating machines. Table 3.2 shows a few of the predefined components found on ATP's extensive palette.

Table 3.2: Components found on ATP software [74]

Selection	Icon	Description
AC source		AC source. Voltage or current. Single or 3-phase. Grounded or ungrounded
BCTRAN	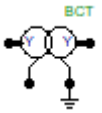	Direct support of BCTRAN transformer matrix modelling
Voltage probe		Specifies a node voltage to ground output
LCC		Single-core cable
Windsyn	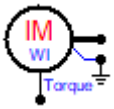	Universal machine with manufacturers data input
Current probe		Specifies current output
Resistor		Pure resistance in Ω
MOV type 3.phase		3. phase current dependent Resistance

3.9.1 Operating Principles of ATP

ATP has built-in models of most electrical components that can be used to design the electrical network. ATP supports most standard components and allows the user to create new objects based on models [74]. The software operates by predicting variables within the electric power network as functions of time, typically initiated by an electrical disturbance. The trapezoidal rule of integration is used to solve the differential equations of system components in the time domain. Interfacing capability to the program modules enables the modelling of control systems and components with nonlinear characteristics [74]. Disturbances such as faults, lightning surges, and switching operations may be simulated using this software.

Using the components available on ATP the network system in this study was simulated with parameters calculated from mathematical modelling. Models such as VSD's that were not available as pre-set blocks were designed using various components such as diodes, capacitors, and thyristors. The plotting facility of the program made it an excellent tool to visualise the effects of overvoltage in the power system. Voltage, current, and harmonic Fourier analysis are just some of the graphs offered in the program. In this study, the harmonic graph was used to observe the magnitude and order of harmonics present before and after the installation of harmonic filters. Also, the overvoltage experienced due to the switching of the harmonic filter as well as the mitigation of the overvoltage using surge arresters, pre-insertion resistors, or controlled switching was observed using the voltage graphs. By comparing the voltage graphs after implementing the various mitigation techniques the best mitigation method was chosen.

3.9.2 Modelling of Components in ATP

The modelling of the different electrical components makes it possible to simulate the electrical network using ATP software. The implementation was modified and used to simulate the numerical problem developed in this chapter using ATP. The results of the simulation were used to compare the nominal voltage supply to the permissible limits of operation when the harmonic filter is switched on or off. If the voltage is found to be higher than the withstand limits of the system, appropriate mitigation techniques may be used. Based on ATP, simulations are performed to show the effectiveness of the mitigation techniques in reducing the switching overvoltage. The computer program simulation was used to find the solution to switching overvoltages in three different industries. Using the ATP results the surge arrester proved to be the best mitigation technique and was the most successful in keeping to the SANS 10142.1 standards as documented in [75].

3.9.3 BCTRAN Model of Transformer

BCTRAN is the supporting routine of the EMTP program which creates an impedance or admittance matrix representation of the transformer, without taking into account the saturate-able core effects, from transformer ratings and factory test data [76]. Equation (3.23) shows the branch impedance matrix of a single-phase multi-winding transformer.

$$[V] = [I][Z] \tag{3.23}$$

The impedance matrix of the transformer, without taking into account the saturate-able core effects can be represented (3 x 3) as shown in equation (3.24) [76].

$$\begin{bmatrix} Z_s & Z_m & Z_m \\ Z_m & Z_s & Z_m \\ Z_m & Z_m & Z_s \end{bmatrix} \tag{3.24}$$

Where Z_s and Z_m are self and mutual impedance, respectively. The basic voltage equation of the transformer model can be shown as equation (3.25) [77].

$$[V] = [I][R] + \left[\frac{dI}{dt}\right][L] \tag{3.25}$$

Simulation errors may occur when the core saturates as the BCTRAN model can calculate the non-linear characteristic of the curve from the factory test data of the transformer but cannot represent it. Therefore excitation may be omitted from the matrix and attached externally at the models terminals in the form of non-linear core elements to model the core transformer [76].

3.9.4 Modelling of Circuit Breakers

The circuit breaker was modelled after the Mayr and Cassie models, which use two differential equations to represent the physical nature of the arc. equation (3.26), represents the differential equation related to Mayr's model of the arc conductance [78]. Mayr's model describes the arc as a cylindrical column whose cross-section remains constant in time with uniform arc temperature.

$$\frac{dg_m}{dt} = \frac{1}{\tau_m}\left(\frac{i_a^{\,2}}{P_o} - g_m\right) \tag{3.26}$$

Whilst equation (3.27), represents the differential equation described by Cassie.

$$\frac{dg_c}{dt} = \frac{1}{\tau_c}\left(\frac{i_a^{\,2}}{U_s^{\,2} - g_c}\right) \tag{3.27}$$

Cassie's model describes the arc as a cylindrical column whose cross-section is variable in time depending on the arc content but with uniform arc temperature.

In equations (3.26) and (3.27), i_a is the circuit breaker current, g_m or g_c is the arc inductance is the τ_m or τ_c= arc time constant, P_0 is the steady-state power loss of the arc, and u_s is the steady-state arc voltage.

The Mayr and Cassie models can work simultaneously to describe the arc behavior of the circuit breaker. These are the bases of all different mathematical modelling of circuit breakers.

3.9.5 Modelling of Variable Speed Drive

Variable speed drives help to improve process control and soft starting capabilities resulting in prolonged equipment life. The VSD is made up of an AC/DC rectifier, DC link capacitor, and DC/AC inverter. A generic modelling technique for a VSD is presented which can be applied to any type of VSD configuration. The per-phase r.m.s. voltage (E) and power source frequency (fg) are the input variables for the model. Active power (P) and reactive power (Q) are the output variables on the VSD side. The model can be readily used in computer simulation tools for power system dynamic studies [79]. The differential equations for this type of VSDs can be written in equations (3.28) to (3.46). The effect of the commutation inductance I_c in front of the VSD is in equation (3.28).

$$V_d = \frac{3\sqrt{6}}{\pi} E - \frac{3}{\pi} l_c \left(2\pi f_g\right) i_d - 2l_c \frac{di_d}{dt} - 2V_{diode} \tag{3.28}$$

$$V_d = r_{dc} i_d + L_{dc} \frac{di_d}{dt} e_d \tag{3.29}$$

$$i_I = i_d - C_{dc} \frac{de_d}{dt} \tag{3.30}$$

$$P = \frac{3}{2}\left(v_{dg} i_{dg} + v_{qg} i_{qg}\right) \tag{3.31}$$

$$Q = \frac{3}{2}\left(v_{qg} i_{dg} - v_{dg} i_{qg}\right) \tag{3.32}$$

$$v_{qg} = \sqrt{2}E \tag{3.33}$$

$$v_{dg} = 0 \tag{3.34}$$

$$i_{dg} = i_{dgcom} + i_{dgcond} \tag{3.35}$$

$$\begin{aligned} i_{dgcom} = {} & \frac{2\sqrt{3}}{\pi} i_d \left[-\cos\left(u - \frac{5\pi}{6}\right) + \cos\left(-\frac{5\pi}{6}\right) \right] \ldots \\ & + \frac{3\sqrt{2}E}{\pi l_c \left(2\pi f_g\right)} \sin u - \frac{3\sqrt{2}E}{4\pi l_c \left(2\pi f_g\right)} \sin 2u - \frac{3\sqrt{2}E}{2\pi l_c \left(2\pi f_g\right)} u \end{aligned} \tag{3.36}$$

$$i_{dgcond} = \frac{2\sqrt{3}}{\pi} i_d \left[-\cos\left(\frac{7\pi}{6}\right) + \cos\left(u + \frac{5\pi}{6}\right) \right] \tag{3.37}$$

$$i_{dg} = i_{qgcom} + i_{qgcond} \tag{3.38}$$

$$i_{dgcom} = \frac{2\sqrt{3}}{\pi} i_d \left[\sin\left(u - \frac{5\pi}{6}\right) - \sin\left(-\frac{5\pi}{6}\right) \right] + \frac{3\sqrt{2}E}{\pi l_c \left(2\pi f_g\right)} \left(\cos u - 1\right) \ldots + \frac{3\sqrt{2}E}{4\pi l_c \left(2\pi f_g\right)} \left(1 - \cos 2u\right) \tag{3.39}$$

$$i_{dgcond} = \frac{2\sqrt{3}}{\pi} i_d \left[\sin\left(\frac{7\pi}{6}\right) - \sin\left(u + \frac{5\pi}{6}\right) \right] \tag{3.40}$$

$$u = \arccos\left[1 - \frac{2 l_c \left(2\pi f_g\right) i_d}{\sqrt{6}E} \right] \tag{3.41}$$

$$v_{qs} = \frac{1}{2} d e_d \tag{3.42}$$

$$v_{ds} = 0 \tag{3.43}$$

$$P_{IM} = \frac{3}{2} \left(v_{ds} i_{ds} + v_{qs} i_{ds} \right) \tag{3.44}$$

$$P_{Invertor} = e_d i_i \tag{3.45}$$

$$P_{Invertor} = P_{IM} \tag{3.46}$$

Where P and Q are the active and reactive power at the input of the VSD in front of the commutation inductor, I_c is the commutation inductor, E is the r.m.s. value of the power source voltage per phase, f_g is the power supply frequency at the input of the VSD, v_d is the DC link voltage after the rectifier, e_d is the DC link voltage before inverter, i_d is the DC link current after the rectifier, C_{dc} is the capacitance of DC link capacitor, $r_{dc}$is the resistance of DC link capacitor, L_{dc} is the inductance of DC link reactor, v_{qg} is the q-axis power source voltage, v_{dg} is the d-axis power source voltage, i_{qg} is the q-axis AC at VSD input, i_{qgcom} is the q-axis AC at VSD input during commutation period, i_{qgcond} is the q-axis AC at VSD input during conduction period, i_{dg} is the d-axis AC at VSD input, I_{dgcond} is the d-axis AC at VSD input

during the conduction period, U is the commutation angle, v_{qs} is the q-axis voltage at inverter output, v_{ds} is the d-axis voltage at inverter output, d is the duty cycle, P_{IM} is the active power at the motor terminal (assuming there is only a short cable between the drive and the induction motor) and $P_{invertor}$ is the active power at the output of the drive.

3.9.6 Modelling of Motor

Induction motors are commonly used in industry because of their reliability, simple operation, and high efficiency. Over the years, various models have been developed by researchers to explain the design of an induction motor. In this study, dynamic modelling is developed using differential equations which is simple for computer simulation. This method of modelling assumes that both stator and rotor windings are symmetric [80]. The model explains the dynamic behaviour of the motor under both transient and steady-state conditions including the constant moment of inertia and load torque for the external system [40]. The differential equations for induction motors are given by equations (3.47) to (3.56).

$$V_{sd} = R_s I_{sd} + \frac{d\varphi_{sd}}{dt} - \omega_s \varphi_{sq} \tag{3.47}$$

$$V_{sq} = R_s I_{sq} + \frac{d\varphi_{sq}}{dt} - \omega_s \varphi_{sd} \tag{3.48}$$

$$V_{rd} = R_r I_{rd} + \frac{d\varphi_{rd}}{dt} - \omega_r \varphi_{rq} \tag{3.49}$$

$$V_{rq} = R_r I_{rq} + \frac{d\varphi_{rq}}{dt} - \omega_r \varphi_{rq} \tag{3.50}$$

$$\varphi_{sd} = L_s I_{sd} + L_m I_{rd} \tag{3.51}$$

$$\varphi_{sq} = L_s I_{sq} + L_m I_{rq} \tag{3.52}$$

$$\varphi_{rd} = L_r I_{rd} + L_m I_{sd} \tag{3.53}$$

$$\varphi_{rq} = L_r I_{rq} + L_m I_{sq} \tag{3.54}$$

$$T_e = 1.5P\left(\varphi_{ds} i_{qs} - \varphi_{qs} i_{ds}\right) \tag{3.55}$$

$$\frac{d\omega_r}{dt} = \frac{P}{2H}\left(T_e - T_m\right) \tag{3.56}$$

Where R_s is the stator resistance, L_s is the total stator inductance, L_{ls} is the stator leakage inductance, L_m is the magnetising inductance, $v_{qs,}i_{qs}$ are the q-axis stator voltage and current, $v_{ds,}i_{ds}$ are the d-axis stator voltage and current, $\psi_{qs,}\psi_{ds}$ are the stator q and d axis fluxes, $\psi_{qr,}\psi_{dr}$ are the rotor q and d axis fluxes, $\omega_r$is the electric angular velocity of the rotor, ω_s is the stator field angular velocity in electrical rad/s, P is the number of pole pairs, T_e is the electromagnetic torque, T_m is the shaft mechanical torque and H is the combined rotor and load inertia constant.

3.9.7 Modelling of Surge Arrester

Metal oxide surge arresters are commonly used in electrical networks to protect against stress and insulation damage due to an overvoltage. The arrester has a simple construction, comprising of one or more columns of cylindrical block varistors [81]. The metal oxide varistor material used in the surge arrester has a highly non-linear voltage versus current characteristic which allows the arrester to limit the voltage to a low value, even for steep impulses with fast response times. There are several models of surge arresters, however, the IEEE metal oxide surge arrester model is the most used. The model includes the non-linear resistance A_0 and A_1, separated by the R-L filter. The inductance $L_1$and resistance R_1 make up the filter found between the two varistors. The inductance L_0 is associated with magnetic fields in the vicinity of the arrester, R_0 stabilizes the numerical integration and C represents the terminal-to-terminal capacitance [81]. The input parameters for this type of surge arrester are given in equations (3.57) to (3.61).

$$L_1 = \frac{15d}{n} \tag{3.57}$$

$$R_1 = \frac{65d}{n} \tag{3.58}$$

$$L_0 = \frac{0.2d}{n} \tag{3.59}$$

$$R_0 = \frac{100d}{n} \tag{3.60}$$

$$C = \frac{100n}{d} \tag{3.61}$$

Where d is the length of arrester columns in meters and n is the number of parallel columns of metal oxide disks.

Chapter 4

Simulation, Results, and Discussion of Results

4.1 Introduction

In verifying the analytical model as analysed in Chapter 3, regarding harmonic filters, computer simulations were conducted using ATP software. ATP has extensive modelling capabilities for the creation of electric machinery, distribution lines, and components. Using this software different combinations of harmonic filters are connected to the electrical network to determine the best filter that can be used to reduce harmonics in the system. Choosing the correct filter will save on operational costs, maintenance on electrical equipment, and downtime in production.

4.2 Analysis of Simulated Network

An electrical network of a power system was considered and is shown in Figure 4.1. Block diagrams of various components such as the voltage source, transformer, and motors are chosen from the ATP library and their input parameters are entered into the software to simulate the network. The component data must be entered into the value field of the attributes page. For the AC voltage source, the amplitude, frequency, and phase angle are required as the main input parameters.

ATP software offers various transformer models such as single-phase and three-phase ideal transformers, single-phase saturable transformers, and BCTRAN transformers. The BCTRAN model is used in this simulation which requires the user to specify the number of phases and windings, the type of core, and the test frequency. The motor is found under induction machines which use the manufacturer's data input such as frequency, power, speed, and efficiency. The VSD is required in the network to control the speed and torque of the induction motor. To simulate the VSD on ATP the frequency, am ratio, switching frequency, and capacitance of the dc bus is required. Chapter 5 provides the lumped parameters of each component found in the electrical network.

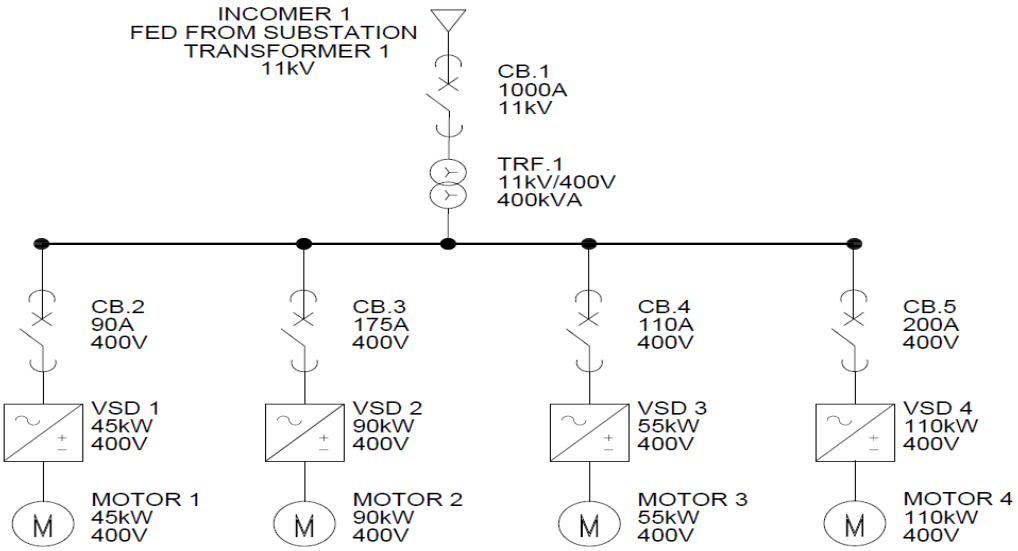

Figure 4.1: Network layout

4.3 Results of ATP Simulation

The electrical network shown in Figure 4.1 was simulated on the ATP software environment to determine the level and order of the harmonics present in the system. The results as shown in Figure 4.2 revealed that the 3rd and 5th order harmonics are the highest with levels present reaching 16.725 V and 11.081 V respectively with a THD of 5.32 %.

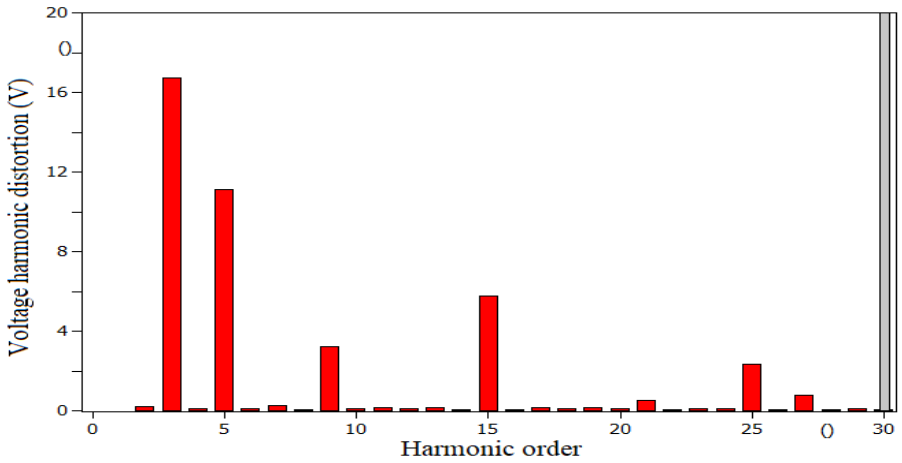

Figure 4.2: Voltage harmonics graph

4.3.1 Mitigation of Harmonics Using Harmonic Filters

A low impedance path for the targeted harmonic frequency is achieved by combining inductors and capacitors to form the harmonic filter. A properly sized filter allows for the unwanted harmonics to be diverted into the filter, preventing them from flowing into the power source. The inductor and capacitor circuit are sized to match the resonance frequency of the harmonic

to be attenuated. As a result, the harmonic current is dissipated as heat by the harmonic filter instead of affecting the utility system and other end-users [30].

4.3.2 Combination of Single and Double-tuned Filter

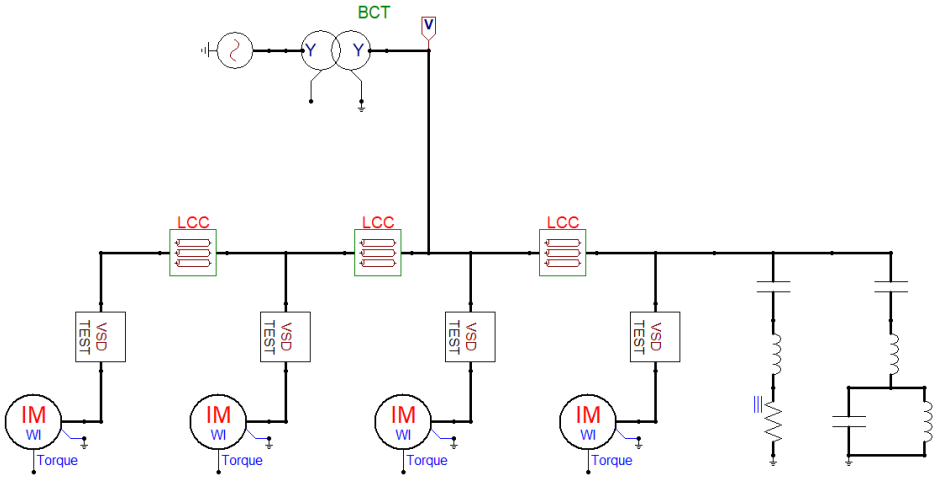

Figure 4.3: Simulation model using single and double-tuned filters

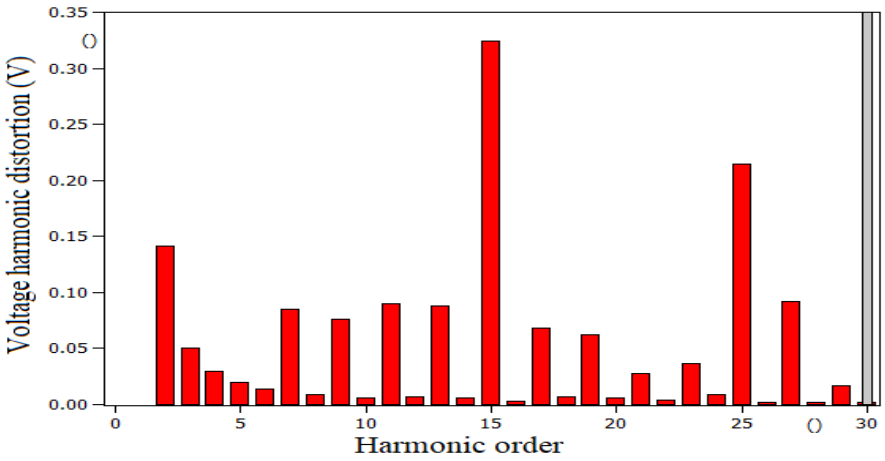

Figure 4.4: Harmonic reduction using single and double-tuned filters

Figure 4.3, shows the installation of a single and double-tuned filter to the existing network. The single-tuned filter can reduce the 3rd harmonic whilst the double-tuned filter can reduce the 3rd and 5th order harmonics simultaneously. According to Figure 4.4, the filters were able to reduce the 3rd harmonic to 0.0501 V and the 5th harmonic to 0.0189 V. The THD has dropped to 0.1119 % keeping it within IEEE 519-1992 limits. Both filters are commonly used in industry to decrease lower order harmonics and be more economical compared to other harmonic filters.

4.3.3 Combination of Single and C-Type Filters

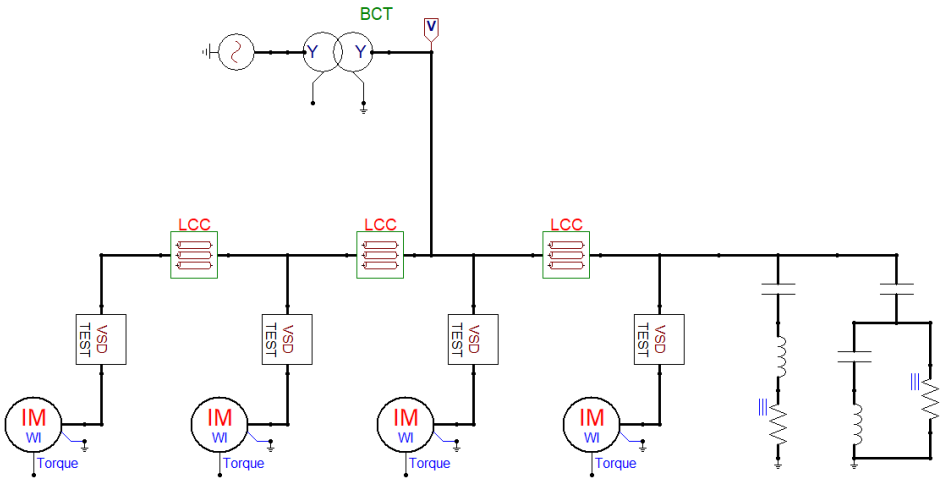

Figure 4.5: Simulation model with single and C-Type filters

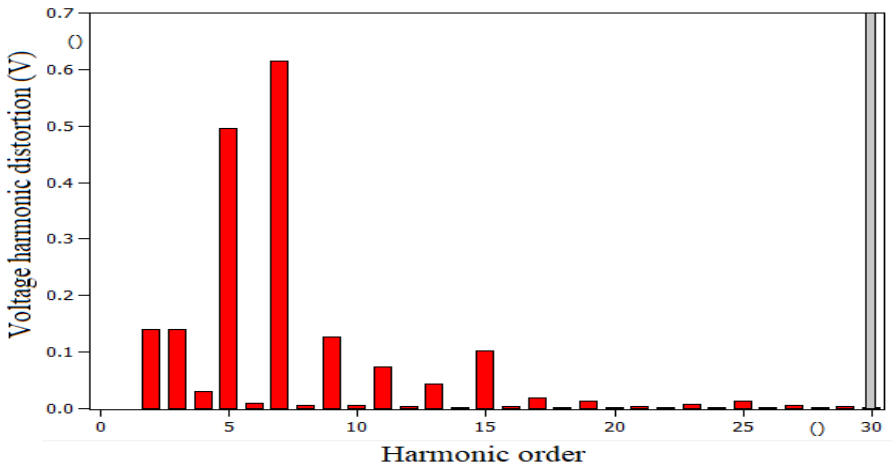

Figure 4.6: Harmonic reduction using single and C-Type filters

The single and C-Type filters are shown in Figure 4.5 are connected to the existing network to eliminate the 3rd and 5th harmonics, respectively. Figure 4.6 shows that the filters reduced the 3rd harmonic to 0.1388 V and the 5th harmonic to 0.4956 V. The THD at the PCC is 0.2016 % which is within the acceptable specified range (THD ≤ 5 %). Compared to the connection of the single and double-tuned filter the combination of the single and C-Type filter produced unsatisfactory results concerning limiting harmonic distortion.

4.3.4 Combination of Double and C-Type Filter

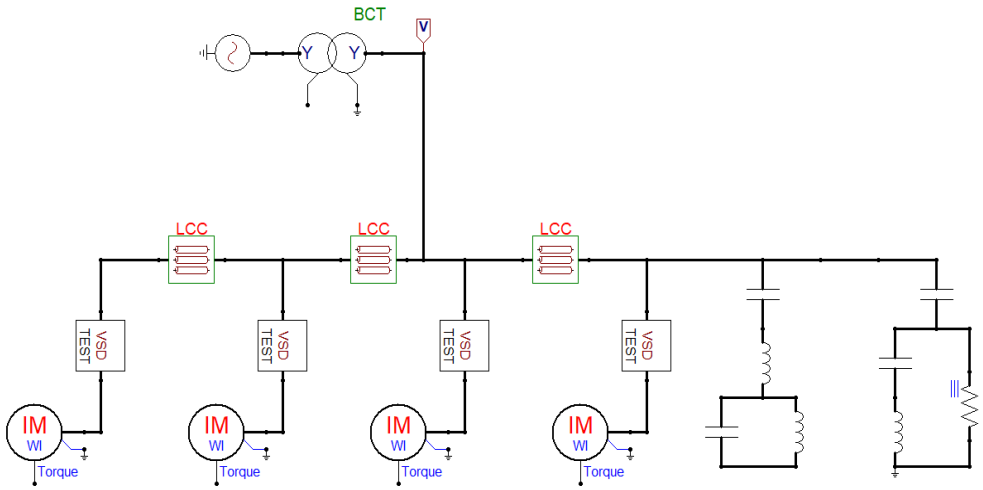

Figure 4.7: Simulation model with double and C-Type filters

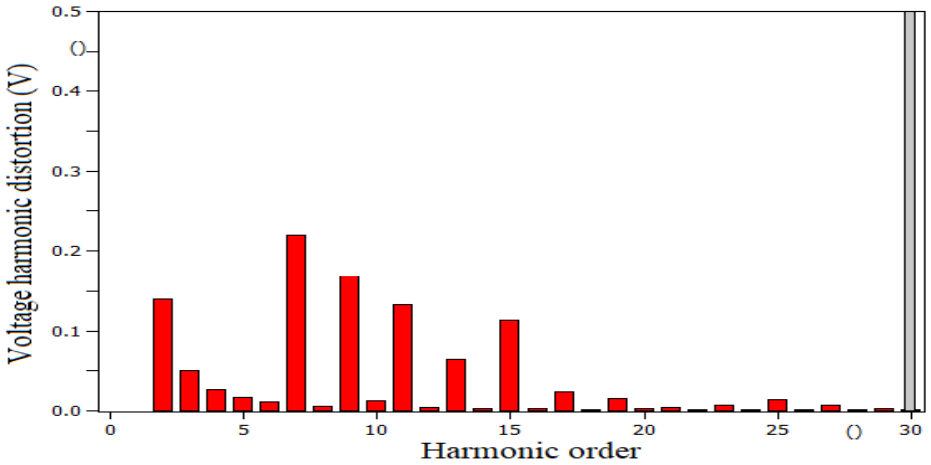

Figure 4.8: Harmonic reduction using double and C-Type filters

The combination of a double and C-Type filter connected to the network is shown in Figure 4.7. The 3rd harmonic is reduced to 0.0503 V and the 5th harmonic is reduced to 0.0165 V. The THD decreased from 5.32 % to 0.1413 % as shown in Figure 4.8. The combination of these two filters will be bulky and subsequently take up a lot of valuable space. Also, the cost of manufacturing and installing both units will be expensive and uneconomical due to the C-Type filters complicated design.

4.3.5 Combination of Single and High Pass Filter

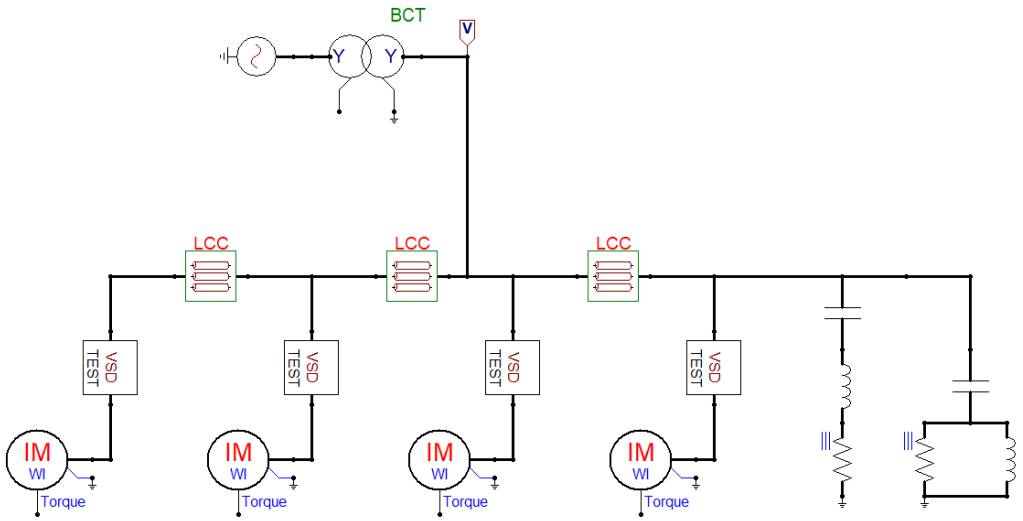

Figure 4 9: Simulation model with single and high pass filter

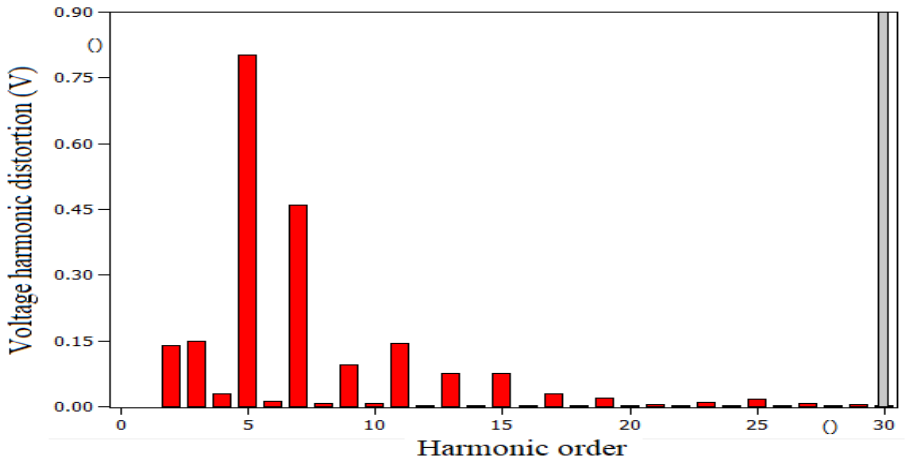

Figure 4.10: Harmonic reduction using single and high pass filter

The connection of a single-tuned filter designed to reduce the 3rd harmonic and a high pass filter designed to reduce the 5th harmonic is shown in Figure 4.9. The 3rd harmonic is reduced to 0.1476 V and the 5th harmonic is reduced to 0.8 V. The value of the THD becomes 0.2339 % as shown in Figure 4.10. These combinations of filters are the least effective and not the best solution for this network.

4.3.6 Combination of Double-tuned and High Pass Filters

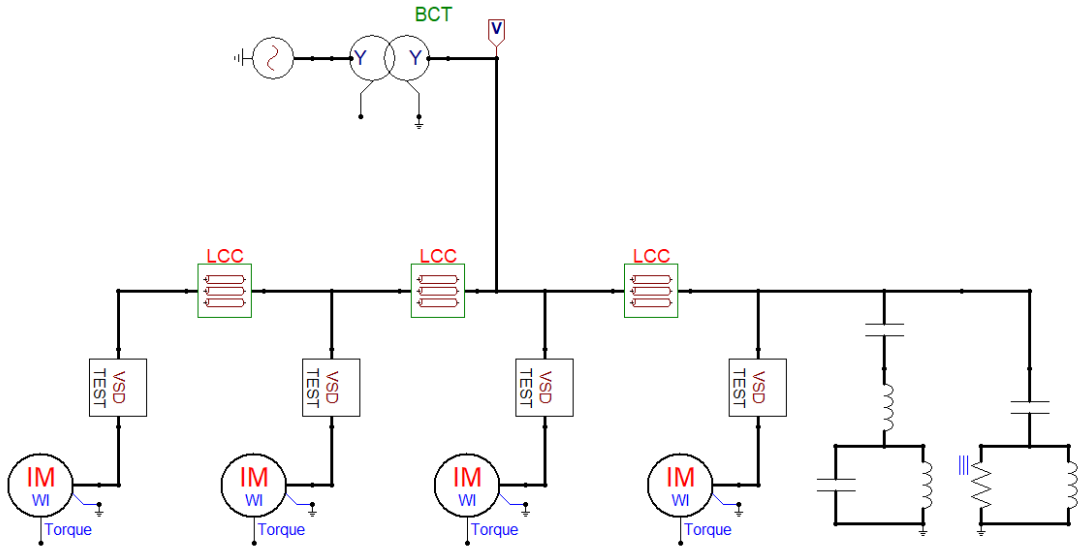

Figure 4.11: Simulation model using double and high pass filters

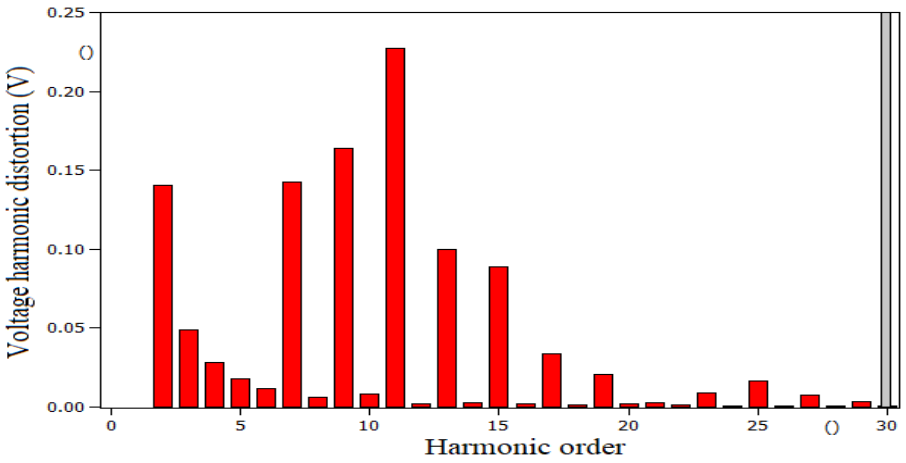

Figure 4.12: Harmonic reduction using double and high pass filters

The last combination is that of a double-tuned and high pass filter as shown in Figure 4.11. The connection of the two filters helped in reducing the 3rd harmonic to 0.0489 V and the 5th harmonic to 0.0176 V. The THD is reduced from 5.32 % to 0.0891 % as shown in Figure 4.12. This combination of filters can be ideally used when there are lower and higher-order harmonics present.

4.4 Summary of Results

Figure 4.13 shows a bar graph that summarises the results of the different filter configurations. The graph shows that for mitigation of harmonics the worst-performing filters were the single and high pass filters whilst the combination of the double and high pass filters closely followed by the combination of single and double-tuned filters proved to be the best. High pass filters

are commonly used to mitigate higher-order harmonics and are therefore unnecessary for this system. This result will be analysed in more detail in Chapter 5.

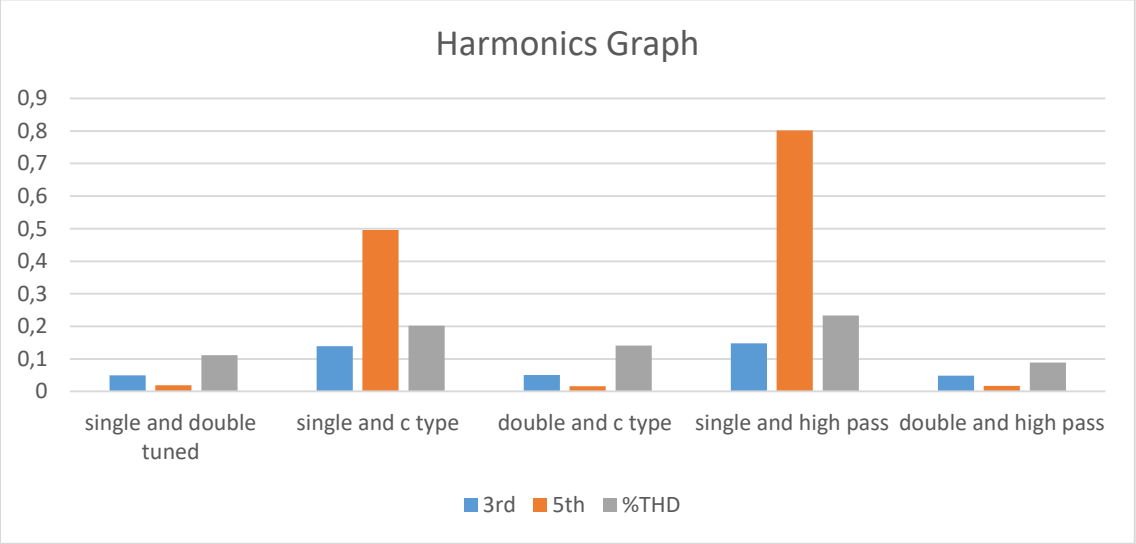

Figure 4.13: Harmonics graph

4.5 Energization of Harmonic Filters

During energization, the harmonic filter is closed to the system which could cause temporary overvoltage to occur. The overvoltage stresses may damage the insulation of various equipment and insulators in the power system. To observe the overvoltage produced by the switching on of the harmonic filter, the two best filter combinations will be simulated on ATP.

4.5.1 Energization of Single and Double-tuned Filters

The filters were closed at 0.04 s, which is at the maximum voltage of phase A. According to the simulation done an overvoltage of 860 V as shown in Figure 4.14 was observed for the energization scenario. This is above the acceptable limit of ± 10 % of the system voltage stipulated by SANS 10142.1.

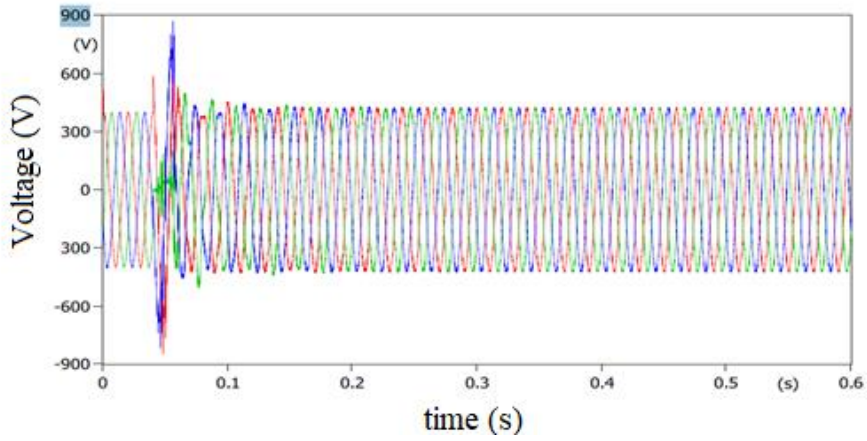

Figure 4.14: Energization of single and double-tuned filter

4.5.2 Energization of Double and High Pass Filters

The closing action of the double and high pass filters produced an overvoltage of 722 V as shown in Figure 4.15. The results show that this filter combination experiences less overvoltage in comparison to the single and double-tuned filters. The overvoltage is still over the voltage tolerance limit in the power system. Therefore, appropriate mitigation measures must be taken.

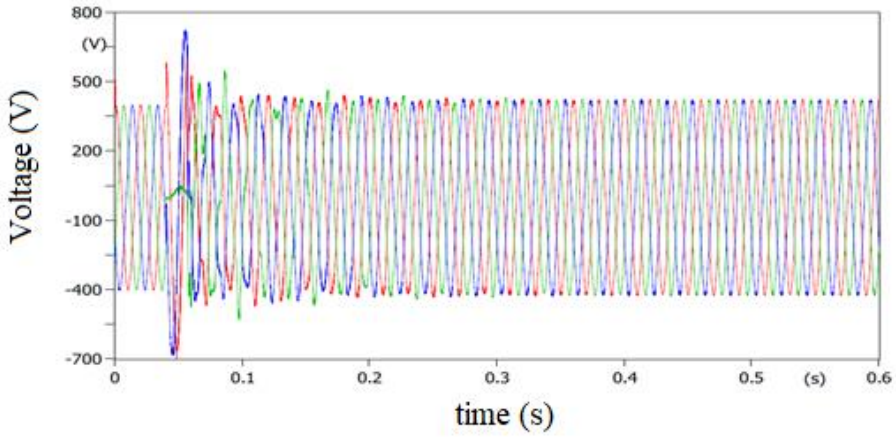

Figure 4.15: Energization of double and high pass filter

4.6 Mitigation Measure of the Overvoltage

Serious damage can be caused to the filter if the overvoltage is greater than the rated voltage of the filter therefore appropriate mitigation measures would be needed, such as pre-insertion resistors, surge arresters, and controlled switching.

4.6.1 Pre-Insertion Resistor

The pre-insertion resistor acts as a resistive element to provide damping to reduce the surge energy. A 2.18 Ω pre-insertion resistor was calculated for this purpose. The resultant waveform

of the simulation in Figures 4.16 and 4.17 shows that overvoltage of 445 V is experienced for the single and double-tuned filter whilst an overvoltage of 463 V is experienced for the double and high pass filters.

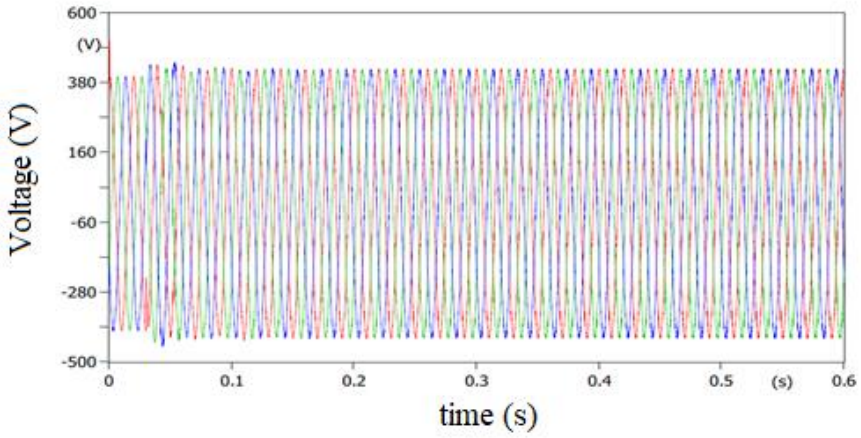

Figure 4.16: Using pre-insertion resistor for single and double-tuned filter

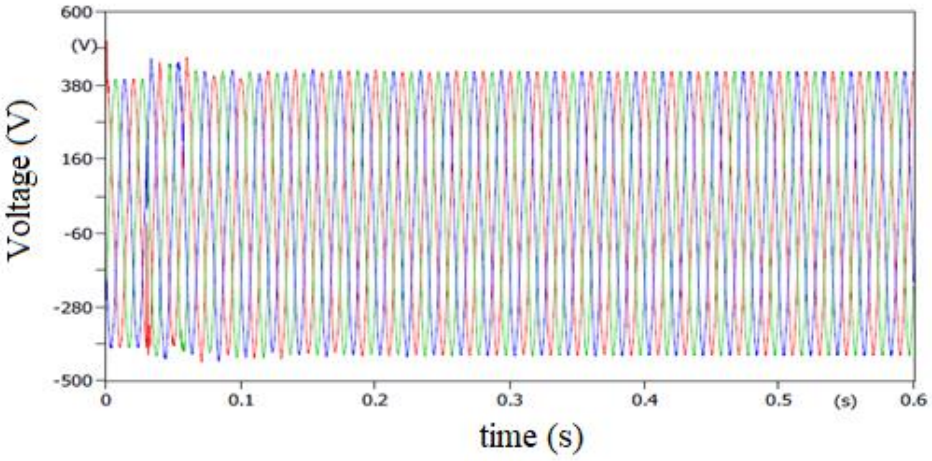

Figure 4.17: Using pre-insertion resistor for double and high pass filter

4.6.2 Controlled Switching

The use of controlled switching has become an effective means of mitigating switching overvoltages, The device minimizes the switching surge by controlling the contact moment during the switching operation of the circuit breaker [50]. In applying controlled switching to mitigate the overvoltage, the circuit breaker is expected to close at the point of least stress. The resultant waveform of the simulation in Figures 4.18 and 4.19 shows that an overvoltage of 792 V is experienced for the single and double-tuned filter whilst an overvoltage of 699 V is experienced for the double and high pass filters.

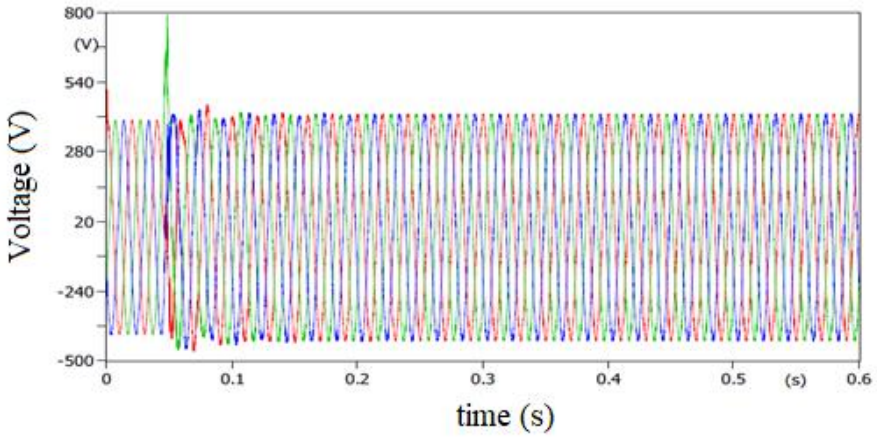

Figure 4.18: Using controlled switching for single and double-tuned filter

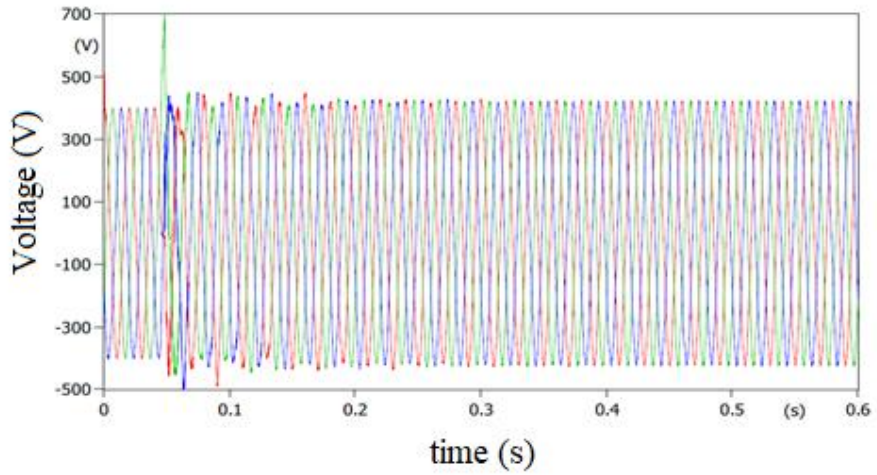

Figure 4.19: Using controlled switching for double and high pass filter

4.6.3 Surge Arrester

Surge arresters are used to protect electrical equipment in the electrical network from overvoltage caused by switching events. In this study the surge arrester is modelled after the IEEE surge arrestor model, however, there are many other existing models of surge arresters available. The resultant waveforms shown in Figures 4.20 and 4.21 show that the surge arrester reduced the overvoltage experienced during energization to 461 V for the single and double-tuned filter and 458 V for the double and high pass filter.

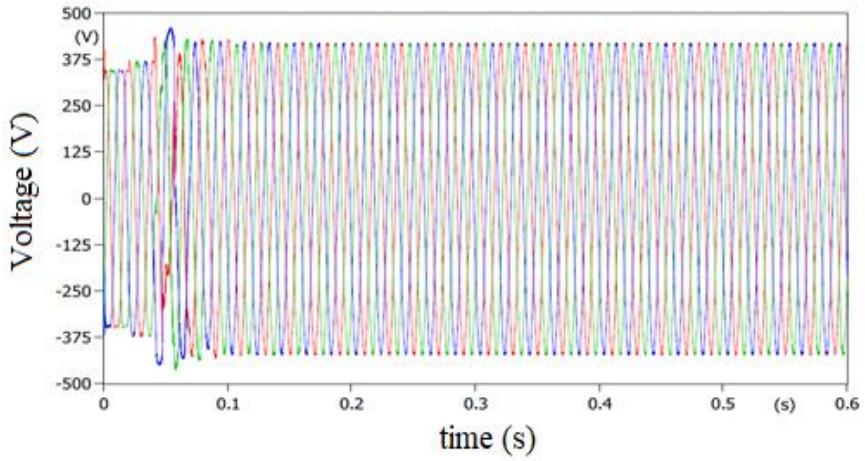

Figure 4.20: Using surge arrester for single and double-tuned filter

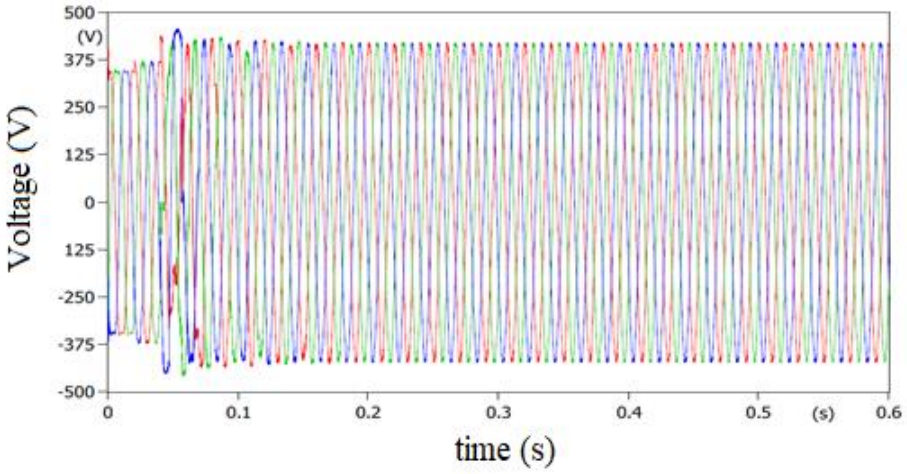

Figure 4.21: Using surge arrester for double and high pass filter

4.7 Summary of Results

From the graph shown in Figure 4.22, the surge arrester was found to be the most successful in mitigating the temporary overvoltage followed by the pre-insertion resistor. Effective placement as well as the high energy dissipation capabilities of modern metal oxide surge arresters allow for the energy produced during the overvoltage to be limited. Controlled switching proved to be the worst-performing mitigation technique and will not be a suitable solution based on this study.

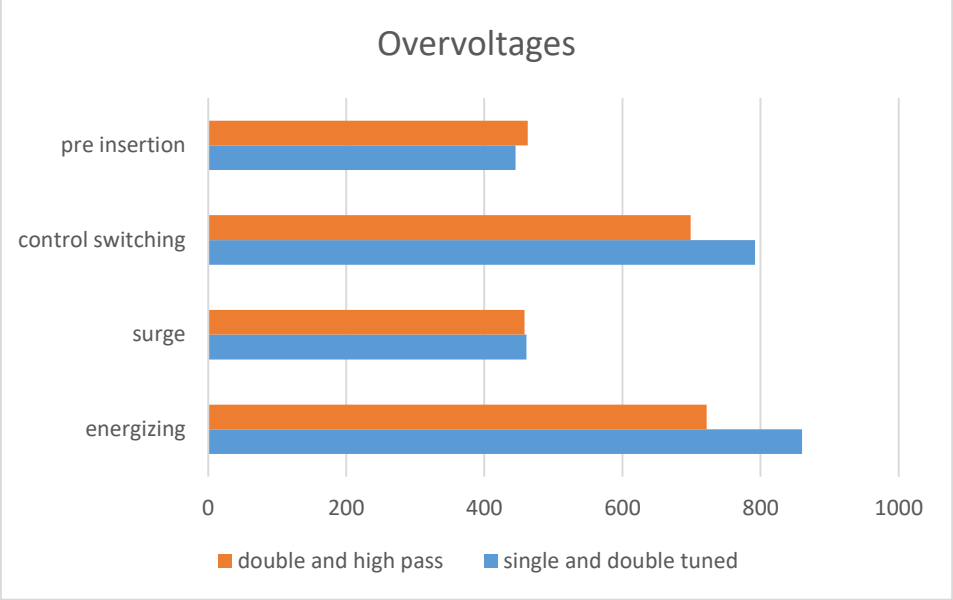

Figure 4.22: Overvoltage graph

Chapter 5
Case Studies

5.1 General Remarks

The aim of embarking on this study was to investigate and mitigate the temporary overvoltage caused by harmonic filters for variable speed drives. To achieve this, to validate the analytical model and computer simulation, case studies were conducted in three different industries. The level and order of harmonics present in these industries were determined using experimental and simulation methods. Using ATP software, the best harmonic filter that would correct the harmonics was chosen. It was found that the switching of the filters produced temporary overvoltage that was greater than the systems withstand levels. Therefore, as will be discussed later, different methods of mitigation were simulated to limit the overvoltage that occurs.

For industrial processing these days, plant engineers are faced with huge challenges of power quality, such as the harmonic distortion of the sinusoidal waveform. These problems have arisen because of the increasing use of non-linear loads. The increased use of these non-linear loads has had a significant impact on the operation of industries, therefore raising concerns among plant engineers and equipment manufacturers. This chapter presents the case studies carried out on harmonics measurements and analysis in various industries and how these problem harmonics were mitigated.

Presented in this chapter are three case studies. These case studies are used to validate the goal that prompt the embarking of the research which was to develop mitigation techniques for overvoltage's caused by harmonic filters. The first case study was carried out in an oil refinery that produces sunflower oil. This refinery employs many VSDs for their operation of extracting and refining the oil from the sunflower seeds. The second case study was done in the soap manufacturing industry. In this industry, the harmonic measurements at various speed drives were done with the help of a power quality analyser to determine where a significant amount of harmonic currents or voltages occur. Finally, the third case study was done in a book-producing company. Book production involves many variable-speed drives used to process large amounts of books. Due to the demand for books, the requirement for this company is a constant operation for the production of a book which requires good power quality to ensure sufficient production capacity. Finally, in these case studies, the benefits gained by these various industries by mitigating these harmonics were also carried out.

5.2 Installation of Network Analyser

An electrical network analyser as shown in Figure 5.1, is normally installed at the industry main incomer panel to record the power quality parameters. When the analyser is connected, data used for the analysis is recorded for approximately 1 week. Split core CT''s are connected around the refinery incoming supply following the flow of the current of the main panel recording data for all three phases. The crocodile clamps, which are colour-coded to red, white, blue, and neutral phases, are connected to each phase. Once the controller is started, it checks each phase, which is visible by LED indication. Once all phases are detected in the correct sequence, the LED stabilises and the recordings begin. The information can be viewed on the controller or transferred to a PC via the memory card. This card is inserted into a PC that contains specialized software to read the graphs obtained during the recording. Quantities such as total harmonic distortion (THD), harmonic order magnitude, power factor, as well as voltage and current distortion can be measured and analysed.

Figure 5.1: The network analyser [82]

5.3 Case Study 1: Harmonics in Oil Refinery

To produce sunflower oil, the sunflower seed is properly prepared for oil removal. The seed is first cleaned to remove any impurities before it is mechanically pressed to remove the oils. Refineries can crush more than 400 tons of sunflower seeds per day. The oil is processed further to produce an edible product. Aside from oil other bye products are produced for consumer use such as soaps and candles. In the oil manufacturing industry, several coupled motors work together simultaneously to produce high-quality products at a high speed. This means that each

motor operates together with precise speed and efficiency. In this plant, there are four induction motors connected to individual VSD's which control the motor's torque and frequency. The impact of harmonic distortion on the electric drives may cause motor failures which can lead to long periods of downtime. This can have huge consequences, resulting in production and monetary losses by the industry.

In modern applications, there is a need to adjust the speed of motors, according to the load demand or machine efficiency. This has made the use of motors to be coupled to the VSD's. There is high reliability, efficiency, and cost-saving in using induction motors in automated industrial applications. With these advantages that the VSD offers, the main disadvantage is the harmonics that it produces. Harmonics are any frequency in the system except for the fundamental frequency and this results in a distortion of the sinusoidal waveform. The resulting impact of harmonic distortion can include failure in motors, overheating of transformers, fuse blowing, and failure in capacitors [83].

The operation of non-linear loads can generate harmonic currents that are harmful to the electrical network. Voltage distortion results from the interaction of these currents with the system impedance versus frequency characteristics [84]. Harmonic voltages increase magnetic core losses in motors and transformers while harmonic current increases losses in motor windings [85]. Variable speed drives have non-linear loads therefore, the harmonics injected at the point of common coupling (PCC) must be considered. Industries are governed by IEEE 519 standards, which limit harmonic currents and harmonic voltages at the metering point. The limits specified are intended to protect the utility and preserve its ability to provide undistorted power to other customers [86].

Typically, 6 pulse rectifiers generate harmonics of the 5^{th}, 7^{th} and 11^{th} order. The harmonic orders found in networks are generally odd-numbered. Higher-order harmonics are generally lower in magnitude. The switching activities on the front end of a standard VSD cause harmonics due to its abrupt pulsations [87]. Once the level and order of the harmonic are identified an effective passive filter can be installed to eliminate the harmful harmonics. The filter is made up of inductance and capacitor combinations. There are various types of passive filters. The most common are single-tuned, double-tuned, high pass, and C-Type filters. The filter is chosen to attenuate a specific range of harmonic frequencies. The harmonic filter reduces harmonic distortion, therefore, improving the efficiency of the electrical system.

5.4 Details of Network Layout

To determine the harmonic levels in the industry, harmonic analysis of the system was conducted and the magnitude and harmonic content were observed. The electrical drawing shown in Figure 5.2 depicts the general layout of the electrical equipment and their ratings for the oil refinery.

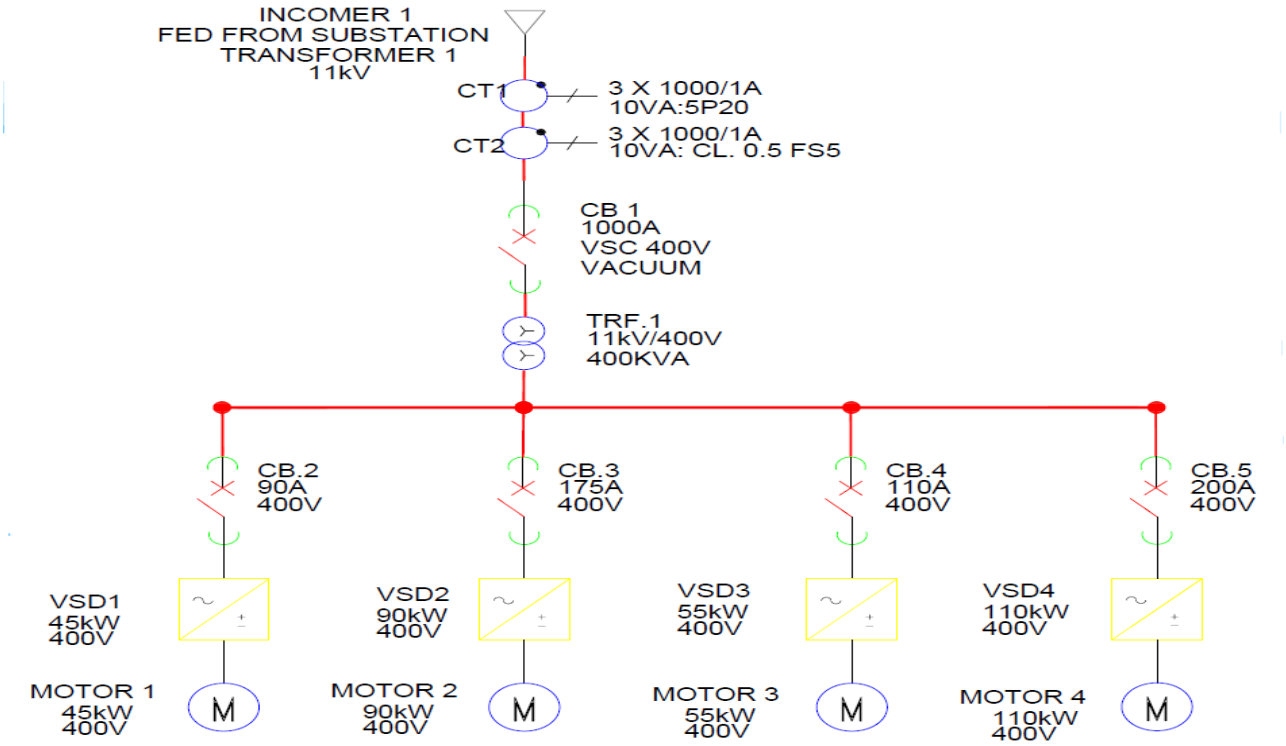

Figure 5.2: Network layout for the oil refinery

This system consists of an 11 kV supply from a mini substation which feeds the total load of the plant. The measuring CTs are connected to the main supply with a ratio of 1000/1. The function of the current transformer is to measure the current of the system by connecting it to a standard ammeter. A 1000 A, 11 kV vacuum circuit breaker is connected before the main transformer to prevent short circuits and overloading if a fault does occur. This prevents damage to the equipment in the system that can be caused by harmful short circuit currents. Transformer 1, steps down the incoming voltage from 11 kV to an operating voltage of 400 V. This modern plant uses a 400 V line to provide voltage to circuit breakers 2, 3, 4, and 5, which are connected to VSD1, VSD2, VSD3, and VSD4 respectively. These VSD's are six pulse drives that are commonly used in industry due to their robustness. The circuit breakers are rated according to the power of the VSD's and is meant to act as a protection device for the sensitive VSD. The breaker will trip if there is an overcurrent thus protecting the VSD from short circuit or fault currents. The ratings of each VSD in the system are based upon the kilowatt and full

load current of the respective motors. The drive controls the motor speed according to the load demand of the system. This allows the motor to run at the most efficient speed according to the load and the production process. Table 5.1 shows the ratings of each of the components in Figure 5.2.

Table 5.1: Component ratings

Components	Ratings
Incomer supply	11 kV
CT 1	1000/1
CT 2	1000/1
CB 1	1000 A
TRF 1	11 kV/400 V
CB2	90 A
VSD 1	45 kW
Motor 1	45 kW
CB 3	175 A
VSD 2	90 kW
Motor 2	90 kW
CB 4	110 A
VSD 3	55 kW
Motor 3	55 kW
CB 5	200 A
VSD 4	110 kW
Motor 4	110 kW
VCB 1	150 A
VCB 2	300 A
CT 3	150/1
CT 4	300/1

5.5 Network Analyser Results for Case Study 1

The network analyser as shown in Figure 5.1 was used to conduct a comprehensive power quality analysis for the Oil refinery which result in various graphs being obtained. The graphs

obtained from the analyser were for the voltage, the current, the power, the power factor, the THDV, and the THDI, which are discussed as follows.

Voltage: The voltage of the system was measured between 414.37 V and 388.59 V as shown in Figure 5.3. As observed from this graph, the voltage was steady throughout the day and reaches its peak in the morning during the start of production for the refinery. As shown, low voltage levels were observed on a Saturday and Sunday due decrease in production.

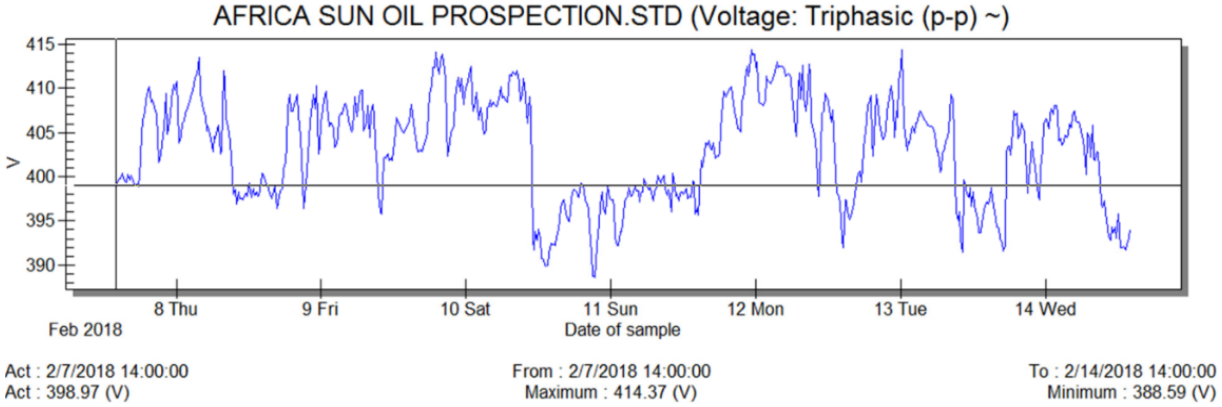

Figure 5.3: Voltage graph

Current: The current of the system was measured between the maximum value of 552.40 A and a minimum value of 148.04 A. Figure 5.4 presents the current levels for seven days. The three phases are balanced with a phase angle of 120° between each phase. The current peaks were recorded on Monday during the start of production and the dips were recorded on Tuesday, possibly due to daily maintenance on the plant.

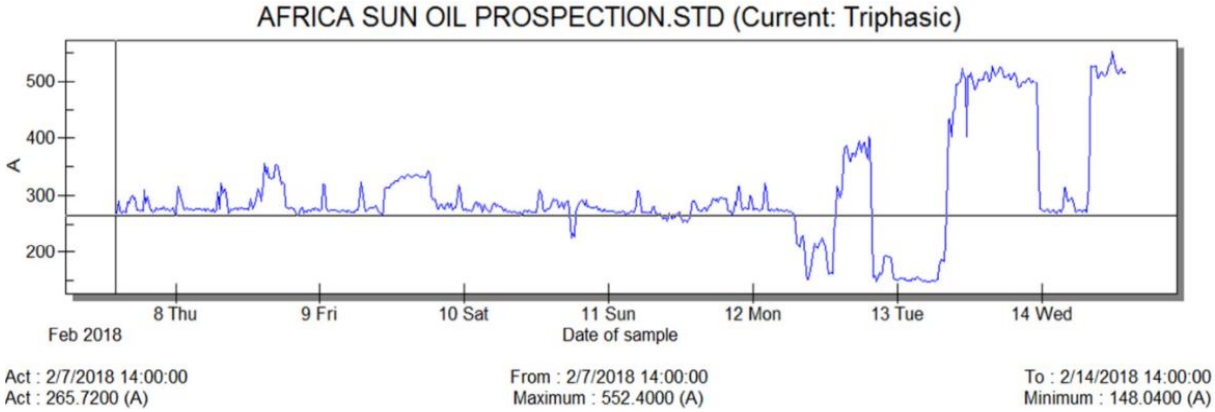

Figure 5.4: Current graph

Power: The power for the system was measured between a maximum value of 300.08 kW and a minimum value of 87.48 kW. The power graph as shown in Figure 5.5 corresponds to the fusion of the voltage and current graphs. The actual power consumed by the system was 141.92 kW. Most powers were consumed during the start of production as expected and remain

steady throughout the rest of the week. This is good for energy conservation as the power consumption remains constant at under 200 kW for the better part of the week.

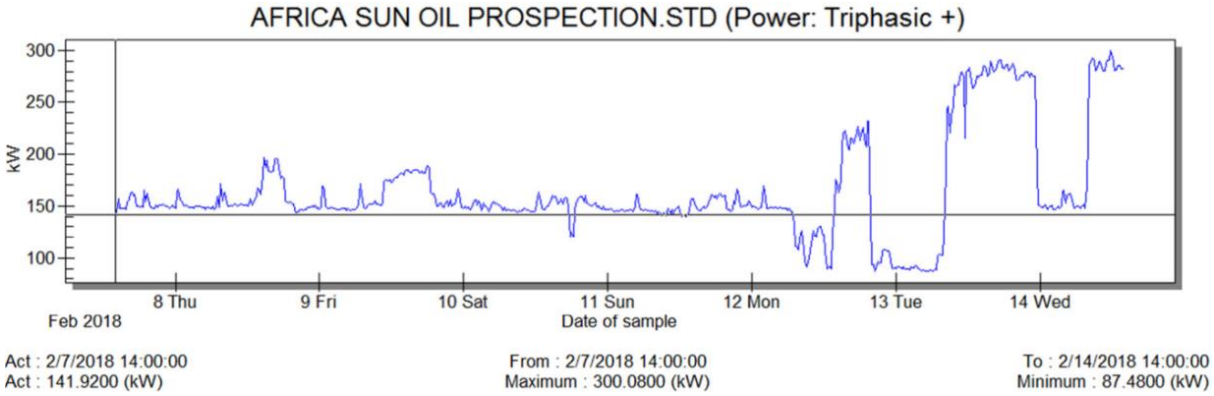

Figure 5.5: Power graph

Power Factor: The power factor of the system was measured between the worst value of 0.715 and the best value of 0.859 as shown in Figure 5.6. The power factor is relatively consistent throughout the week, however, does not reach the desired power factor of at least 0.9. During the start of production of the plant, there is a higher magnetizing current, therefore, the power factor is low. The inductive loads such as motors or transformers can cause the current to lag the voltage, thereby dropping the power factor.

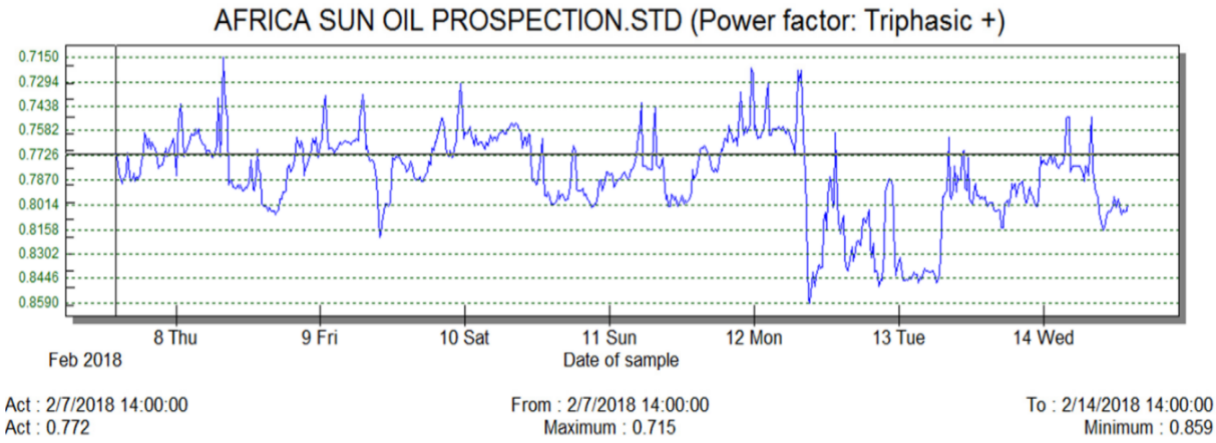

Figure 5.6: The power factor graph

THDV: The THDV (total harmonic voltage distortion), shown in Figure 5.7 runs at an average value of 0.7% but reaches a maximum value of 1.8%. Voltage distortion is measured at the PCC, between the refinery and utility. The highest levels are experienced on a Monday during the start of production. Voltage distortion in an electrical system may cause transformer heating, voltage flicker and proves troublesome to the communication systems. The use of harmonic filters can help decrease voltage distortion.

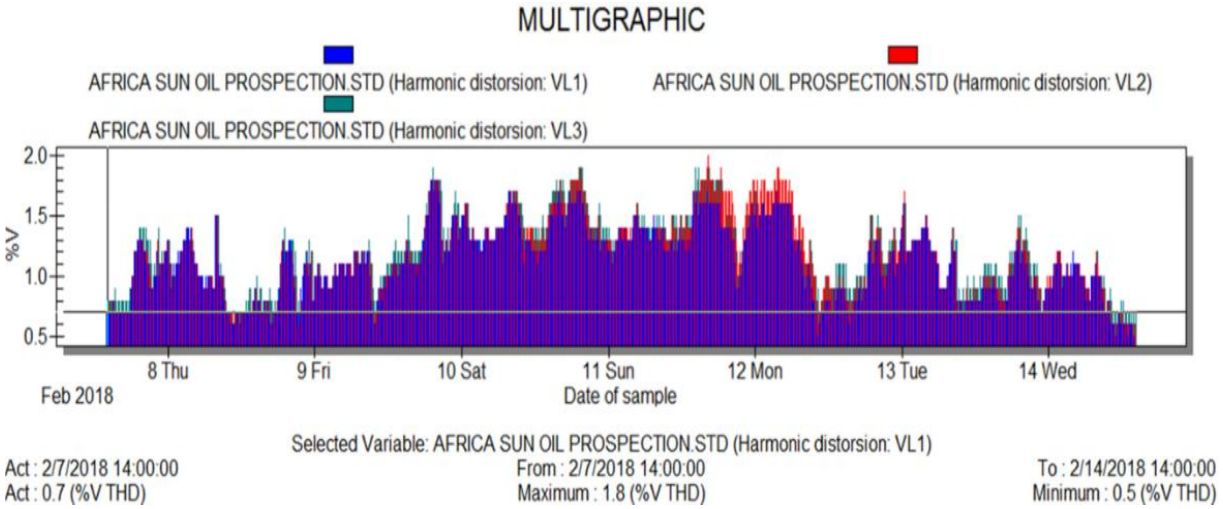

Figure 5.7: The voltage THD graph

THDI: The THDI (total harmonic current distortion), shown in Figure 5.8 runs at an average value of 1.7 % but reaches a maximum value of 4.9%. Current distortion is measured at the point of common coupling (PCC). This prevents the harmful current distortion from entering the utility supply. The lowest current distortion is found over the weekend when the plant is not running at full capacity. Consumers may be charged for high current distortion levels and are encouraged to keep it within IEE 519-1992 standards.

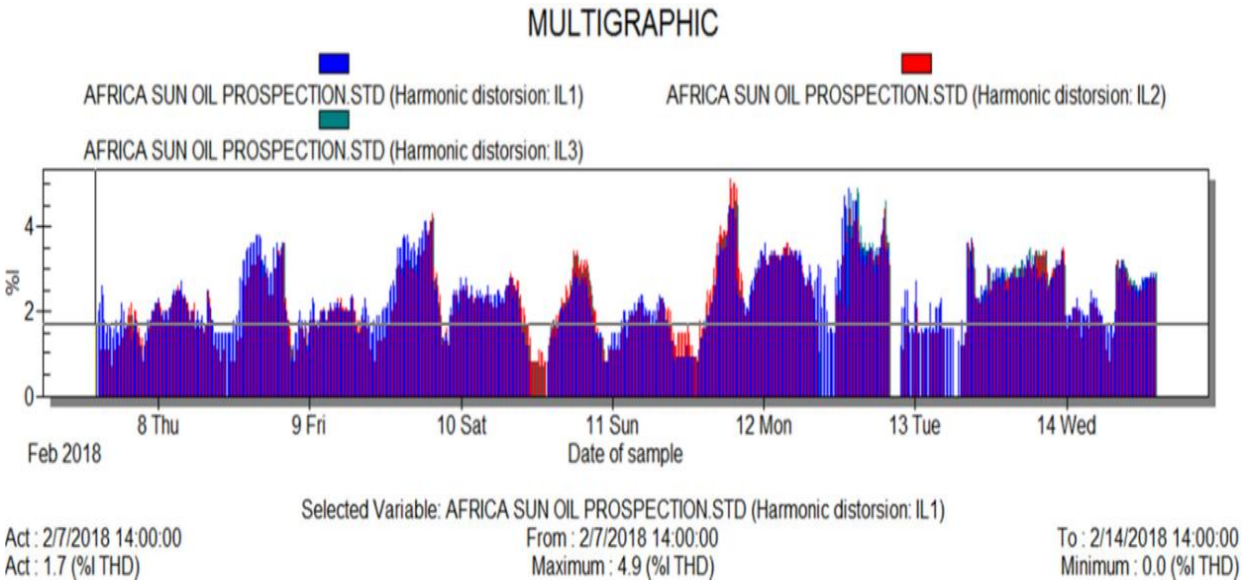

Figure 5.8: Current THDI graph

5.6 System Modelling in ATP: Case Study 1

The ATP/EMTP software was used to model the electrical network of the oil refinery and the network for this refinery is shown in Figure 5.9. The supply voltage for the system is 11 kV which is stepped down by the main transformer to an operational voltage of 400 V. The

transformer is modelled by using the BCTRAN model available on the ATP. The transformer is connected to the main bus through a 7 m long cable. The cables were modelled using the *PI* model. To investigate the harmonics produced during the operation of the variable speed drive, each drive was modelled on ATP with their switching frequencies to represent the rate at which the DC bus voltage is switched on and off during the pulse width modulation process. Each drive is connected to a squirrel cage motor of individual power ratings. The drives are connected through 3 m long cables. The drive controls the output torque and speed to the motor which is dependent on the load demand on the system.

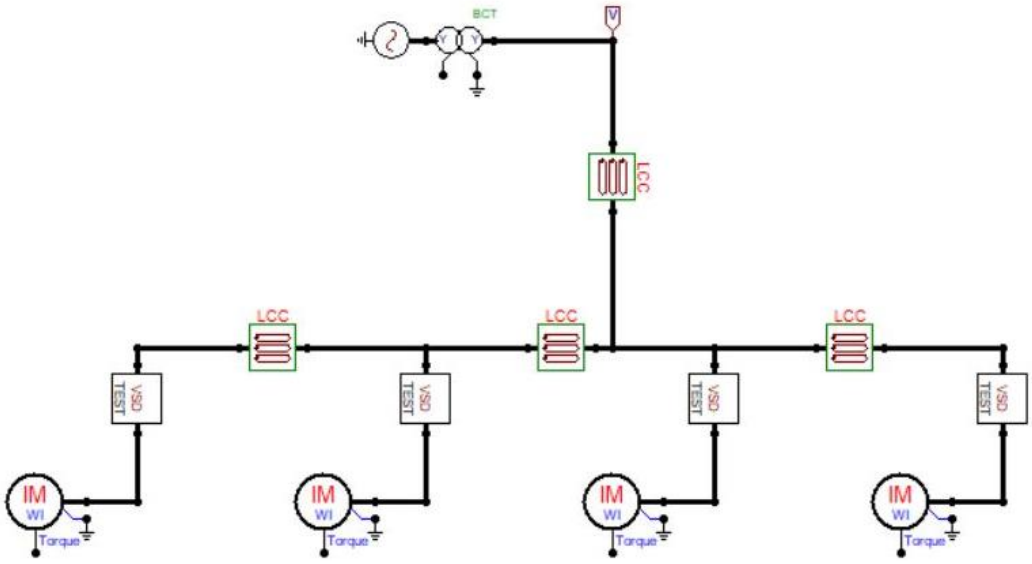

Figure 5.9: ATP simulation model

5.6.1 Modelling of AC Voltage Source

The 3-phase voltage source was modelled using ATP software. The amplitude was 7777 V, which is the peak value for the 3-phases measured in a root mean square voltage ($V_{r.m.s.}$). The $V_{r.m.s.}$ of a sinusoidal waveform is determined by multiplying the peak voltage value by 0.707. The source is grounded to provide a common reference point in the electrical system. The frequency is standard at 50 Hz, which is synchronised with the national grid in South Africa. The starting time (Start A), is -1 seconds to include the steady-state. The stop time (Stop A) is 100 seconds, which cuts off the voltage to the simulated network. Table 5.2 shows the details of the AC voltage source.

Table 5.2: Source parameters

Parameter	Value
Amplitude (kV)	11
Frequency (Hz)	50
Start A (sec)	-1
Stop A (sec)	100
Number of phases	3. Phase

5.6.2 Modelling of Transformer

The transformer number of phases, the number of windings, and the test frequency are specified. The BCTRAN model can be used for single or three-phase transformers with any number of windings. In the part related to the structure of the transformer, the number of phases, number of windings, and test frequency need to be specified. Under the rating tab, the line-to-line voltage levels, the power, the connection, and the phase shift for each winding must be added [88]. The transformer connections are star/star and its power rating is 0.5 MVA. Table 5.3 shows the data of the main transformer as it is modelled on ATP.

Table 5.3: Transformer parameters

Parameter	Value
Vector group	Dyn11
Rated power	0.5 MVA
Open-circuit voltage (%)	100
Open-circuit current (%)	0.55
Open-circuit losses (kW)	1.6
Short-circuit impedance HV-LV (%)	3.2
Short-circuit impedance losses (kW)	1.56

5.6.3 Modelling of Variable Speed Drives

The variable speed drive was modelled to measure the harmonics it produces when powering a motor in an industrial setting. The frequency (Hz), Am ratio, switching frequency, and capacitance of the dc bus is required to model the drive on ATP. The switching frequency refers to the DC bus voltage being switched on and off to produce a smoother sine wave. The DC-link capacitor is meant to filter out ripple voltage and current and act as an energy storage

device. This component maintains the reliability and long life of the drive and the value of the capacitor can be evaluated using equation (5.1).

$$C = \frac{(2P_0 th)}{n(V_s^2 - V_p^2)} \tag{5.1}$$

Where P_0 is the power rating of the drive-in watts, th is the holding time, usually 50ms, n is the drive efficiency, V_s is the secondary voltage and V_p is the primary voltage. Table 5.4 describes the parameters for the variable speed drive.

Table 5.4: VSD parameters

Parameters	VSD 1	VSD 2	VSD 3	VSD 4
Frequency (Hz)	50	50	50	50
Am ratio	0	0	0	0
Switching Freq (Hz)	150	250	250	250
Capacitor (µfµf)	319400	245800	663800	770700

The VSD block diagram is shown in Figure 5.10 which consists of a rectifier, DC link, and the inverter. The value of the DC link capacitor is 319400 µf and was calculated using equation (5.1). The process of rectification results in the AC power being converted to DC power. This DC power is stored in the DC-link is converted by the inverter back to AC at the necessary frequency and voltage, making it suitable for the operation of the motor.

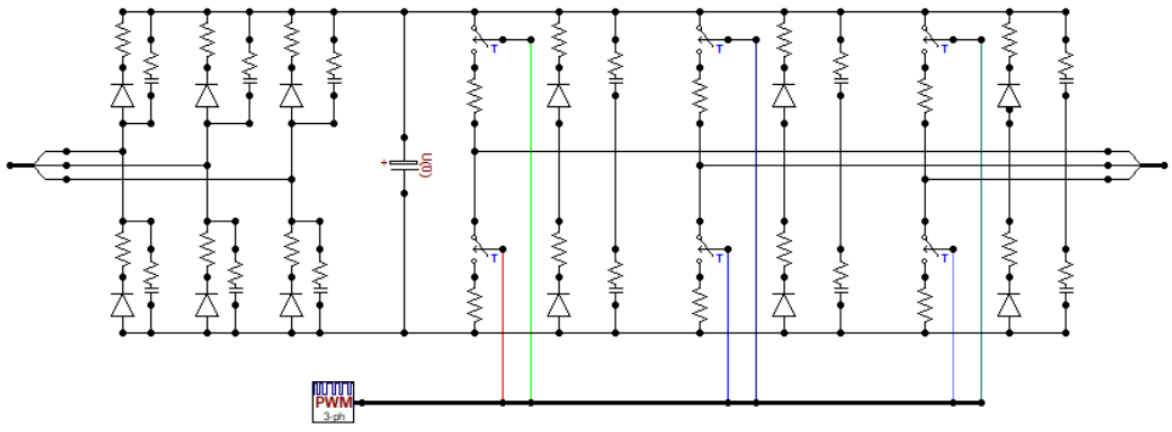

Figure 5.10: VSD internal schematic diagram

5.6.4 Modelling of Motors

The motor was modelled to match most datasheet performance values. The motor drives various loads in the oil refinery including mixers, conveyor belts, packaging machinery, etc.

The motor was modelled, using the single cage rotor model on the ATP and was set to start at 0.02 s at the rated speed of 1800 rpm. The full load torque is the rated torque that was taken from the nameplate of the induction motor. This torque indicates when the motor is run under normal operating conditions. The maximum torque of the motor occurs during the start of production and is the maximum torque that the motor can develop during its operation. The starting current of a motor is usually 6 to 7 times higher than the rated motor current in p.u. The starting torque is the maximum torque that the motor requires during start-up and is always higher than its static torque requirement. The three-phase squirrel-cage induction motor is commonly used in industry due to its simple operation and reliability. As indicated earlier, there are four motors in the electrical network with individual power ratings. Each motor is connected to a suitable drive, which controls the speed, torque, and direction of the motor. Table 5.5 describes the parameters for the four motors as modelled on ATP.

Table 5.5: The description of parameters for motors

Parameters	Motor 1	Motor 2	Motor 3	Motor 4
Frequency (Hz)	50	50	50	50
Voltage L-L (kVr.m.s.)	0.283	0.283	0.283	0.283
Power (HP)	61.183	47.586	122.366	149.558
Speed (rpm)	1800	1800	1800	1800
Power Factor	0.8	0.8	0.8	0.8
Efficiency (pu)	0.75	0.75	0.75	0.75
Slip (%)	0.72	0.72	0.72	0.72
Start current (pu)	7	7	7	7
Start torque (pu)	0.5	0.5	0.5	0.5
Load torque (pu)	1	1	1	1
Max torque (pu)	1.5	1.5	1.5	1.5

5.7 Simulation Results

For case study 1, based on the modelling of the network as presented in Figure 5.2, simulation was carried out using the ATP software. The simulation results obtained from the ATP software is presented as follows: voltage and harmonics graphs

- **Voltage Graph**

Figure 5.11 shows the voltage waveform starting at 0 s and ending at 0.2 s. From this graph, the 3-phase, 50 Hz voltage sine wave reaches a maximum value of 400 V. The sine wave is smooth and has a small amount of harmonic distortion as seen at the peak of the wave. This is caused by the harmonics produced during the operation of the VSD's. The voltage provided by the voltage source becomes slightly distorted however this is negligible unless higher-order harmonics are considered.

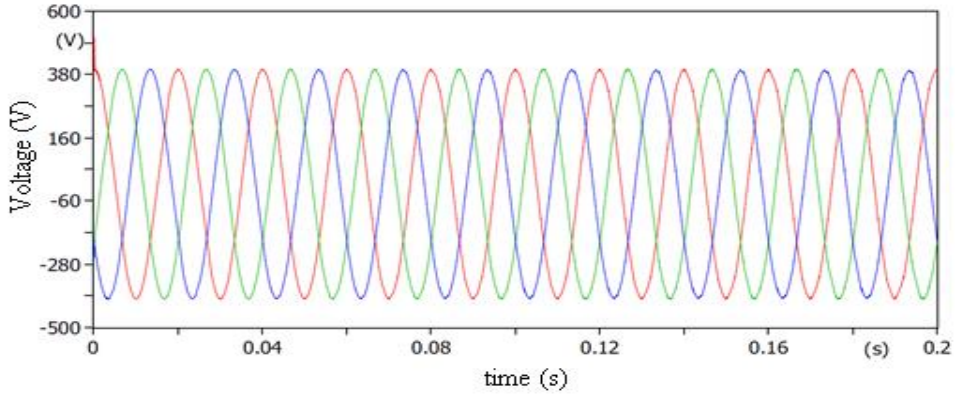

Figure 5.11: The voltage against time graph

- **Harmonics Graph**

The dominant harmonics as can be seen in Figure 5.12 are the 3rd and 5th order harmonics. The 3rd harmonic reaches a maximum value of 16.725 V whilst the 5th harmonic reaches a maximum value of 11.081 V. The total harmonic distortion of the system was found to be 5.32 %. According to IEEE 519-1992, harmonic voltage distortion on a 400 V power system is limited to less than 5 %, and individual harmonic orders are limited to 3 % [31]. The negative effects of having higher lower order harmonics can lead to an increase in core losses for motors and transformers, nuisance tripping of circuit breakers, and blowing of fuses. Due to this, the use of harmonic filters to mitigate harmful harmonics has become necessary for this industry.

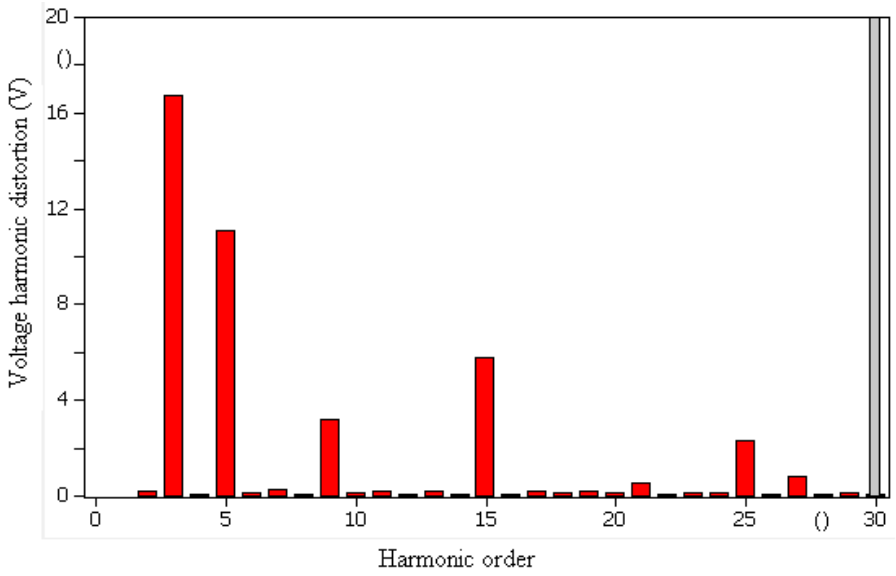

Figure 5.12: The voltage harmonics harmonic against time graph

5.8 Mitigation of Harmonics

The non-linear characteristics of industrial loads such as VSD's used in conjunction with pumps, fans, and compressors have made harmonic distortion a common occurrence in power systems. The presence of harmonics in a system reduces the life expectancy of equipment due to overheating and stress on electrical cables. Because of the requirements for power quality as stipulated by IEEE-519 standards, the level of harmonic distortion must be limited at the PCC. To reduce harmonics in the system, harmonic filters are installed. The filters help to mitigate harmonic distortion and increase the system's power factor. The filters are comprised of linear components such as inductors, resistors, and capacitors to attenuate the flow of harmonics through them. There are several types of harmonic filters available, each with its special characteristics of attenuation.

5.8.1 Harmonic Filters

As discussed in Chapter two, four types of harmonic filters are commonly used for harmonic attenuation, namely Single-tuned, double-tuned, C-Type, and high pass filters. The filters are connected in parallel with the power system to provide a low impedance path for a given frequency. Therefore, the harmonic distortion is reduced to the required levels. The single and double-tuned filters are usually used to target specific harmonic orders, while the C-Type and high pass filters are used to filter a wider range of frequencies. Choosing the correct harmonic filter is determined by the level and order of harmonics present in the system. Each of these filters was applied to Case Study 1 as discussed as follows:

5.8.1.1 Single-tuned Harmonic Filter

The single-tuned filter is the simplest and most common type of filer used in industry to suppress lower-order harmonics. It has low maintenance requirements because of fewer components however the major disadvantage of this filter is that it can only mitigate one type of harmonic in the system. Single-tuned filters (3^{rd} and 5^{th}) are modelled as shown in Table 5.6. The values for the resistor, inductor, and capacitor are determined by equations (2.1), (2.2), and (2.3).

Table 5.6: Single-tuned filter parameters

Harmonic	Q_f (KVAr)	R_f (Ω)	C_f (µf)	L_f (mH)
3^{rd}	275	0.0476	4863.067	0.2315
5^{th}	275	0.0147	5252.11	0.0772

5.8.1.2 Simulation of the Single-tuned Harmonic Filter

Modelling the operation of the single-tuned filter in the oil refinery network was done using the ATP software. Two single-tuned filters were connected in parallel to mitigate the 3^{rd} and 5^{th} order harmonics as shown in Figure 5.13. The filter was connected to the system via a 2 m long cable. A contactor was used to control the filter, which switches on and off according to the network requirements to improve the power quality of the system. The filters are modelled using the parameters for *R, L,* and *C* documented in Table 5.6 for the 3^{rd} and 5^{th} harmonics. The filter is connected to the main bus to attenuate the harmonics caused by the operation of the VSD's.

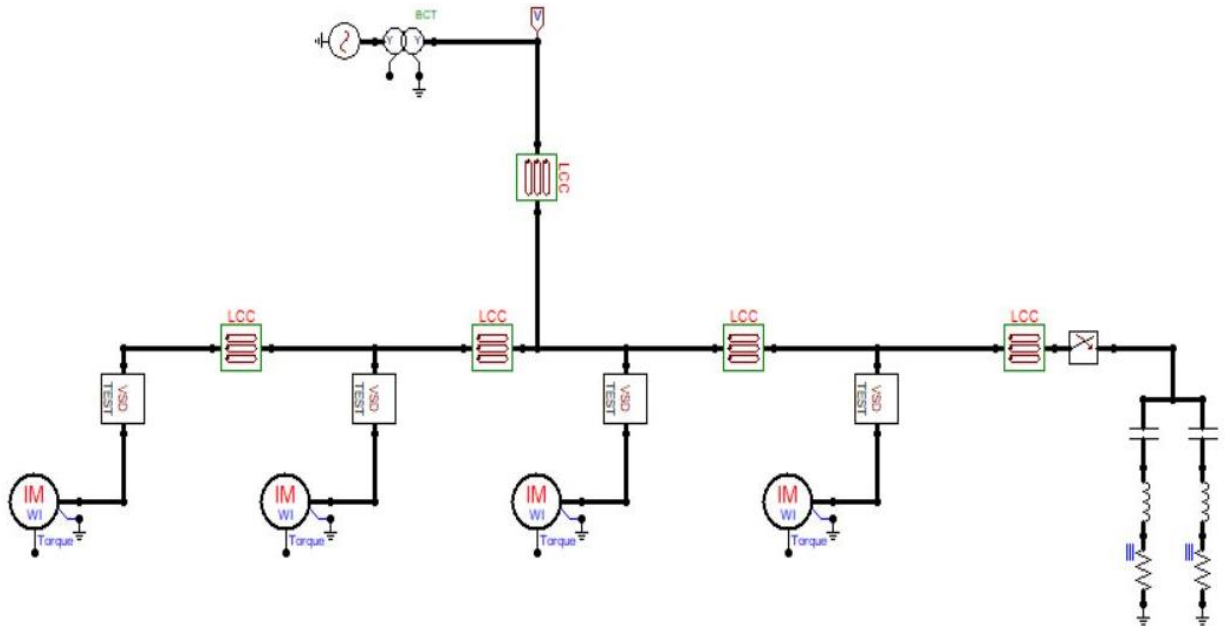

Figure 5.13: Simulation model with single-tuned filter

5.8.1.3 Results from the Single-tuned Filter Simulation

The connection of the single-tuned filter to the network has resulted in a considerable reduction of the 3rd and 5th harmonics as observed in Figure 5.14. The 3rd harmonic has decreased from 16.725 V to 0.13998 V and the 5th harmonic has decreased from 11.081 V to 0.0774 V. There is a 99.16% decrease in the 3rd harmonic and a 99.3 % decrease in the 5th harmonic due to the connection of the two single-tuned filters. The total harmonic distortion is 0.1381% compared to 5.32 % before the connection of the filter. This brings the THD within IEEE 519-1992 harmonic limits. The results show that the connection of the two single-tuned filters connected in parallel is a possible solution to the reduction of the harmonics in the system.

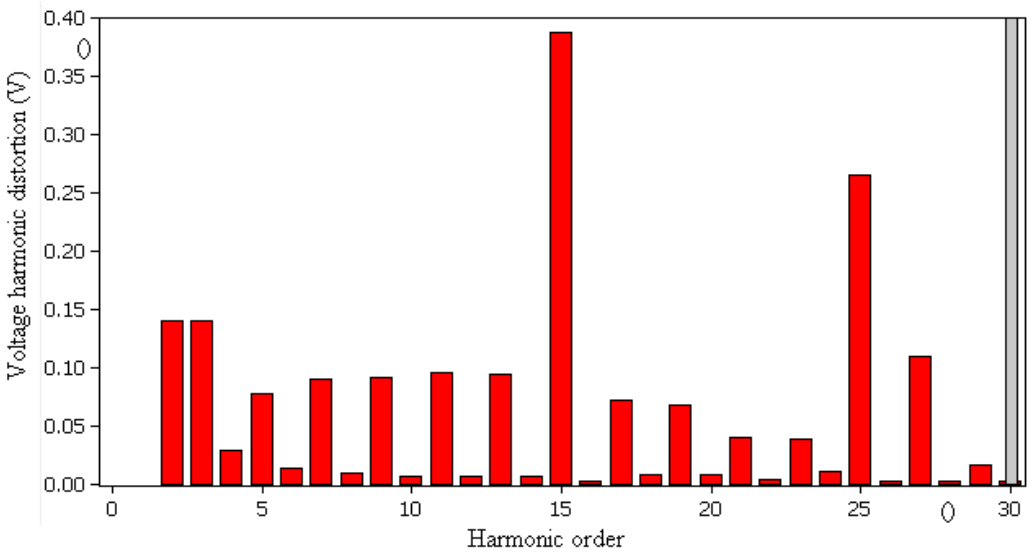

Figure 5.14: Harmonics simulation result for the single-tuned filter

5.8.2.1 Conventional Double-tuned Harmonic Filter

Double-tuned filters can suppress two different harmonic frequencies at the same time. The filter is designed by using the equivalent method where the filter values are calculated by using two single-tuned filters connected in parallel. The impedances of both double-tuned filters and two single-tuned parallel filters are the same. The double-tuned filter is known to have better performance in mitigating low order harmonics compared to two single-tuned filters. The reactive power requirement is also less compared to a single-tuned filter [25]. The values of the double-tuned filter are presented in Table 5.7.

Table 5.7: Lumped parameters for double-tuned filter

Harmonic	Q_f(KVAr)	C_1(μF)	L_1(mH)	C_2(μF)	L_2(mH)
3rd and 5th	275	10115.177	0.05789	47452.56	0.01642

5.8.2.2 Simulation of the Conventional Double-tuned Filter

The double-tuned filter can attenuate two lower-order harmonics by modelling two single-tuned filters connected in parallel. This filter is presented in Figure 5.15, and it has the benefit of being both cost-effective and easy to design with minimal maintenance. The value for L_1, C_1, L_2, and C_2 was obtained from the parameters of two single-tuned filters connected in parallel as given in Table 3.7. The filter is switched on via a circuit breaker and can suppress both the 3rd and 5th harmonics simultaneously.

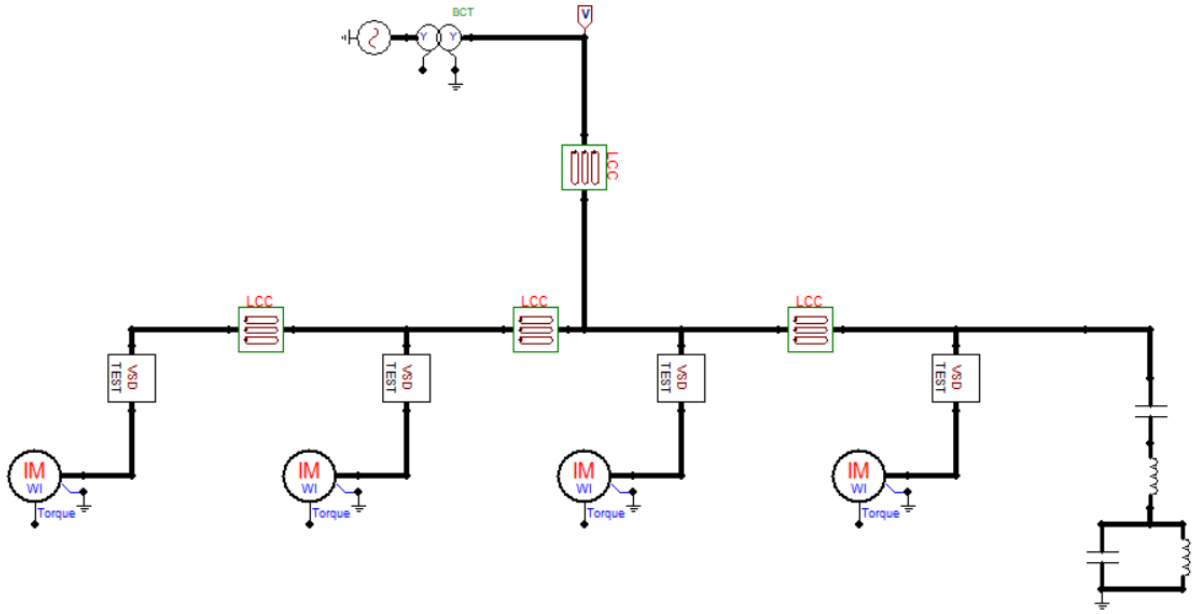

Figure 5.15: Simulation model with double-tuned filter

5.8.2.3 Results from the Double-tuned Filter Simulation

The harmonics graph as shown in Figure 5.16 displays a significant decrease for both the 3rd and 5th harmonics. The 3rd harmonic decreased from 16.725 V to 0.096 V and the 5th harmonic decreased from 11.081 V to 0.019 V. There was a 99.4 % decrease for the 3rd harmonic and a 99.8 % decrease for the 5th harmonic due to the connection of the double-tuned filter. The THD has dropped to 0.136 and is within IEEE 519-1992 harmonic limits of a maximum 5 % distortion for a 400 V system. The results show that a double-tuned harmonic filter can successfully reduce two lower-order harmonics simultaneously in the system.

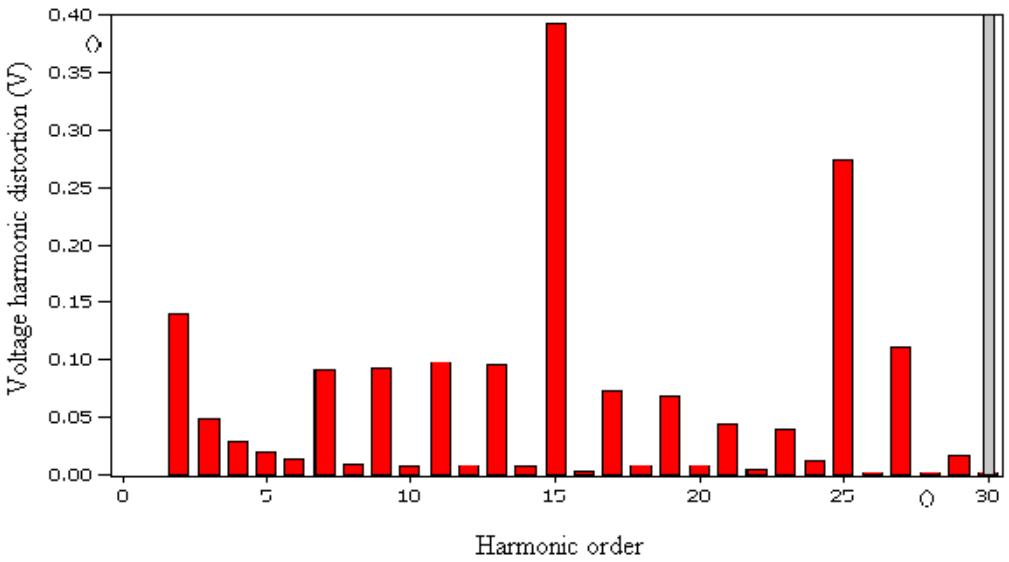

Figure 5.16: Harmonics simulation result for the double-tuned filter

5.8.3.1 C-Type Harmonic Filter

The filter is configured using *R*, *L*, C_1 (main capacitor), and C_2 (auxiliary capacitor). The C-Type filter is used to improve the performance of the system, reduce harmonic distortion, and increase power factor in an industrial setting [89]. Parameters used for the C-Type filter are given in Table 5.8.

Table 5.8: Lumped parameters for C-Type filter

Harmonic	Q_f(KVAr)	C_1(μF)	C_2(μF)	L(mH)	R(Ω)
3rd	275	5409	0.04376	0.2315	0.01497
5th	275	5409	0.1313	0.7716	0.00287

5.8.3.2 Simulation of C-Type Harmonic Filter

The two C-Type filters are connected in parallel to attenuate the 3rd and 5th harmonics as shown in Figure 5.17. The filter is connected to the network via a 2 m long cable and is modelled on ATP to investigate the change in the harmonic levels during its operation. The C-Type filter can provide reactive power with the ability to avoid parallel resonance. It allows the filtering of lower-order harmonics with minimal power losses. The filter is energised by closing the circuit breaker.

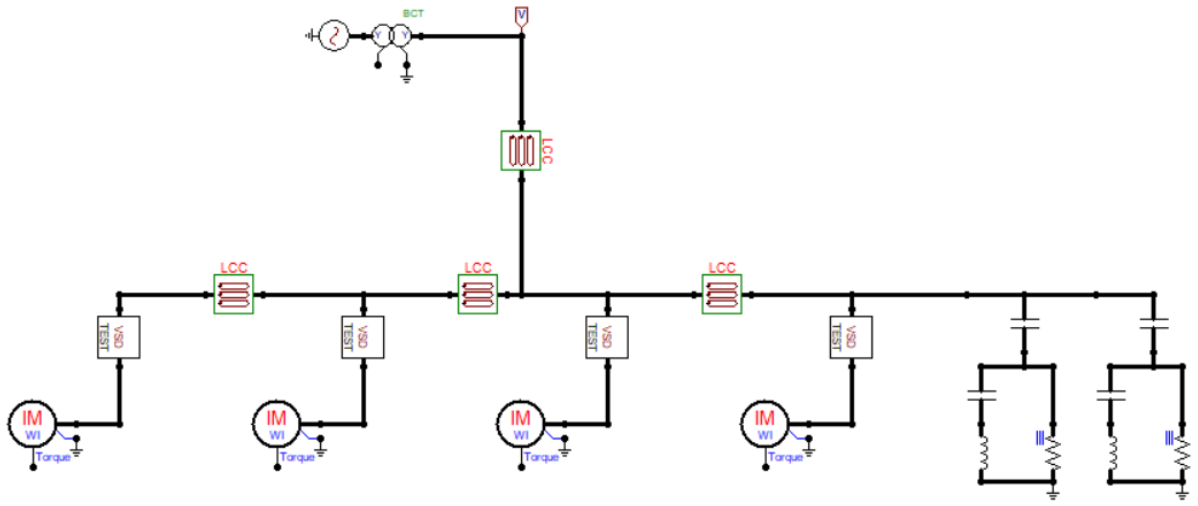

Figure 5.17: Simulation Model with C-Type Filter

5.8.3.3 Results of C-Type Filter Simulation

Based on the results obtained from the harmonics graph as shown in Figure 5.18, the C-Type filter has met the requirements by reducing the 3rd and 5th harmonics. The 3rd harmonic was reduced from 16.725 V to 0.2933 V while the 5th harmonic was reduced from 11.081 V to 0.7299 V. There was a 98.2 % decrease for the 3rd harmonic and a 93.4 % decrease for the 5th harmonic due to the connection of the C-Type filter. The THD is 0.194 % compared to 5.32 % of the original network. This is well within IEEE 519-1992 harmonic standards for a 400 V system. This makes the C-Type filter a suitable option to reduce lower-order harmonics and improve THD in the system.

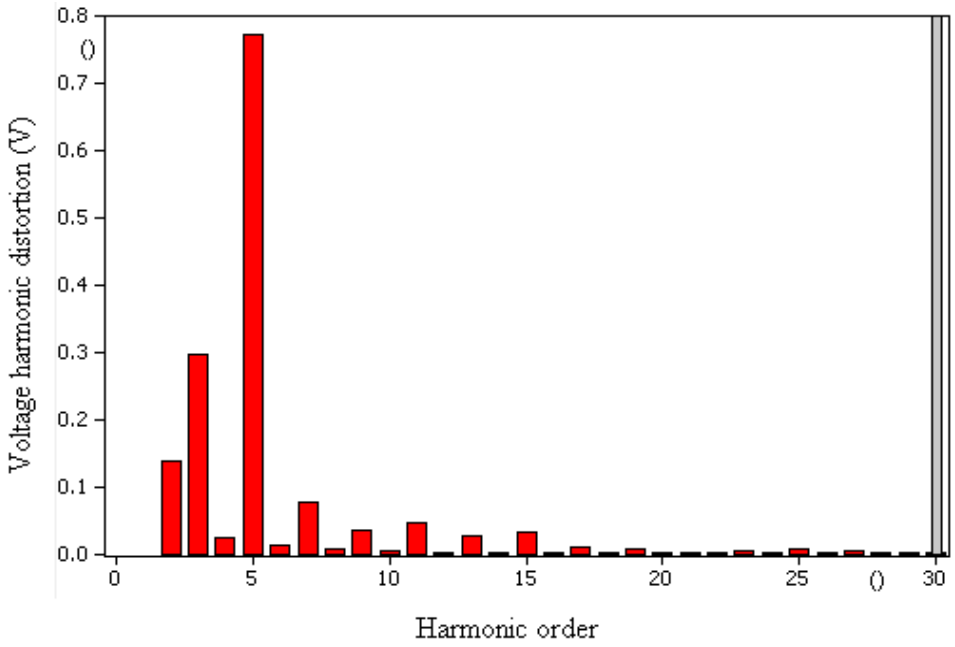

Figure 5.18: Harmonics simulation result for the C-Type filter

5.8.4.1 Second-order High Pass Filter

The damping resistor found in this high pass filter reduces the quality factor, which in turn increases the bandwidth of the filter, making it possible to attenuate a range of harmonic frequencies. Designing the high pass filter for low order harmonics results in the fundamental frequency losses in the damping resistor being very high [1]. Therefore, the filter is used mainly to eliminate high order frequencies. Parameters used for the second-order high pass filter are presented in Table 5.9.

Table 5.9: The lumped parameters for the second-order high pass filter

Harmonic	Q_f (KVAr)	C (µF)	L (mH)	R (Ω)
3rd	275	4863.1	0.2314	0.0476
5th	275	5252	0.0771	0.01469

5.8.4.2 Simulation of Second-order High Pass Filter

The second-order high pass filter was modelled using ATP software to determine how it would suppress the dominant harmonics of the system. The two high pass filters were connected in parallel to attenuate the 3rd and 5th harmonics. Each filter was made up of a reactor and a resistor in parallel with a series capacitor shown in Figure 5.19. This filter attenuates a wide range of frequencies and decreases the energy losses at the fundamental frequency.

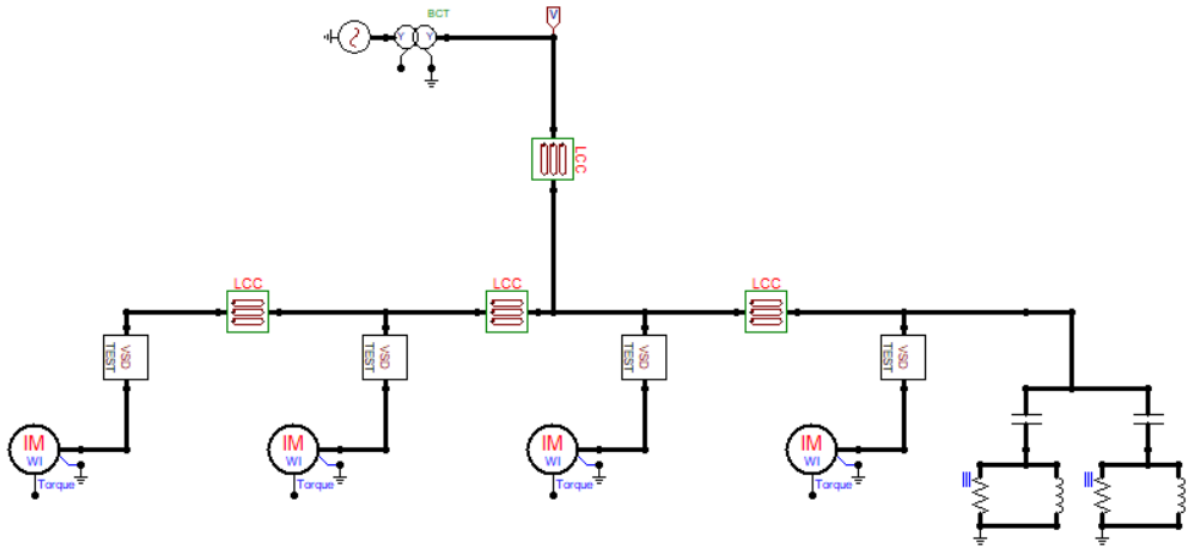

Figure 5.19: Simulation model using second-order high pass filter

5.8.4.3 Results from the Second-order High Pass Filter Simulation

The results from the harmonics graph as presented in Figure 5.20, revealed a measurable decrease in both the 3rd and 5th harmonics. The 3rd harmonic was decreased from 16.725 V to

0.387 V while the 5th harmonic was decreased from 11.081 V to 0.795 V. There is a 97.6 % decrease for the 3rd harmonic and a 92.8% decrease for the 5th harmonic. The resultant THD is 0.223 % within IEEE 519-1992 limits, compared to 5.32 % THD of the original circuit.

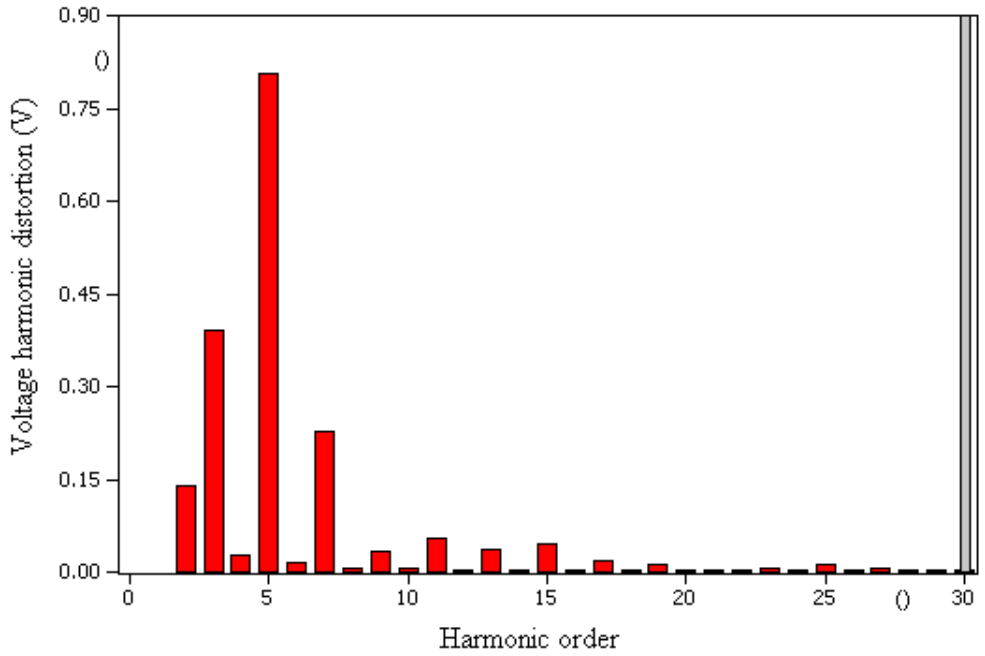

Figure 5.20: Harmonics simulation result for the second-order high pass filter

5.9 Harmonic Filter Analysis and Results for Case Study 1

The use of harmonic filters in the oil refinery is important to mitigate harmonic distortion that may be harmful to system equipment. Simulation of the four different harmonic filters was performed using ATP software to identify the best performing filter to suppress the 3rd and 5th harmonics. From the results presented in Table 5.10, the double-tuned filter proved to be the most effective whilst the single-tuned filter was found promising. The high pass filter provided the lowest improvement in THD levels, making it the worst-performing filter.

This is expected as the double-tuned filter has a higher quality factor compared to the high pass filter, providing maximum attenuation of the two harmonics. The filter also experiences negligible losses with the absence of a damping resistor. The damping resistor in the high pass filter reduces the quality factor, therefore, increasing the bandwidth making it suitable for a wider range of higher-order harmonic frequencies. The filter is also complex making it more expensive to design. Therefore, in this case, the double-tuned filter is best suited to suppress two lower-order harmonics at the same time.

Table 5.10: Results of filter simulations

	Original Network	Single-tuned	Double-tuned	C-Type	High pass
3rd harmonic	16.725	0.13998	0.096	0.2933	0.387
5th harmonic	11.081	0.0774	0.019	0.7299	0.795
THD (%)	5.32	0.1381	0.136	0.1944	0.223

5.9.1 Energization of Harmonic Filters

Energization of the harmonic filters can cause a temporary overvoltage that can stress the insulation of electrical equipment and damage them with frequent occurrence [90]. When the contacts of the circuit breaker are energized, a resulting overvoltage occurs. The main purpose of the simulation was to determine the peaks of temporary overvoltage caused by filter circuits when being operated in the electrical system. To close all three phases simultaneously, the breaker could close at the peak voltage (90°) resulting in the worst scenario that could be experienced [6]. The energization simulation results for all the four filters are presented in Figures 5.21(a) to 5.21(d), conducted using the ATP to determine which filter experiences the highest and lowest overvoltage levels. The filters were energized at 0.04 s which is the maximum voltage of phase A.

Based on the simulation results, the overvoltage experienced was found to be 887 V for the single-tuned filter, 910 V for the double-tuned filter, 732 V for the C-Type filter, and 788 V for the high pass filter. These results were over the voltage tolerance limit in the power system according to SANS 10142.1. The overvoltage observed during energization was highest for the double-tuned filter and the lowest for the C-Type filter. This is due to the absence of a resistor in the design of the double-tuned filter. The resistor provides damping to suppress the magnitude of the overvoltage that occurs during switching. The results of the simulations are tabulated in Table 5.11.

Table 5.11: Overvoltage during energization

Filter	Overvoltage experienced during energization
Single-tuned filter	887 V
Double-tuned filter	910 V
C-Type filter	732 V
High pass filter	788 V

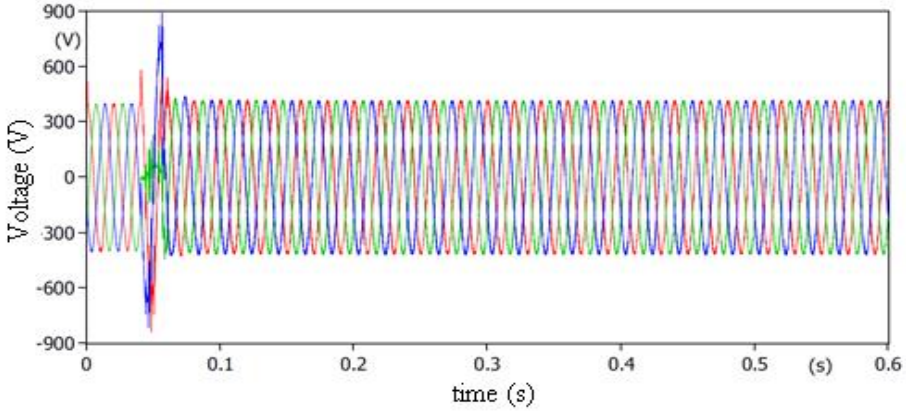

Figure 5.21(a): Energization of single-tuned filter

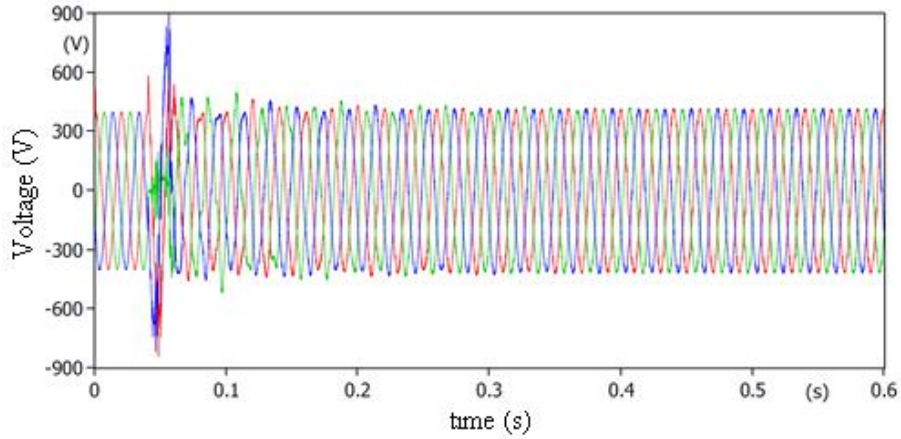

Figure 5.21(b): Energization of double-tuned filter

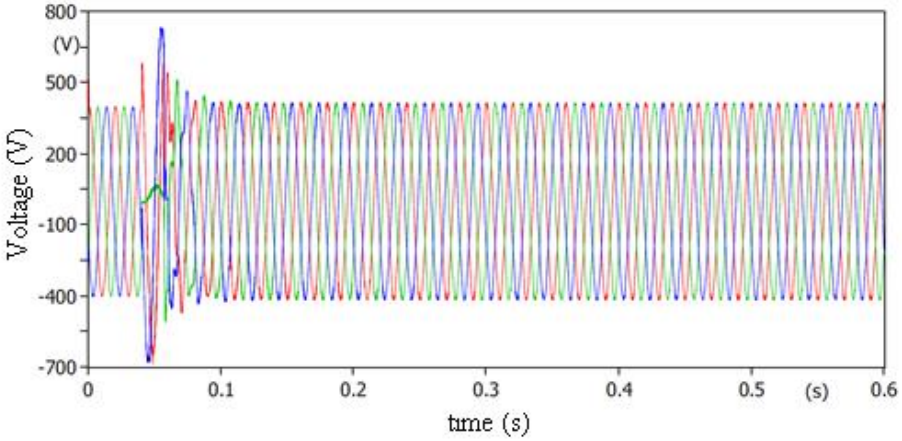

Figure 5.21(c): Energization of C-Type filter

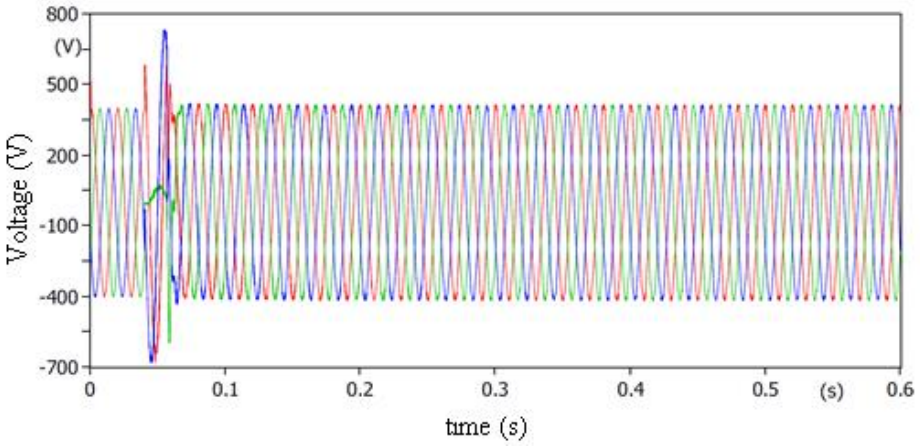

Figure 5.21(d): Energization of high pass filter

5.9.2 De-Energization of Harmonic Filters

Opening of the circuit breaker de-energizes the harmonic filter causing high overvoltage and stress on the electrical system. The circuit breaker contacts do not open simultaneously during operation. There is a finite time before circuit breaker interruption. Before interruption occurs, an arc is formed between the breaker contacts and may persist for several cycles. To observe the switching operations of the harmonic filters, the filters were simulated using ATP software and the results of the simulations are presented in Figures 5.22(a) to 5.22(d). Based on the simulations done, the overvoltage experienced was found to be 875 V for the single-tuned filter, 909 V for the double-tuned filter, 853 V for the C-Type filter, and 876 V for the high pass filter when the circuit breaker was opened at 0.04 s.

From the results obtained it is found that the double-tuned filter experienced the highest overvoltage levels, whilst the C-Type filter experienced the lowest overvoltage levels during the de-energization scenario. As in the case of energization, the de-energization of the double-tuned filter experienced the highest overvoltage levels. This is also due to the absence of a resistor in its configuration which helps to suppress the overvoltage that occurs when the harmonic filter is switched off. Constant switching of the harmonic filter can cause over voltages to occur. Table 5.12, presents the values of the overvoltage experienced during de-energization for the four filters.

Table 5. 12: Overvoltage during de-energization

Filter	Overvoltage experienced during de-energization
Single-tuned filter	875 V
Double-tuned filter	909 V
C-Type filter	853 V
High pass filter	876 V

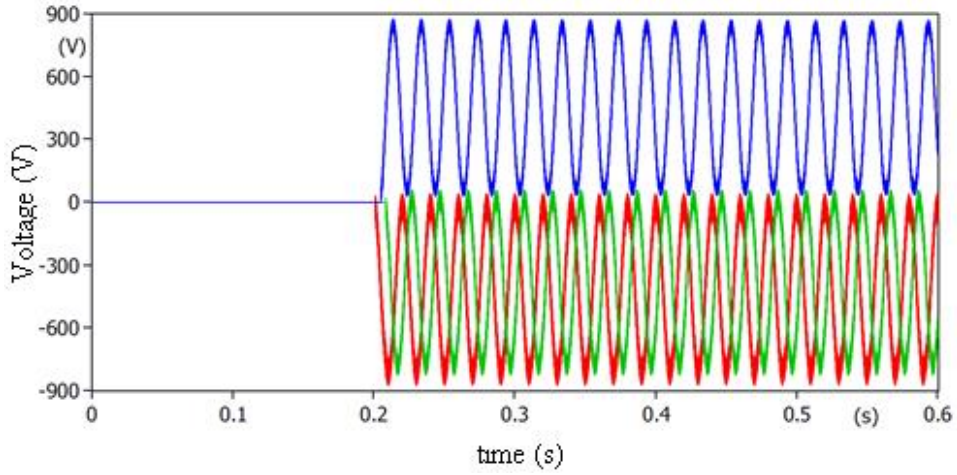

Figure 5.22(a): De-energization of single-tuned filter

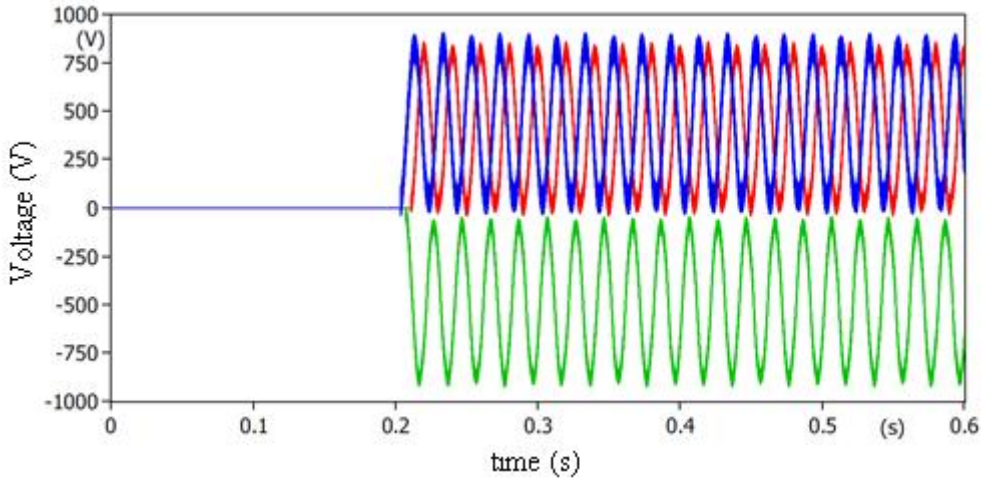

Figure 5.22(b): De-energization of double-tuned filter

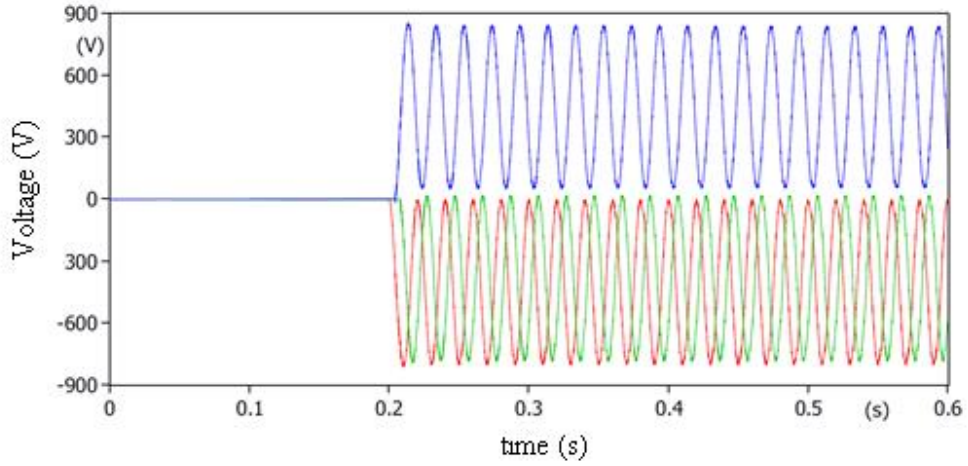

Figure 5.22(c): De-energization of C-Type filter

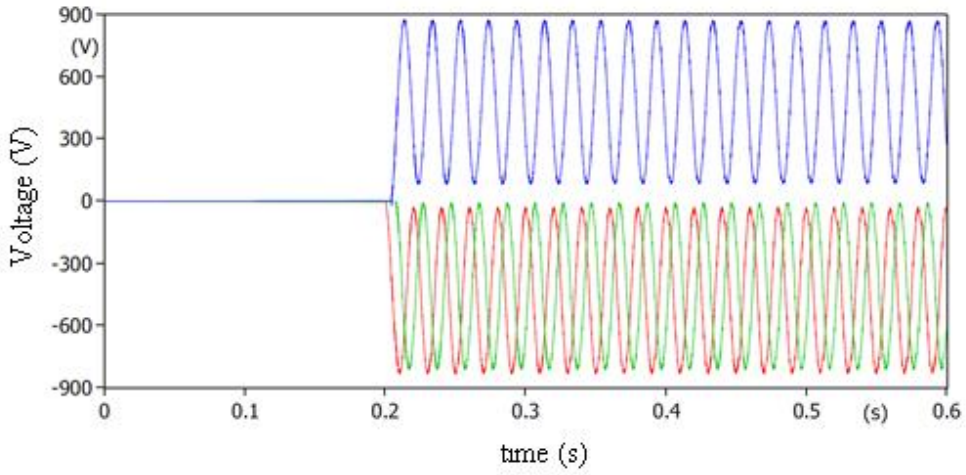

Figure 5.22(d): De-energization of high pass filter

5.10 Mitigation of Overvoltage for Case Study 1

If the withstand level of the system and the harmonic filter is lower than the observed overvoltage, mitigation measures would be needed to combat this. As a result, the electrical equipment and filter could be damaged. Therefore, the use of pre-insertion resistors, surge arresters, and controlled switching is considered to observe the effects it may have on mitigating the overvoltage.

5.10.1 Pre-Insertion Resistor

A bypass resistor is inserted across the circuit breaker contacts which close before the filter is energized. The pre-insertion resistor needed for this purpose may be calculated by using equation (5.2):

$$R_{pr} = \frac{1}{2}\sqrt{\frac{L_r}{C_r}} \tag{5.2}$$

The four filters are simulated on ATP and the resultant waveforms are presented in Figures 5.23(a) to 5.23(d). The double-tuned filter experiences the highest overvoltage levels during energization. This is due to the absence of a damping resistor in the configuration of the filter. The resistor is meant to help dampen the magnitude and duration of the overvoltage to within system limits. To help achieve this effect, a pre-insertion resistor is placed in the circuit before energization. The installation of the resistor increases the overall losses in the circuit which decreases the value of the peak voltage. Therefore the double-tuned filter has the highest reduction in overvoltage and the C-Type filter has the lowest reduction when a pre-insertion resistor is used. The results of the simulation upon the implementation of the pre-insertion resistor are tabulated in Table 5.13.

Table 5.13: Mitigation using a pre-insertion resistor

Filter	Resistor value	Overvoltage Before	Overvoltage After
Single-tuned filter	0.087 Ω	887 V	465 V
Double-tuned filter	0.018 Ω	910 V	446 V
C-Type filter	0.034 Ω	732 V	461 V
High pass filter	0.087 Ω	788 V	449 V

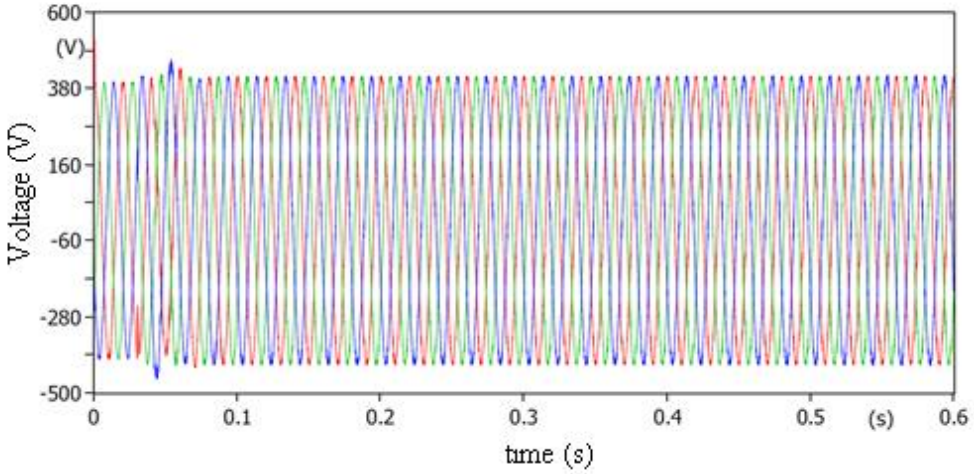

Figure 5.23(a): Using pre-insertion resistor for single-tuned filter

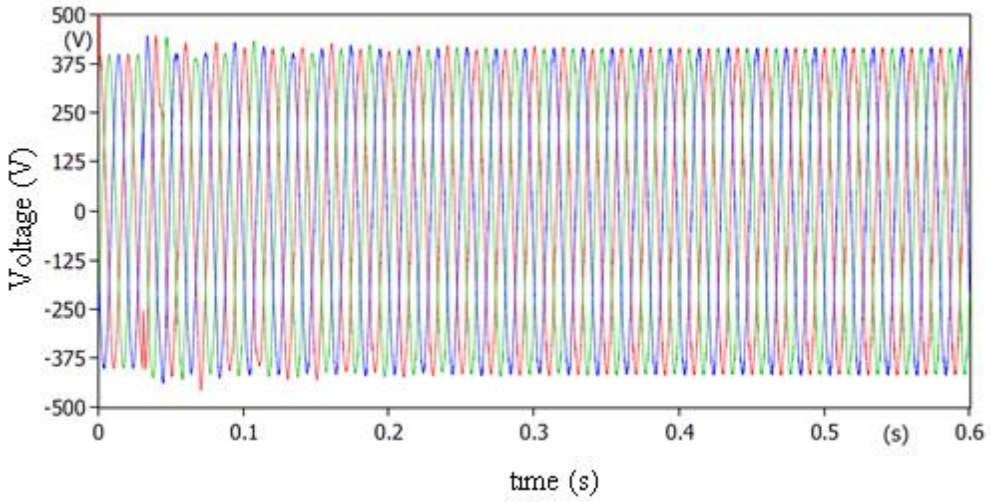

Figure 5.23(b): Using pre-insertion resistor for double-tuned filter

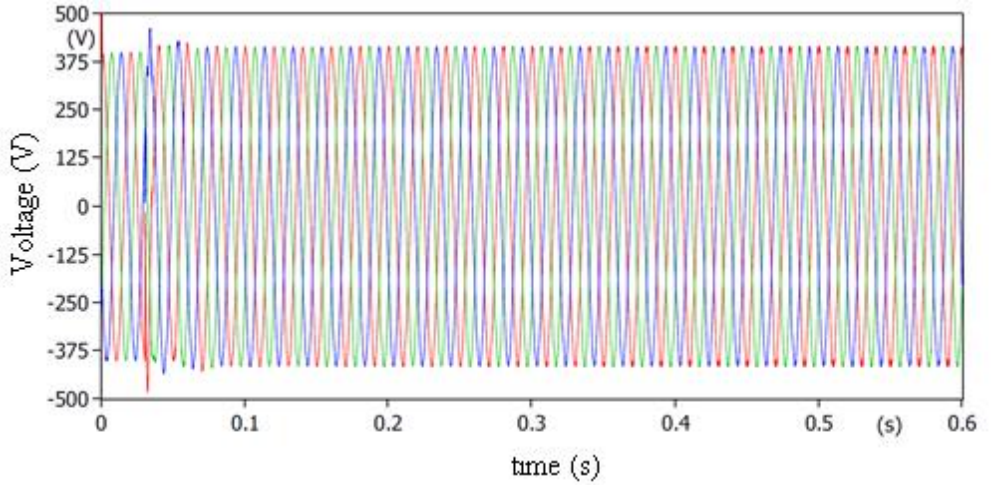

Figure 5.23(c): Using pre-insertion resistor for C-Type filter

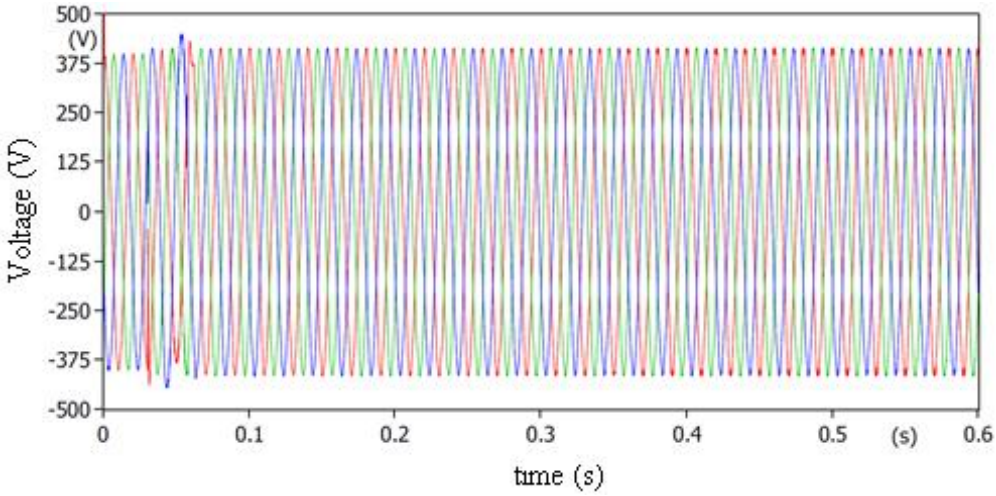

Figure 5.23(d): Using pre-insertion resistor for high pass filter

5.10.2 Controlled Switching

Controlled switching has proved to be one of the most efficient methods of mitigating switching overvoltages. The method involves closing individual phases in the circuit breaker when the system experiences the least amount of stress. All four filters were simulated using ATP to observe the effects that the controlled switching would have on the resultant waveform. Using phase A as a reference, the closing signal issued at 0.04 s is delayed by 0.005 s to give a controlled closing time of 0.045 s. The controlled closing time of phase B is 0.0516 s and phase C is 0.0483 s. Figures 5.24(a) to 5.24(d) show the resultant voltage waveform of the simulation. The double-tuned filter showed the best results with a reduction of 416 V after using controlled switching. The worst performing filter was the C-Type filter with a reduction of 34 V followed by the high pass filter with a reduction of 92 V. The results of the simulation are tabulated in Table 5.14.

Table 5.14: Mitigation using controlled switching

Filters	Overvoltage Before	Overvoltage After
Single-tuned filter	887 V	792 V
Double-tuned filter	910 V	494 V
C-Type filter	732 V	698 V
High pass filter	788 V	696 V

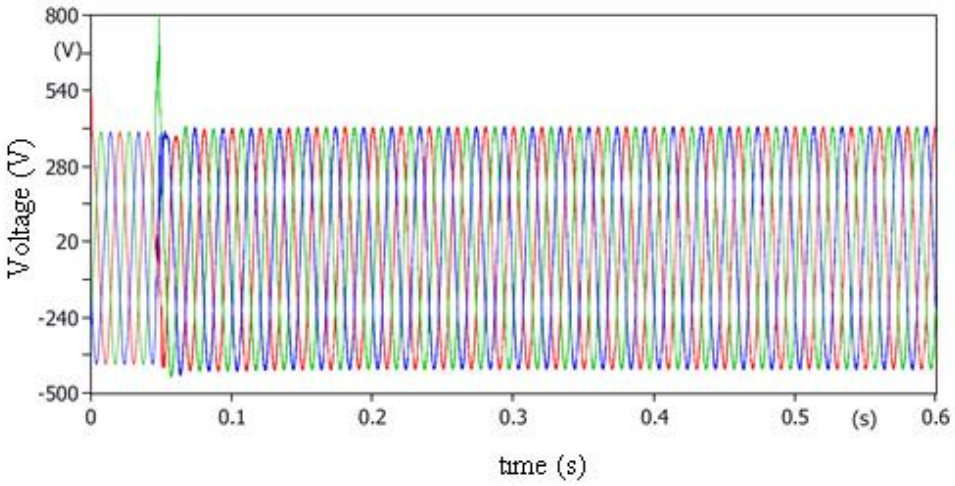

Figure 5.24(a): Using controlled switching for single-tuned filter

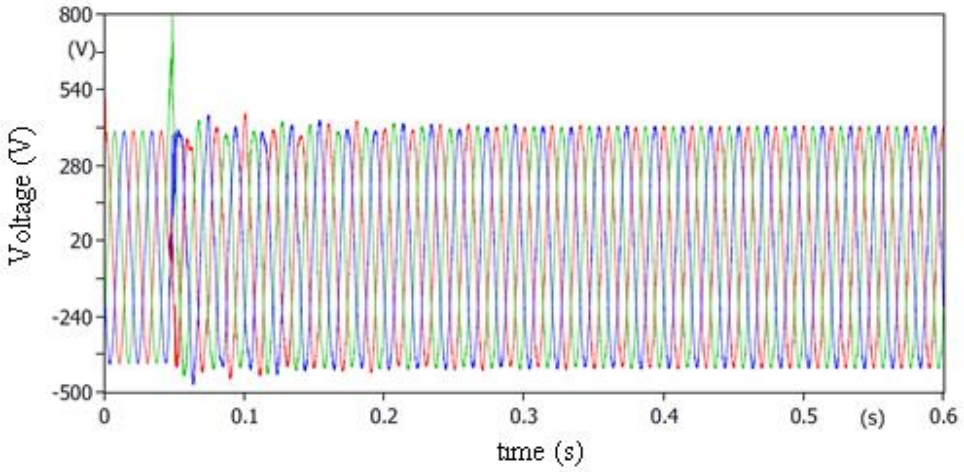

Figure 5.24(b): Using controlled switching for double-tuned filter

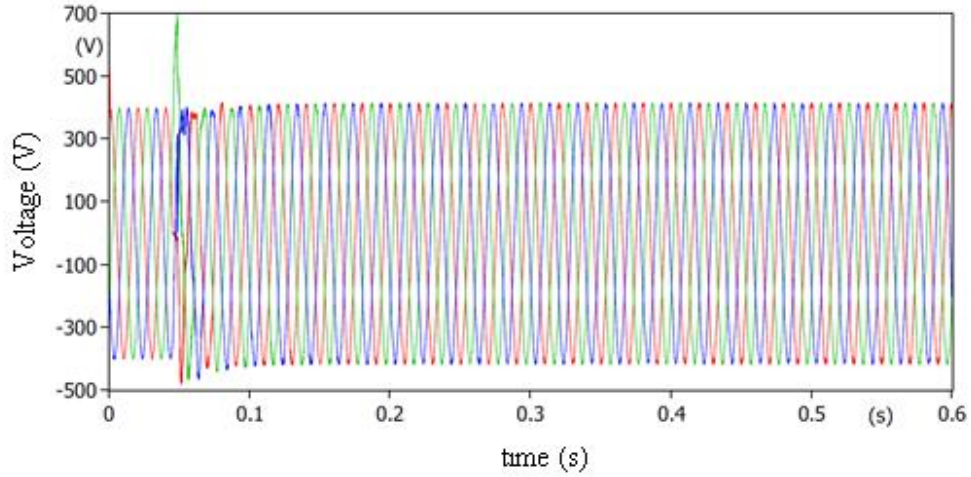

Figure 5.24(c): Using controlled switching for C-Type filter

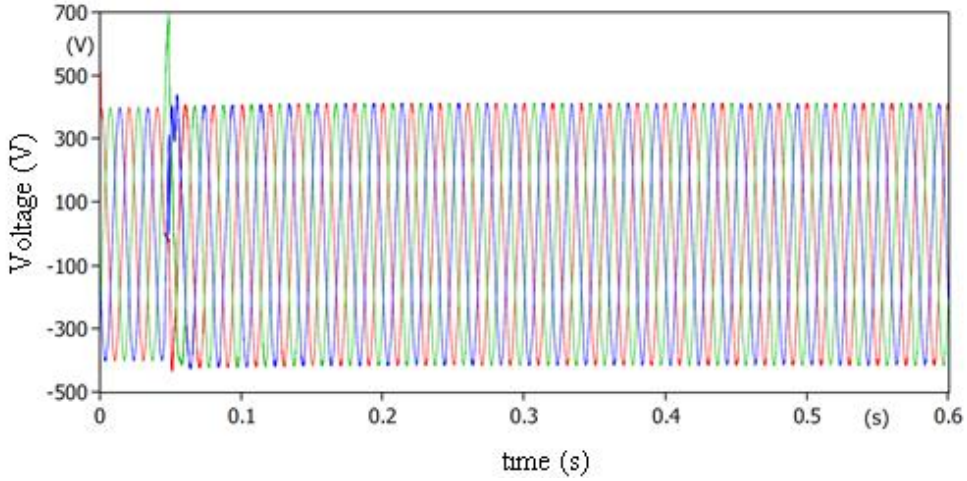

Figure 5.24(d): Using controlled switching for high pass filter

5.10.3 Surge Arrester

Surge arresters help in mitigating overvoltage caused by the switching operation of the harmonic filter. Metal oxide surge arresters investigated were modelled after the IEEE surge arrestor model. The model is comprised of two non-linear resistances A_0 $A_0$and A_1A_1 which are separated by an *RL* filter. The *V-I* characteristics of the two non-linear resistors were determined according to the IEEEANSI C62.1993 standard, with the value of the residual voltage estimated for a current impulse of 3 kA and 30/60 µs.

The placement of the surge arrester plays an important role in its ability to limit the surge. For this study, the surge arrester was placed between the circuit breaker and supply cable to limit the overvoltage caused during switching. Figures 5.25(a) to 5.25(d), show the voltage waveforms of the circuit breaker for the four filters using ATP software during controlled switching. When the surge arrester was connected to the network during energization, the overvoltage of the double-tuned filter was reduced to 400 V whilst the C-Type filter experiences the lowest reduction in overvoltage with a value of 317 V. The results of the simulations are tabulated in Table 5.15.

Table 5.15: Mitigation using surge arrester

Filters	Overvoltage before	Overvoltage after
Single-tuned filter	887 V	408 V
Double-tuned filter	910 V	400 V
C-Type filter	732 V	415 V
High pass filter	788 V	406 V

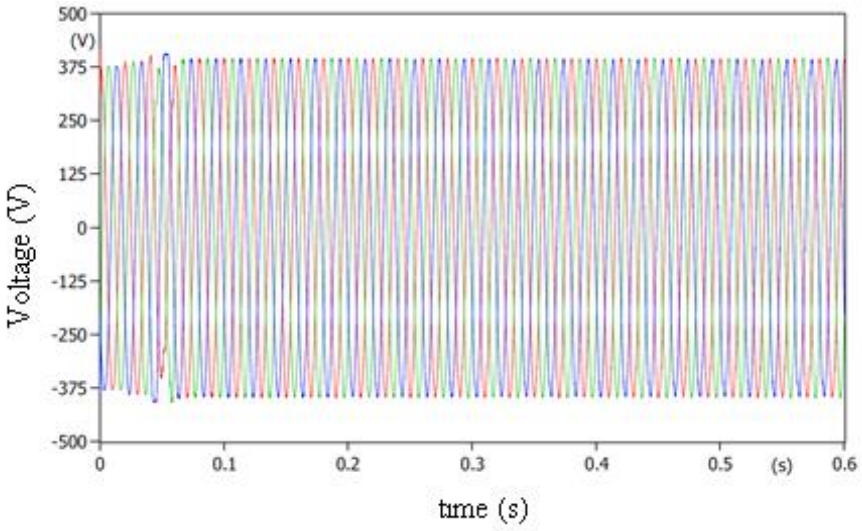

Figure 5.25(a): Using surge arrester for single-tuned filter

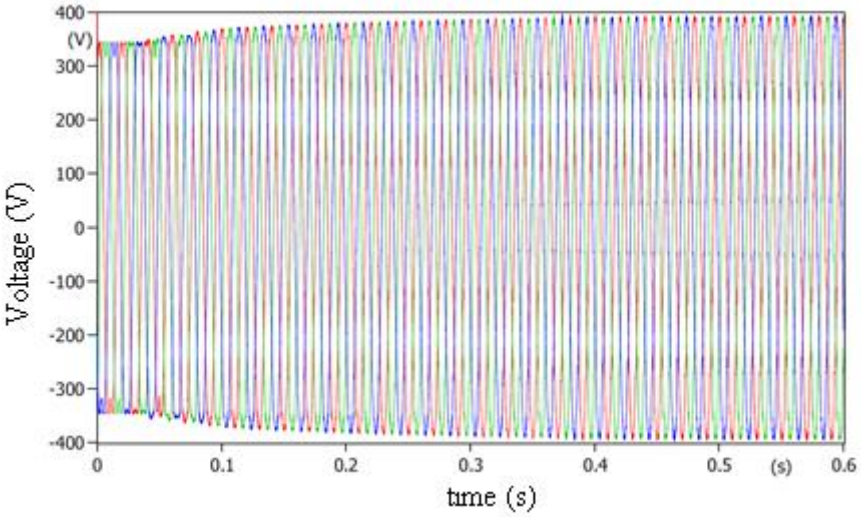

Figure 5.25(b): Using surge arrester for double-tuned filter

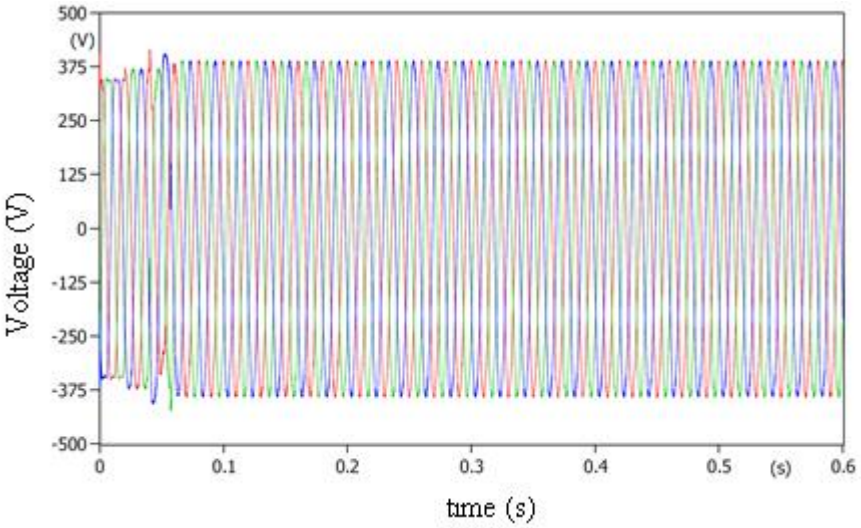

Figure 5.25(c): Using surge arrester for C-Type filter

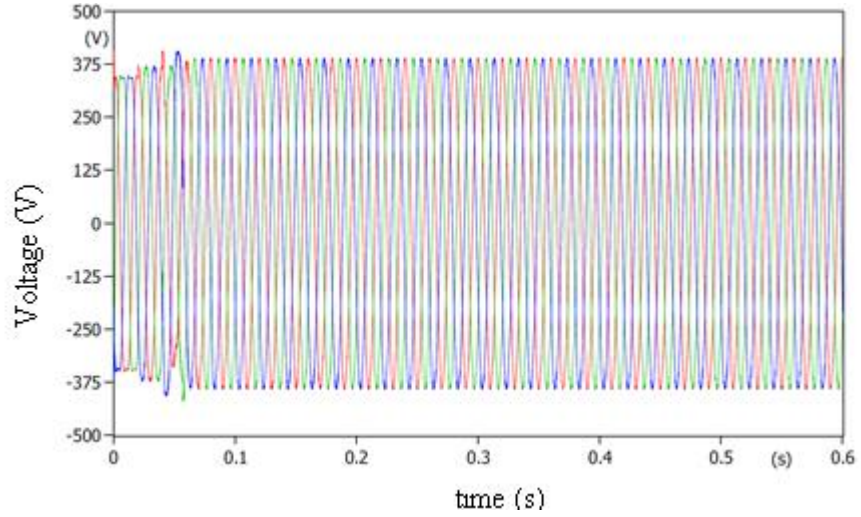

Figure 5.25(d): Using surge arrester for high pass filter

5.10.4 Conclusion on the Mitigation Methods

For mitigation of energization, the most effective method to limit the overvoltage caused by the switching operations of the harmonic filter proved to be the surge arrester. However, the pre-insertion resistor was found promising as it effectively reduced the overvoltage by approximately 50%. Using a control switching device, proved to be the least effective method of mitigation. The surge arrester has a higher energy absorption capacity compared to using a controlled switching device. The effective placement of the surge arrester in the power system would allow for maximum suppression of the overvoltage compared to using a pre-insertion resistor or controlled switching device.

5.11 Case Study 2: Harmonics in Soap Manufacturing Industry

The manufacturing of soap can be a complex and involved process that requires the refining of raw materials to produce the final product. Soap is created by mixing fats and oils with a base. The industrial production of soap involves the continuous addition of fat and removal of the product by heating and cooling. Various colorants and fragrances are added to the product before it is sold to the consumer. This high-precision process of heating and cooling requires the use of motors and VSD's. The VSD controls the speed and frequency of the motors to produce a safe and high-quality product for public use. The operation of these motors can produce harmonic distortion that may pose a threat to the power quality.

5.12 Details of Network Layout

The harmonic content of the system was determined by installing a harmonic analyser as discussed in section 5.2, at the main incomer panel. A harmonic analysis can thereafter be conducted from the graphs extracted to determine the level and order of harmonics present in the system. The electrical network shown in Figure 5.26 depicts the general layout of the electrical equipment and their ratings for the soap manufacturing industry.

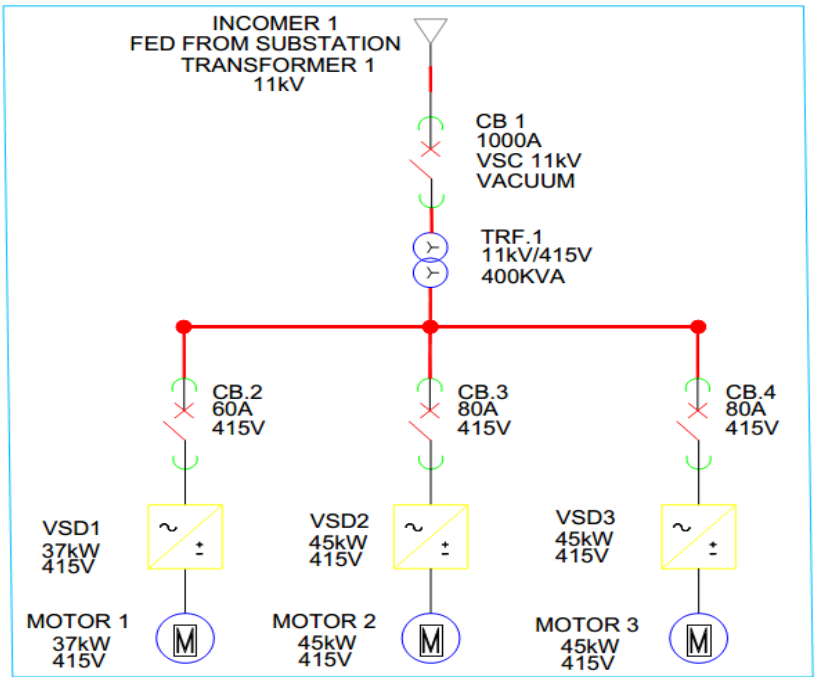

Figure 5.26: Network layout for the soap manufacturing industry

The soap manufacturing industry network consists of an 11 kV supply from a voltage source of an 11 kV substation. The system is protected by a 1000 A, 11 kV vacuum circuit breaker that will trip when a fault is detected. This prevents short circuit current from damaging the electrical equipment. Transformer 1 steps down the 11 kV to 415 V and has a fault level of 400 kVA. Circuit breakers 2, 3, and 4 are connected to VSD1, VSD2, and VSD3 respectively. The circuit breakers protect the VSD's and are rated according to the motor current. The kilowatt ratings of each VSD are chosen according to the motor's power rating. The motor runs at 1800 rpm and has a frequency of 50 Hz. The ratings of each component are presented in Table 5.16.

Table 5.16: Component ratings

Components	Ratings
Incomer supply	11 kV
CB 1	1000 A
TRF 1	11 kV/415 V
CB 2	60 A
CB 3	80 A
CB 4	80 A
VSD 1	37 kW
VSD 2	45 kW
VSD 3	45 kW
Motor 1	37 kW
Motor 2	45 kW
Motor 3	45 kW

5.12.1 The Network Analyser Results

To determine the harmonics, present a harmonic analyser is installed to create a detailed report of any power quality issues. The report presents the level and order of harmonics in the system. The following parameters were measured during the analysis, voltage, current, power (kW), power factor, and harmonics.

The network analyser as shown in Figure 5.1, was also installed to create a detailed report of any power quality issues for case study 2 to obtain various graphs. For this company, the report provides details on harmonic orders with high levels of harmonic distortion. Also similar to case study 1, the parameters measured during the analysis were for the voltage, the current, the power, the power factor, the THDV, and the THDI, discussed as follows.

Voltage: The voltage of the system was measured between a maximum value of 437.59 V and a minimum value of 406.02 V as shown in Figure 5.27. As observed from this graph, the actual voltage used in the plant is 416 V and remains steady during production. The maximum voltage used is on a Saturday as this plant runs for 24 hours.

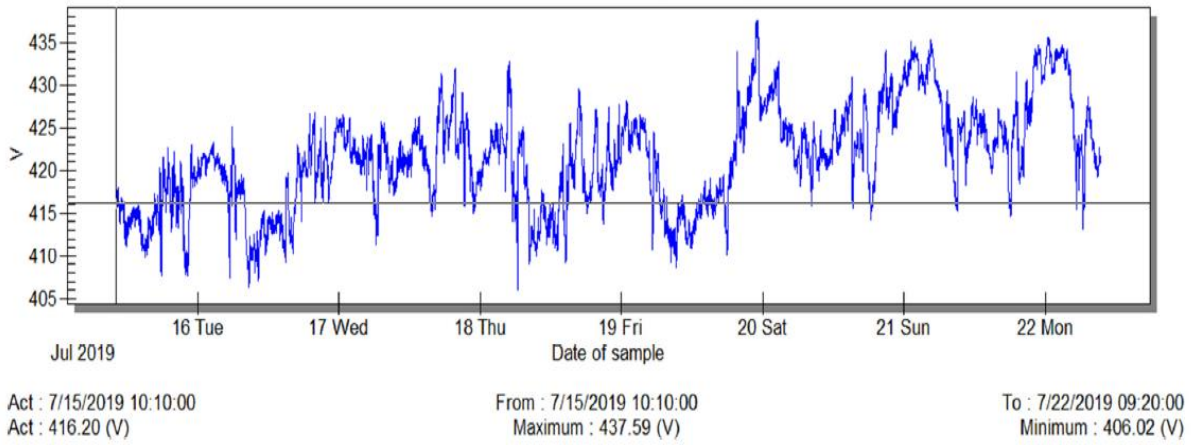

Figure 5.27: Voltage graph

Current: The current of the system was measured between a maximum value of 192 A and a minimum value of 0 A. Figure 5.28, represents the current consumption over the week, measuring the points of maximum and minimum usage. The current peaks on a Saturday as production increases during off-peak periods.

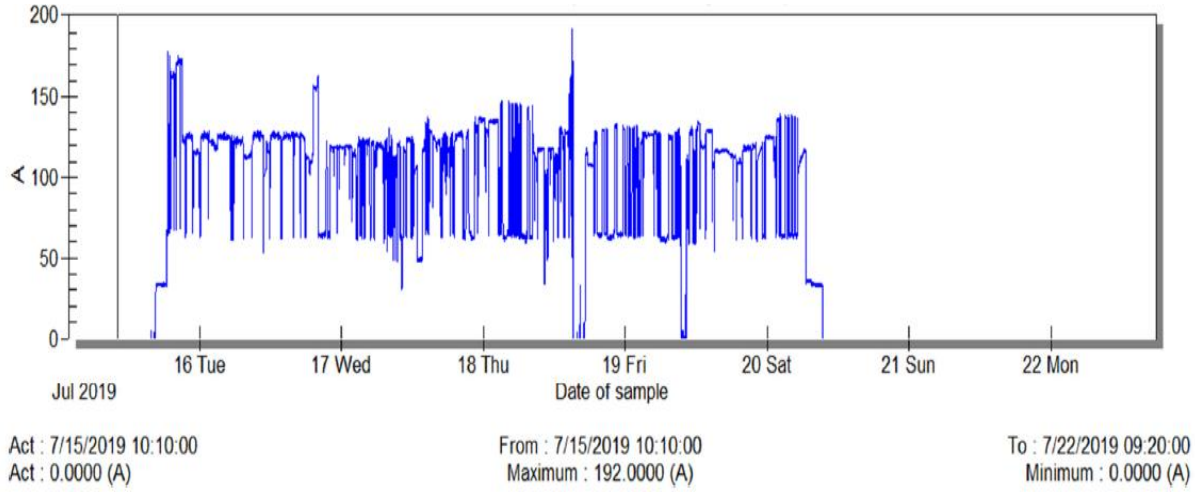

Figure 5.28: Current graph

Power: The power graph as shown in Figure 5.29, indicates that the system was measured between a maximum value of 126.52 kW and a minimum value of 0 kW. The power is supplied via the mini substation that is fed from Eskom's supply. This industry is charged on a TOU (time of use) tariff and is billed according to peak and off-peak times. Therefore, maximum power usage is consumed closer to the weekend where power demand is at its lowest.

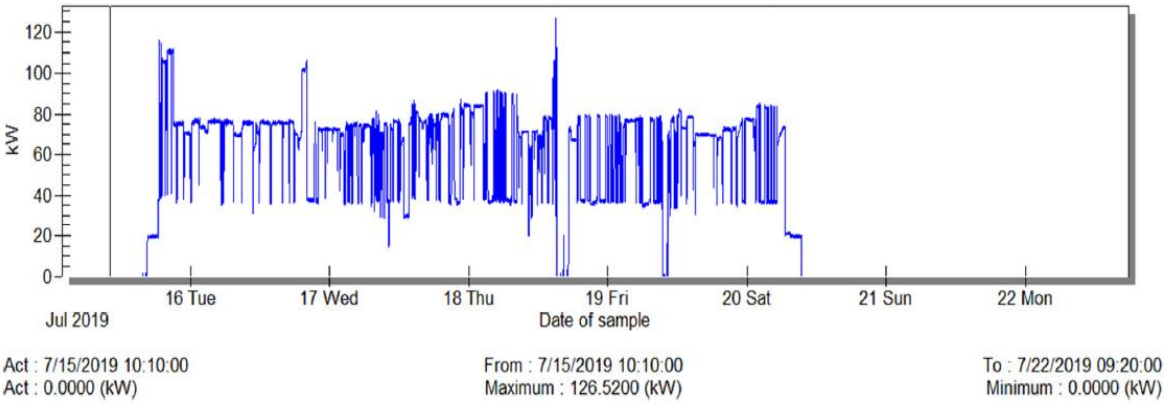

Figure 5.29: Power graph

Power Factor: The power factor of the system reaches a maximum value of 0.146. A higher power factor close to unity eliminates the power factor penalty and reduces peak kW billing demand. As shown in Figure 5.30, the power factor of the system fluctuates according to the load and without power factor correction this will cost the company money due to the energy consumed.

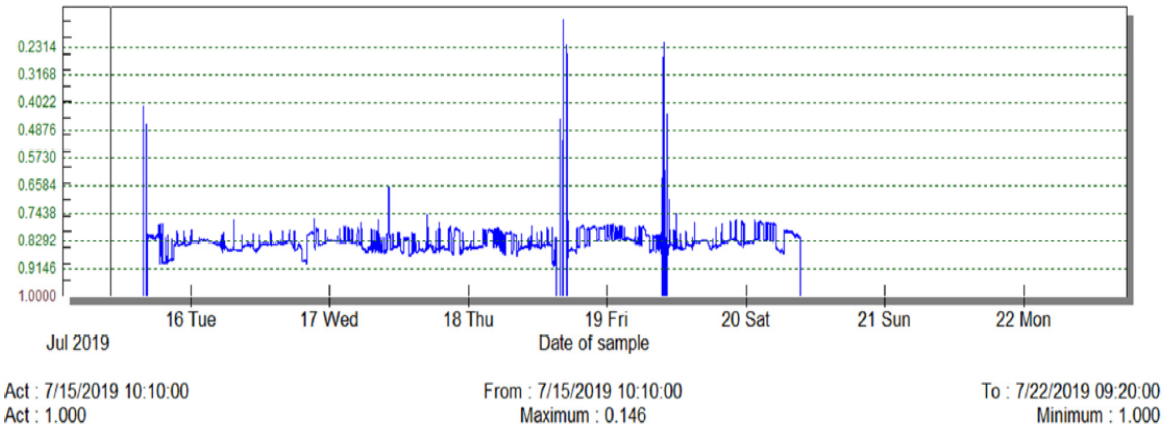

Figure 5.30: Power factor graph

THDV: The harmonics in this system run at an average of 2.1% but reach a maximum of 4.8% as observed in Figure 5.31. The increased usage of non-linear loads over the weekend causes high voltage distortion levels. The use of a harmonic filter will help reduce the THDV caused by the non-linear loads in the system.

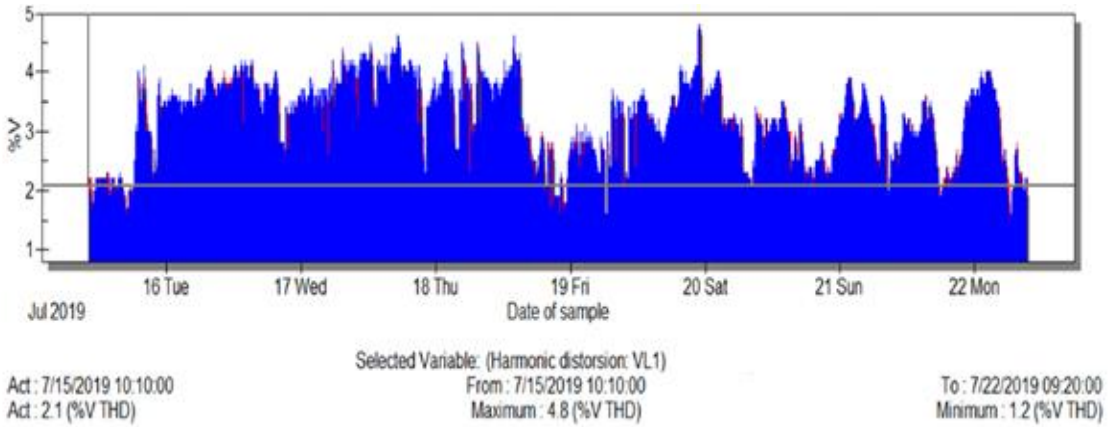

Figure 5.31: Voltage THD graph

THDI: The harmonics in the system run at an average of 0% but reach values as high as 59.7% as shown in Figure 5.32. A current waveform that is purely sinusoidal has no harmonic distortion and consists of a single frequency. The introduction of current harmonics to the system will distort the current waveform harming a wide range of power system equipment.

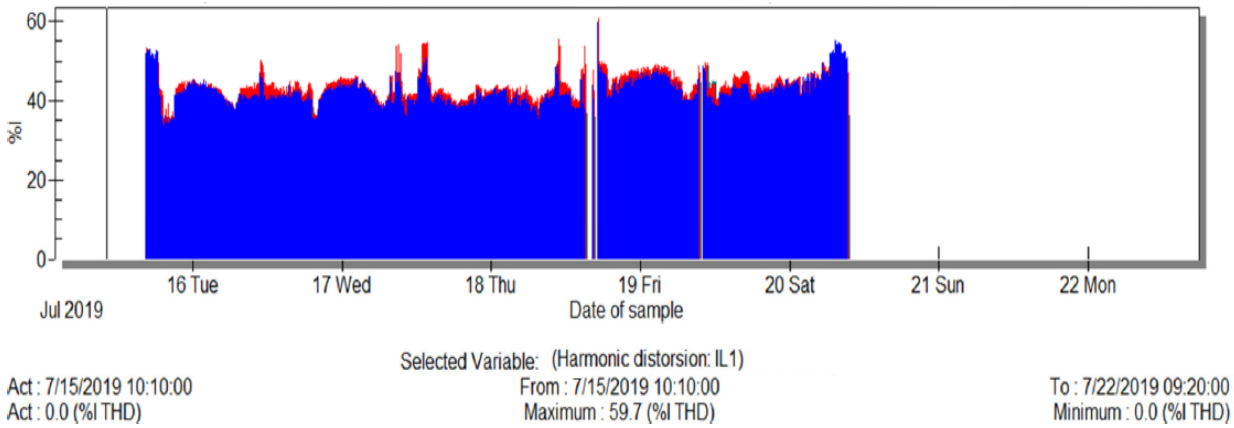

Figure 5.32: Current THDI graph

5.13 System Modelling in ATP: Case Study 2

To model the switching activities of the harmonic filters in the soap industry using ATP/EMTP software as presented in Figure 5.33. The incoming voltage of 11 kV is stepped down by the main transformer to 415 V. The layout of the soap industry for the ATP model, with its main VSD's and motors are shown in Figure 5.26. The main transformer 11 kV/415 V was modelled by using the BCTRAN model on the ATP. The transformer was connected to the VSD's through a 7 m long cable. The cables were modelled using the *PI* model. Each VSD was modelled with individual switching frequencies that affect system efficiency. The VSD's are

connected to individual motors that are presented by using a single cage rotor model on ATP software.

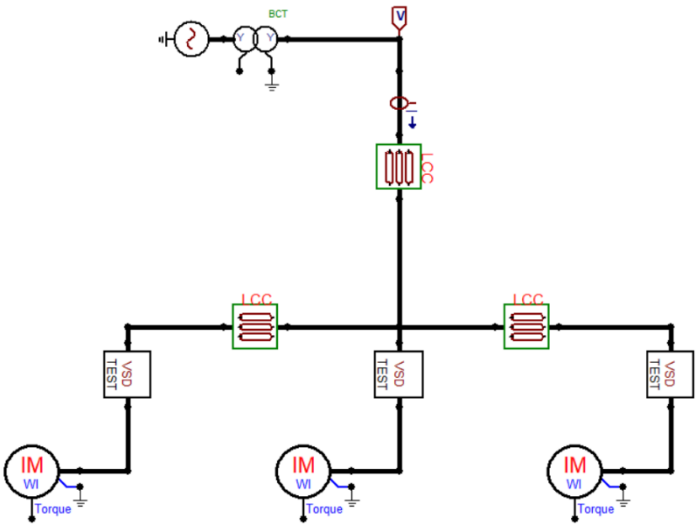

Figure 5.33: ATP simulation model

5.13.1 Modelling the AC Voltage Source

The voltage source is modelled on ATP to represent an 11 kV supply from a distribution substation. The source is modelled according to that presented in section 5.6.1 in case study 1, with the source parameters presented in Table 5.17.

Table 5.17: Source parameters

Parameter	Value
Amplitude (V)	11000
Frequency (Hz)	50
Start A (sec)	-1
Stop A (sec)	100
Number of phases	3. Phase

5.13.2 Modelling of Transformer

A 3-phase, 50 Hz copper-wound transformer steps down, with the incoming voltage from 11 kV to 400 V, it has a vector group of Yy0 and a power rating of 0.5 MVA. Using the BCTRAN model on ATP, the structure and ratings of the transformer were specified and Table 5.18 shows the specifications for the main transformer as modelled on ATP.

Table 5.18: Transformer parameters

Parameter	Value
Vector group	Yy0
Rated power	0.5 MVA
Open-circuit voltage (%)	100
Open-circuit current (%)	0.55
Open-circuit losses (kW)	1.6
Short-circuit impedance HV-LV (%)	3.2
Short-circuit impedance losses (kW)	1.56

5.13.3 Modelling of Variable Speed Drives

The variable speed drive was modelled using ATP, to control the speed and frequency of the 3-phase motor. The standard frequency of 50 Hz was used with a switching frequency of 150 Hz. The structure of the VSD was modelled in three parts; the rectifier, the DC link, and the invertor. The diodes have an ignition voltage of 0.7 V chosen from standard silicon control diode ignition voltage. Table 5.19 parameters are used to model the variable speed drive.

Table 5.19: VSD parameters

Parameters	VSD 1	VSD 2	VSD 3
Frequency (Hz)	50	50	50
Am ratio	0	0	0
Switching freq (Hz)	150	250	250
Capacitor (μf)	308300	319400	319400

5.13.4 Modelling of Motors

The electric motor is modelled on ATP, with the values for speed, efficiency, and slip taken from industry standards and the motor's nameplate details. The system is made up of three motors each with its power ratings. As in case study one, the motor was represented by using a single cage rotor model on ATP and is set to start at 0.02 s at the rated speed of 1800 rpm. ATP simulation allows for an easy model implementation, where the results obtained match the expected behaviour for the motor. Table 5.20, shows the parameters of the motor drive.

Table 5.20: Motor parameters

Parameters	Motor 1	Motor 2	Motor 3
Frequency (Hz)	50	50	50
Voltage L-L (kVrms)	0.283	0.283	0.283
Power (hp)	49.61	60	60
Speed (rpm)	1800	1800	1800
Power factor (cos phi)	0.8	0.8	0.8
Efficiency (pu)	0.75	0.75	0.75
Slip (%)	0.72	0.72	0.72
Start current (pu)	7	7	7
Start torque (pu)	0.5	0.5	0.5
Load torque (pu)	1	1	1
Max torque (pu)	1.5	1.5	1.5

5.14 Simulation Results

For case study 2, the simulation results obtained from the ATP software are presented as voltage and harmonic graphs.

- **Voltage Graph**

The voltage wave form reaches a maximum of 415 V with a frequency of 50 Hz. The simulation starts at 0 s and ends at 0.35 s. The 3 phase waveform is uniform with negligible harmonic distortion. The sine wave has a periodic time of 0.02 s. Figure 5.34, shows the resultant voltage waveform of the system.

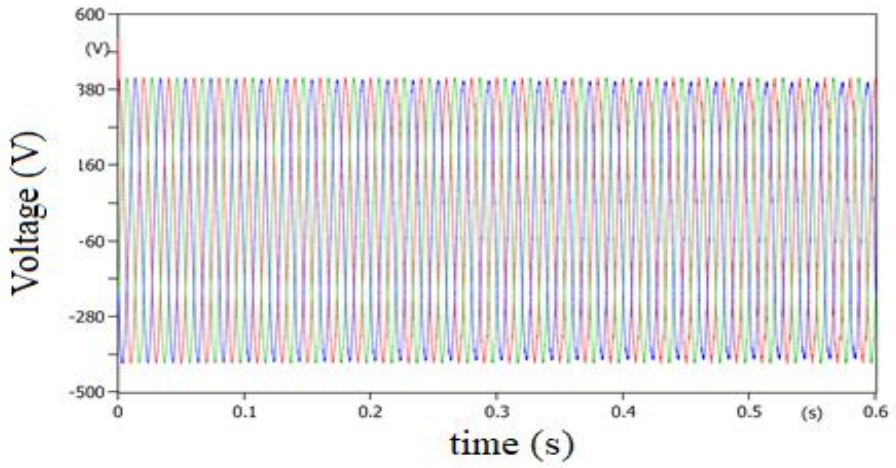

Figure 5.34: Voltage simulation graph

- **Harmonics Graph**

Figure 5.35, represents the harmonics of the system and was extracted from the power factor analyser seen in Figure 5.1. The dominant harmonics are the 3rd and 5th order harmonics, similar to the results found in case study one. The 3rd harmonic reaches a maximum of 20.015 V and the 5th harmonic reaches a maximum of 13.756 V. The THD of the system was found to be 6.623 %. This is over the power system limit of 5 % THD according to IEE 519-1992 [31]. To conform to IEE 519-1992 standards, harmonic filters can be installed to mitigate harmful harmonics.

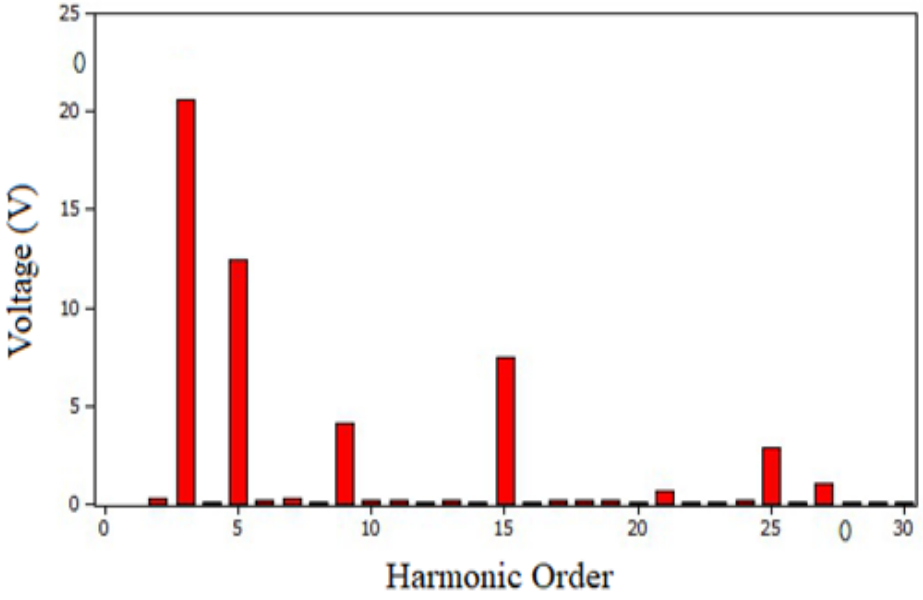

Figure 5.35: Harmonics simulation graph

5.15 Mitigation of Harmonics

5.15.1 Harmonic Filters

Similar to case study 1, the same process was done where the four harmonic filters were employed to mitigate harmonics for case study 2.

5.15.1.1 Single-tuned Harmonic Filter

The single-tuned harmonic filter will be simulated to determine if it can successfully reduce the THD of the system and bring the 3rd and 5th harmonics to an acceptable level. The filter was made up of a resistor, inductor, and capacitor connected in series. The values of *R*, *L*, and *C* can be found by using equations (2.1), (2.2), and (2.3). Values of the filter used are given in Table 5.21.

Table 5.21: Single-tuned filter parameters

Parameter	Q_f (KVAr)	R_f (Ω)	C_f (μf)	L_f (mH)
3rd	42.32	0.333	695.26	1.619
5th	42.32	0.1999	750.88	0.5397

5.15.1.2 Simulation of Single-tuned Harmonic Filter

Figure 5.36, presents the simulation of the single-tuned harmonic filter on ATP. The two single-tuned filters are connected to the network to attenuate the 3rd and 5th harmonics. The parameters for *R*, *L*, and *C* are given in Table 5.21.

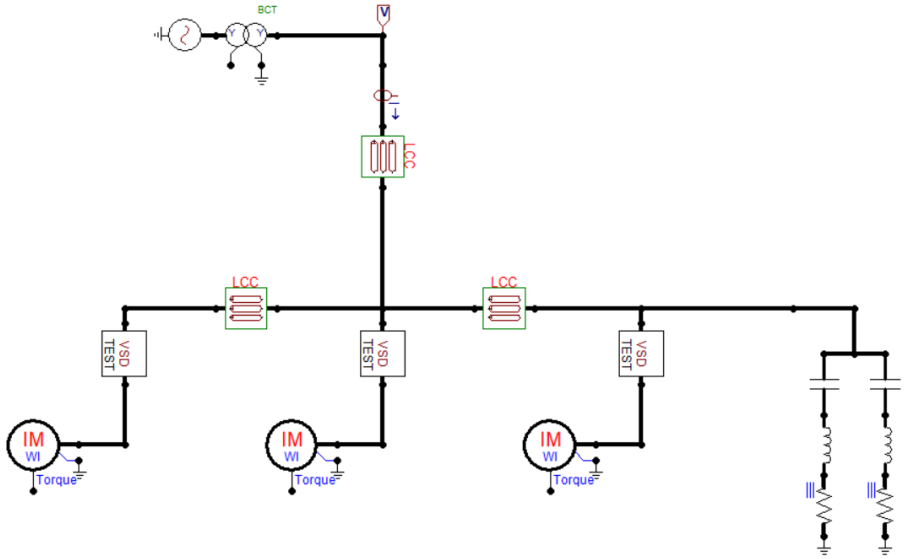

Figure 5.36: Simulation model with single-tuned filter

5.15.1.3 Results of Single-tuned Filter Simulation

The results obtained as presented in Figure 5.37, show that the connection of the single-tuned filter to the system has resulted in a decrease of the 3rd and 5th harmonics. The 3rd harmonic has decreased from 20.015 V to 0.869 V and the 5th harmonic has decreased from 13.756 V to 0.508 V. There is a 95.66 % decrease in the 3rd harmonic and a 96.3 % decrease in the 5th harmonic. The THD is now 0.6814 % compared to 6.623 %, well within the IEE 519-1992 standards. The results show that the use of a single-tuned filter may be a plausible solution to mitigating harmonics in this case study.

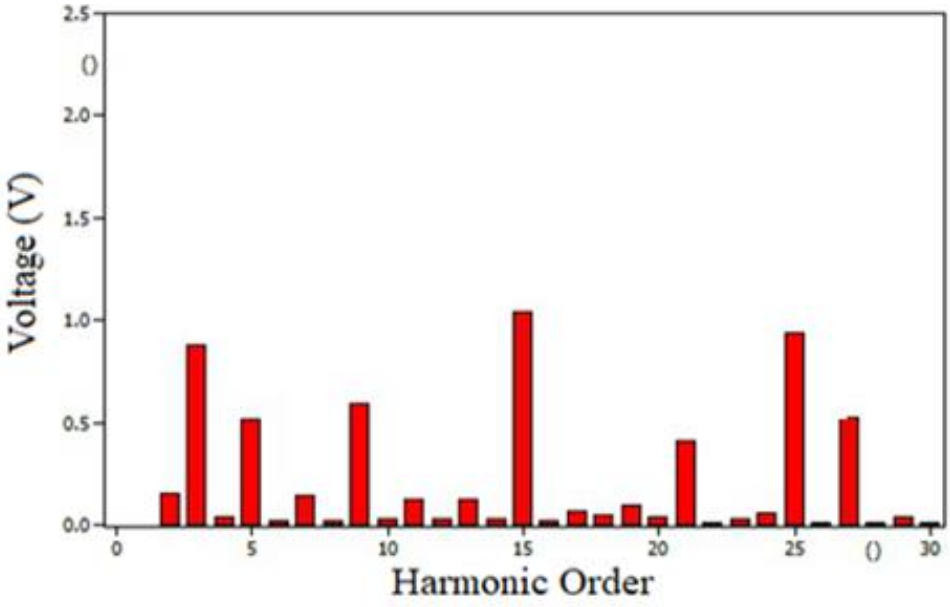

Figure 5.37: Harmonics simulation with single-tuned filter

5.15.2.1 Conventional Double-tuned Harmonic Filter

The double-tuned filter is widely used in the industry which performs similar to that of an active filter. A conventional double-tuned filter has a simple design and takes a small space. The filter consists of a parallel resonant circuit connected in series with a series resonant circuit. The combination of series and parallel resonant circuits offers a low impedance path for the two resonant frequencies [86]. Table 5.22 documents the parameters used for the double-tuned filter.

Table 5.22: Lumped parameters for double-tuned filter

Parameter	Q_f (KVAr)	C_1 (µf)µf)	L_1 (mh)	C_f (µf)	L_2 (mh)
3^{rd} and 5^{th}	42.32	404.6	1.447	1897.14	0.411

5.15.2.2 Simulation of Conventional Double-tuned Filter

The simulation of the double-tuned filter on ATP is shown in Figure 5.38. A double-tuned filter and two parallel single-tuned filters have the same function that both of them can filter two different frequency harmonics [91]. Using the parameters of two single-tuned filters as can be found in Table 4.7, the double-tuned filter was designed.

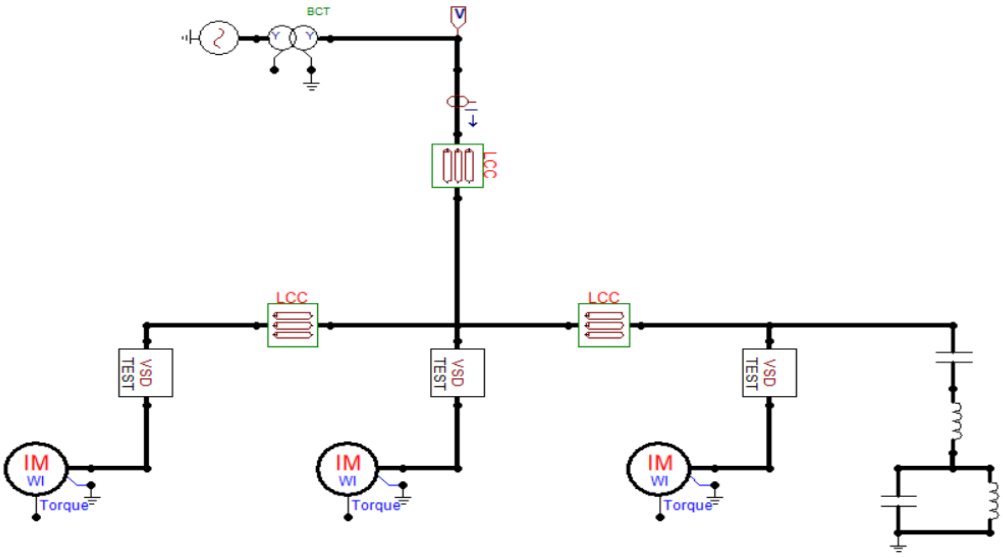

Figure 5.38: Simulation model with double-tuned filter

5.15.2.3 Results from the Double-tuned Filter Simulation

The harmonics graph seen in Figure 5.39, shows that the installation of the double-tuned filter has successfully attenuated the 3rd and 5th harmonics. The 3rd harmonic has decreased from 20.015 V to 0.377 V, whilst the 5th harmonic has decreased from 13.756 V to 1.809 V. There is a 98.1% decrease in the 3rd harmonic and an 86.85 % decrease in the 5th harmonic due to the connection of the double-tuned filter. The THD has decreased from 6.623 % to 0.7825 %, within IEEE 519-1992 limits. The results prove that the double-tuned filter is an acceptable solution to mitigating the two lower-order harmonics.

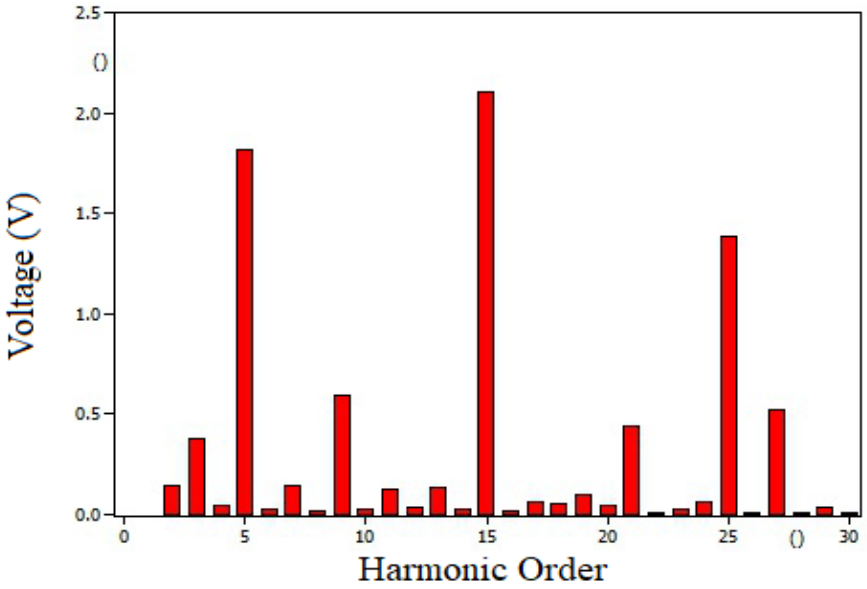

Figure 5.39: Harmonic graph for the double-tuned filter

5.15.3.1 C-Type Harmonic Filter

The C-Type harmonic filter is different compared to the 2nd and 3rd order filters in that its components *L* and *C* elements which are parallel to the resistor are resonant at the fundamental frequency, thus reducing the power loss on the damping resistor *R*. The filter does well in suppressing high-frequency harmonics due to its flat impedance characteristic above the tuned frequency [4]. The parameters to model the filter on ATP are shown in Table 5.23.

Table 5.23: Lumped parameters for C-Type filter

Parameter	Q_f (KVAr)	C_1	C_1(µf)	L (mH)	R (Ω)
3rd	42.32	782.167	6257.33	1.619	0.732
5th	42.32	782.167	18772.01	0.5397	0.1408

5.15.3.2 Simulation of C-Type Harmonic Filter

To determine the effects that the C-Type filter will have on the system harmonics the filter is simulated on ATP and is represented by Figure 5.40. The filters are modelled to suppress the 3rd and 5th harmonics with minimal losses when tuned to low frequencies. The C-Type filter is connected via a 2-meter long cable to the network to effectively compensate reactive power, improve system performance and reduce harmonic distortion of the system.

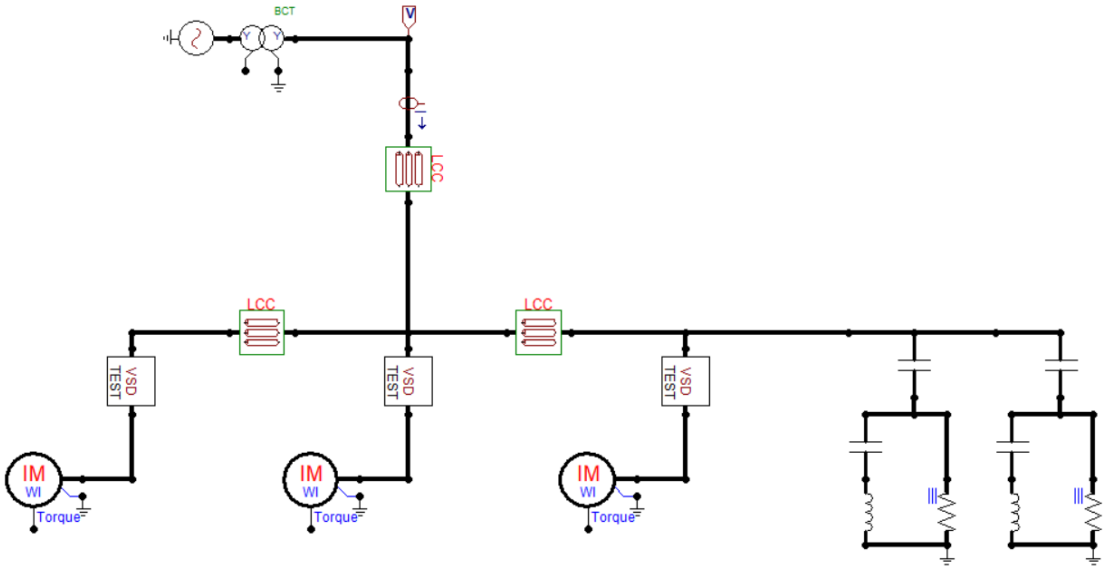

Figure 5.40: Simulation model with C-Type filter

5.15.3.3 Results from the C-Type Filter Simulation

Figure 5.41, presents the harmonic results after the C-Type filter was connected to the electrical network. The 3rd harmonic decreased from 20.015 V to 1.968 V and the 5th harmonic decreased from 13.756 V to 1.002 V. This has resulted in a 90.17 % decrease for the 3rd harmonic and a

92.7 % decrease for the 5th harmonic. The THD has improved to 0.5475 %. The C-Type filter is a possible option to reduce harmonic distortion and will be compared to the other filters to deduce the best possible solution.

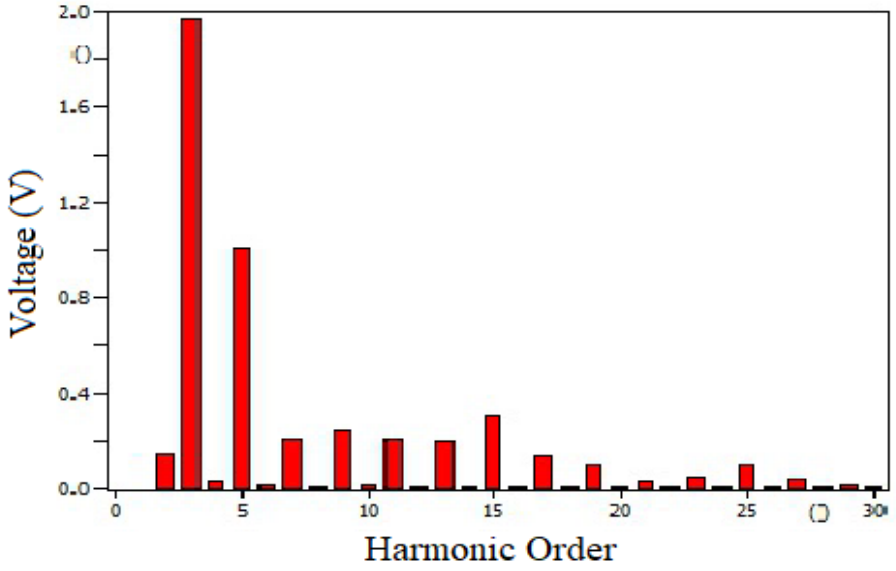

Figure 5.41: Harmonic reduction with C-Type filter

5.15.4.1 Second-order High Pass Filter

The second-order high pass filter is commonly used and consists of a capacitor in series with a parallel combination of a resistor and inductor. It can be used to eliminate a wide range of frequencies. The filter may be used to eliminate high order harmonics (17th harmonic and above), by providing a low impedance for high frequencies but stopping low ones. The parameters for simulating the filter on ATP can be found in Table 5.24 below.

Table 5.24: Lumped parameters for second-order high pass filter

Parameter	Q_f (KVAr)	C(µf)	L(mH)	R(Ω)
3rd	42.32	695.26	1.619	2.32
5th	42.32	750.88	0.539	0.7187

5.15.4.2 Simulation of Second-order High Pass Filter

The second-order high pass filter was modelled using ATP simulation to determine the effects it would have in reducing the 3rd and 5th harmonics. Figure 5.42, shows the modelling of the filter on ATP. Two high pass filters are connected in parallel to the network to decrease harmonic distortion and therefore improve system efficiency.

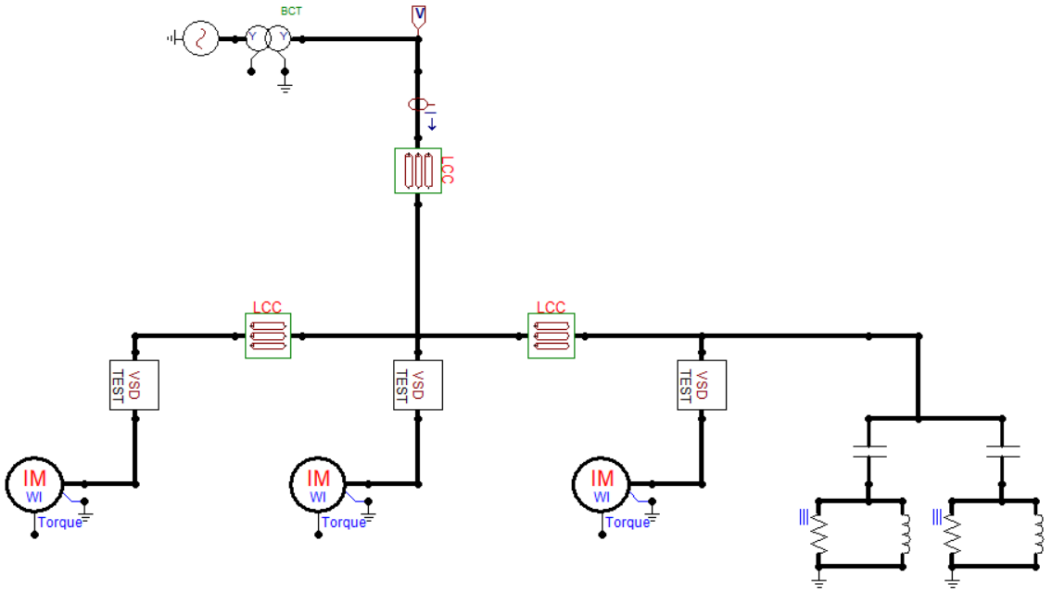

Figure 5.42: Simulation model using second-order high pass filter

5.15.4.3 Results from the Second-order High Pass Filter Simulation

The results of the harmonics present in the system after the installation of the filter are represented in Figure 5.43 below. The graph shows a decrease in the 3rd and 5th harmonics and therefore an improvement in the THD. The 3rd harmonic decreased from 20.015 V to 1.541 V and the 5th harmonic decreased from 13.756 V to 1.073 V. There is a 92.3 % reduction of the 3rd harmonic and a 92.1 % decrease for the 5th harmonic. The THD has improved from 6.623 % to 0.4909 %. Therefore the second-order high pass filter can also be considered as a solution to improving harmonic distortion.

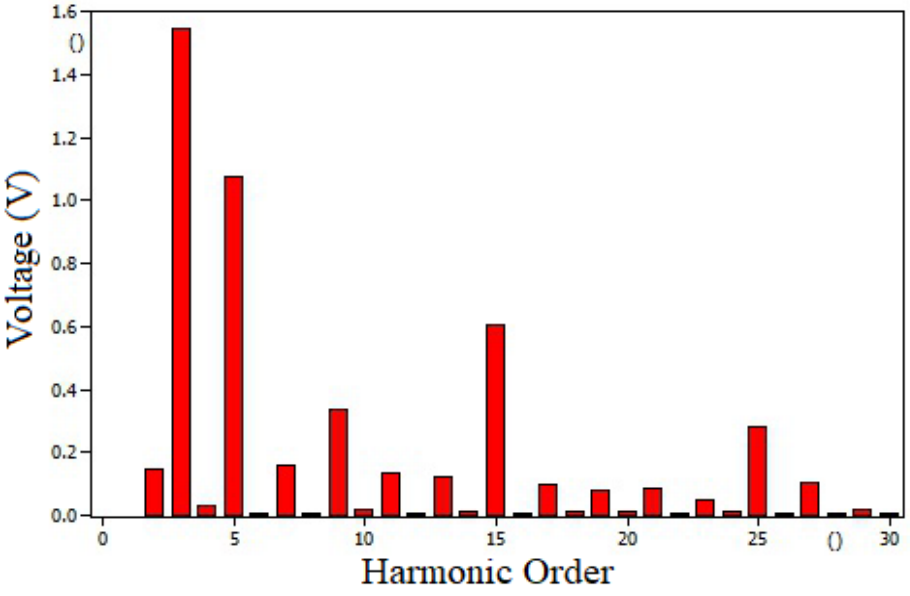

Figure 5.43: Harmonic reduction with second-order high pass filter

5.16 Harmonic Filter Analysis and Results for Case Study 2

To determine the best performing filter to successfully mitigate the two lower-order harmonics, all four filters were simulated with the help of ATP software. The results show the effects that the harmonic filter has on the reduction of the 3rd and 5th harmonics and the subsequent improvement on the THD levels. According to the results compiled in Table 5.25 below, the best performing filter is the single-tuned filter and the worst performing filter is the C-Type filter. The single-tuned filter has better performance at the tuning frequency compared to the C-Type filter when reducing harmonic content. The single-tuned filter is designed to reduce lower-order harmonics below the tuning frequency, whereas the C-Type filter is designed to reduce higher-order harmonics above the tuning frequency. The single-tuned filter has a high-quality factor which provides maximum attenuation of one harmonic. The C-Type filter has a low-quality factor making it suitable for a range of harmonic frequencies greater than the cut-off frequency. Therefore, the design of a C-Type filter is meant to mitigate higher-order harmonics usually up to the 23rd harmonic.

Table 5.25: Results of filter simulations

	Original network	Single-tuned	Double-tuned	C-Type	High pass
3rd harmonic	20.015	0.869	0.377	1.968	1.541
5th harmonic	13.756	0.508	1.809	1.002	1.073
THD (%)	6.623	0.6814	0.7825	0.5475	0.4909

5.16.1 Energization of Harmonic Filters

To simulate the switching activities of each filter during energization, the use of ATP software was employed. During energization, the filter is closed to the system which may cause overvoltage to occur. One possible cause is the charging of the capacitors during the energization of the filter. This causes a resultant voltage across the filter at the point of closing. Another possible cause may be experienced when the breaker closes at the peak voltage 90^{O}, which could occur on any three phases as the breaker tries to close all three phases simultaneously. The energization simulations of all four filters seen in Figures 5.44(a) to 5.44(d), were conducted using ATP to determine which filter experiences the highest and lowest overvoltage levels. According to the simulation done the overvoltage experienced was found to be 963V for the single-tuned filter, 987 V for the double-tuned filter, 798 V for the C-Type filter, and 788 V for the high pass filter. The overvoltage observed during energization

was highest for the double-tuned filter and the lowest for the high pass filter as seen in Table 5.26.

Table 5.26: Overvoltage during energization

Filter	Overvoltage experienced during energization
Single-tuned filter	963 V
Double-tuned filter	987 V
C-Type filter	798 V
High pass filter	788 V

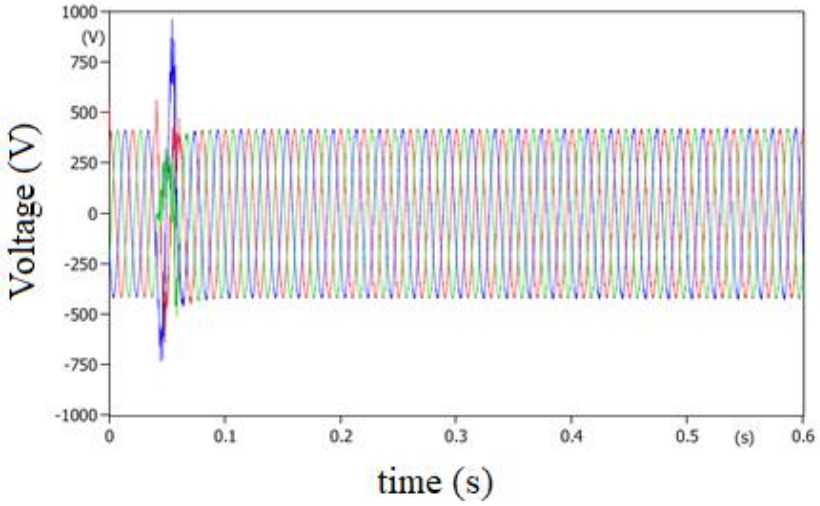

Figure 5.44(a): Energization of single-tuned filter

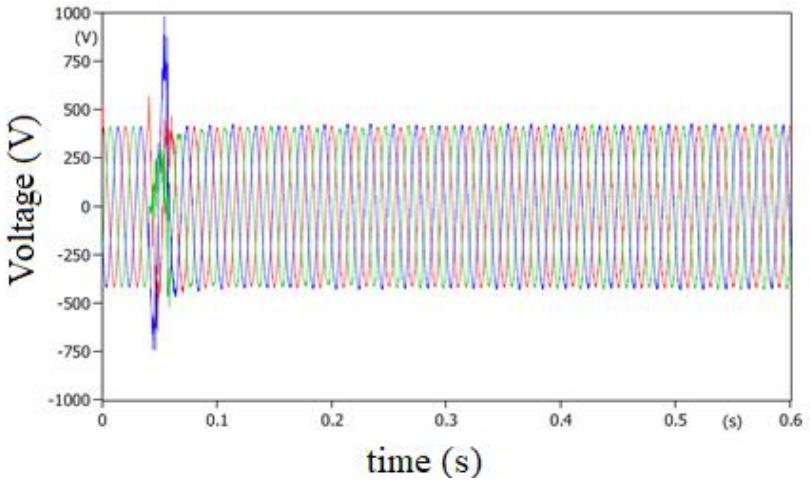

Figure 5.44(b): Energization of double-tuned filter

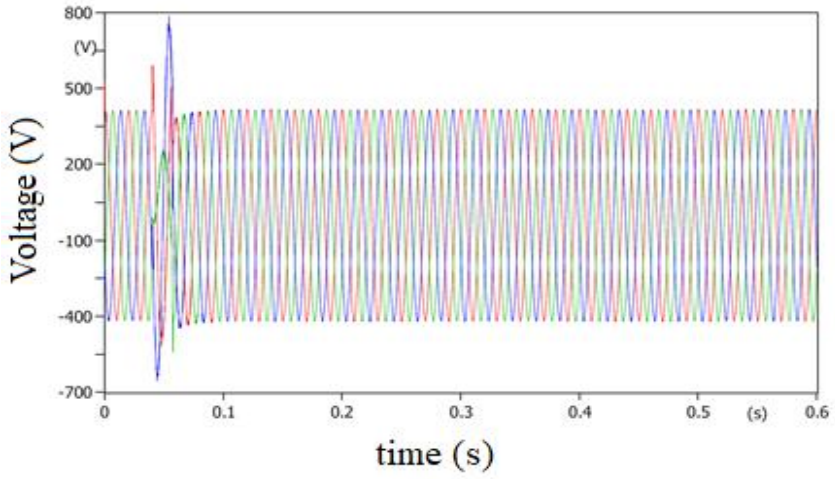

Figure 5.44(c): Energization of C-Type filter

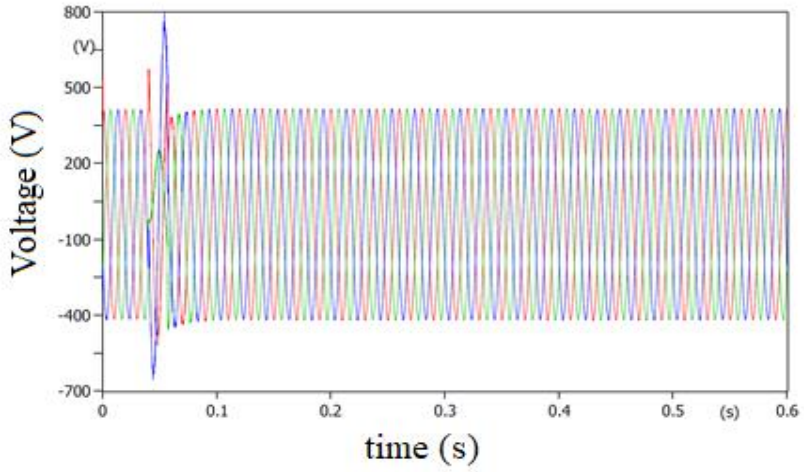

Figure 5.44(d): Energization of high pass filter

5.16.2 De-Energization of Harmonic Filters

In many applications, harmonic filters are switched daily causing temporary overvoltage across components of the filter that may exceed the voltage at the bus. During de-energization the filter is opened to the system, causing interruption to the circuit. To study the switching of the harmonic filters, the filters were simulated as shown in Figures 5.45(a) to 5.45(d), with the aid of ATP software. According to the simulation done the overvoltage experienced was found to be 1007 V for the single-tuned filter, 1017 V for the double-tuned filter, 942 V for the C-Type filter, and 973 V for the high pass filter when the circuit breaker was opened at 0.04 s. According to the results compiled in Table 5.27, the double-tuned filter experienced the highest overvoltage levels, whilst the C-Type filter experienced the lowest overvoltage levels during the de-energization scenario.

Table 5.27: Overvoltage during de-energization

Filter	Overvoltage experienced during de-energization
Single-tuned filter	1007 V
Double-tuned filter	1017 V
C-Type filter	942 V
High pass filter	973 V

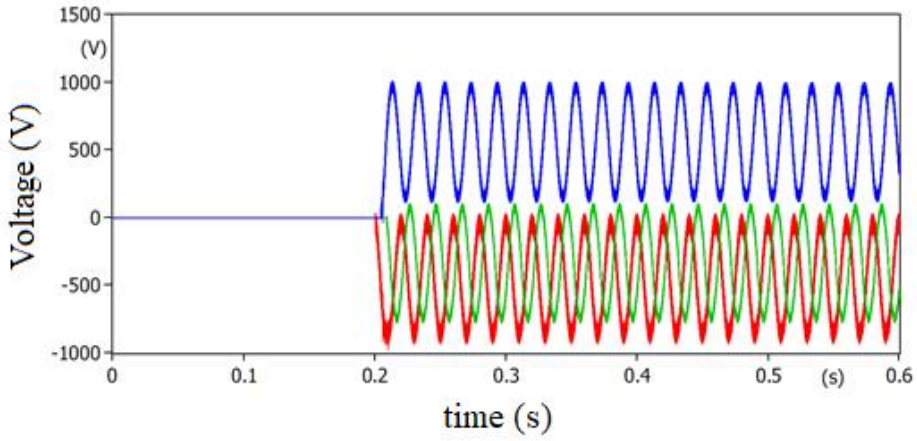

Figure 5.45(a): De-energization of single-tuned filter

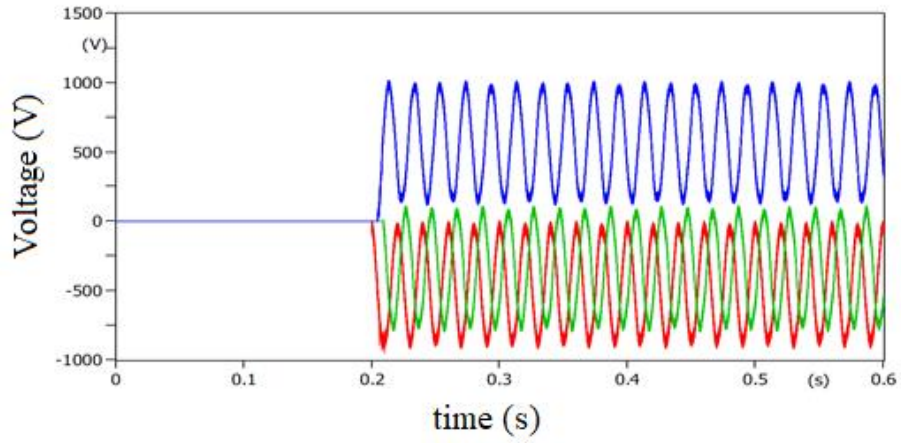

Figure 5.45(b): De-energization of double-tuned filter

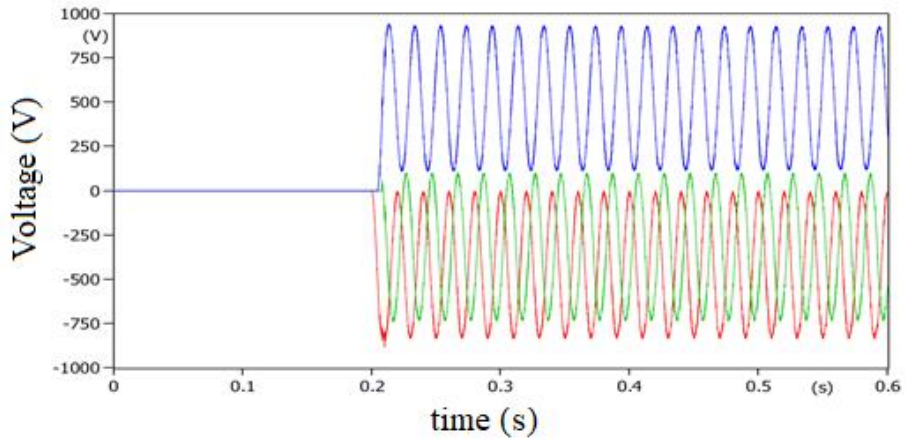

Figure 5.45(c): De-energization of C-Type filter

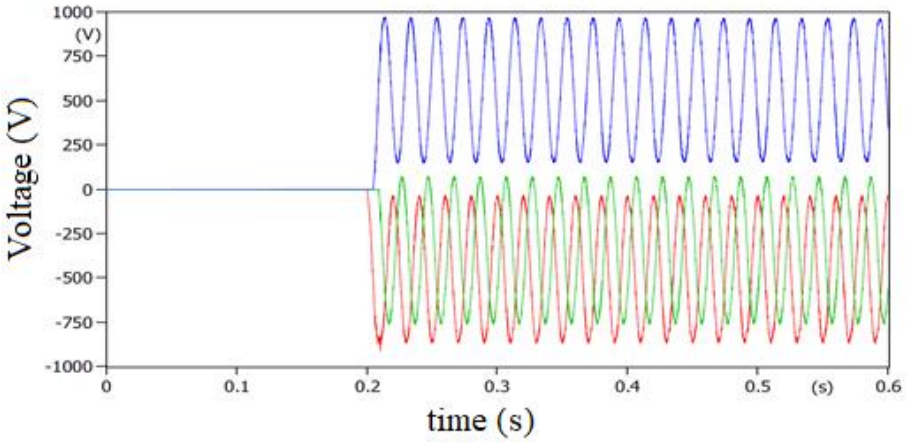

Figure 5.45(d): De-energization of high pass filter

5.17 Mitigation of Overvoltage for Case Study 2

To reduce the temporary overvoltage caused by the switching of the harmonic filter, various mitigation techniques must be discussed. Therefore, the use of pre-insertion resistor, controlled switching, and sure arrester are explored.

5.17.1 Pre-Insertion Resistor

The use of a pre-insertion resistor can be an effective measure to mitigate overvoltage by acting as a bypass across the circuit breaker before the filter is energized. Figures 5.46(a) to 5.46(d), show the resultant voltage waveform of the simulations conducted on ATP. When the pre-insertion resistor is connected to the network during energization, the overvoltage of the double-tuned filter is reduced the most by 560 V whilst the high pass filter experiences the lowest reduction in overvoltage with a value of 347 V. The results of the simulation upon the implementation of the pre-insertion resistor are tabulated in Table 5.28 below.

Table 5.28: Mitigation using pre-insertion resistor

Filters	Resistor value	Overvoltage before	Overvoltage after
Single-tuned filter	0.611	963 V	474 V
Double-tuned filter	0.146	987 V	427 V
C-Type filter	0.142	788 V	425 V
High pass filter	0.61	798 V	451 V

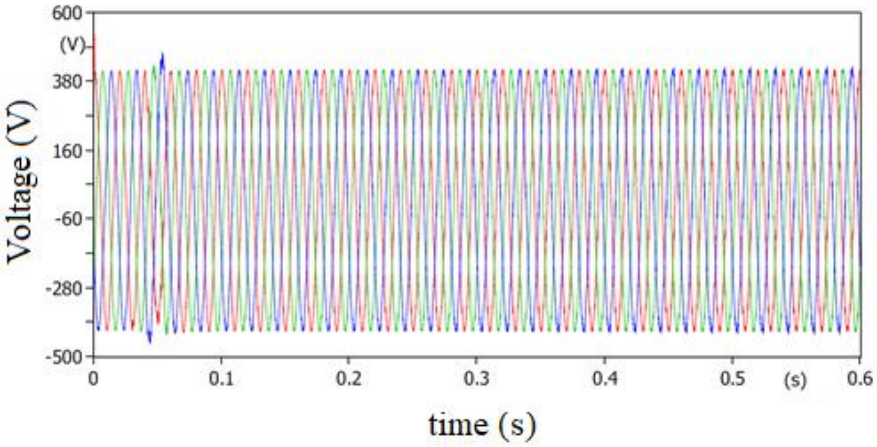

Figure 5.46(a): Using pre-insertion resistor for single-tuned filter

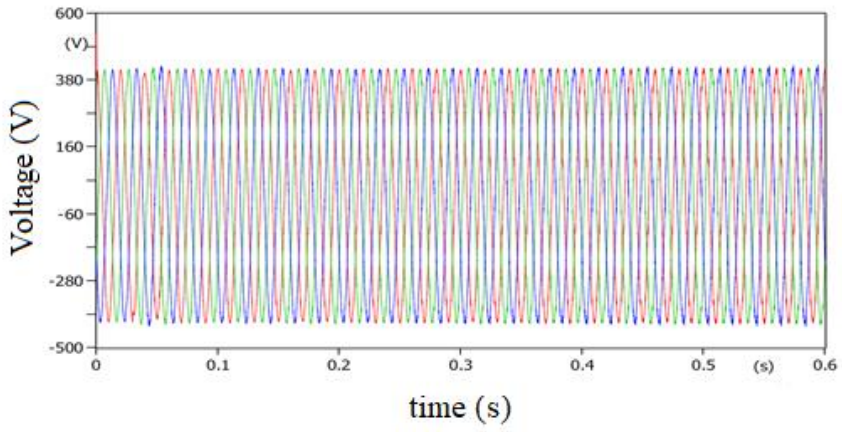

Figure 5.46(b): Using pre-insertion resistor for double-tuned filter

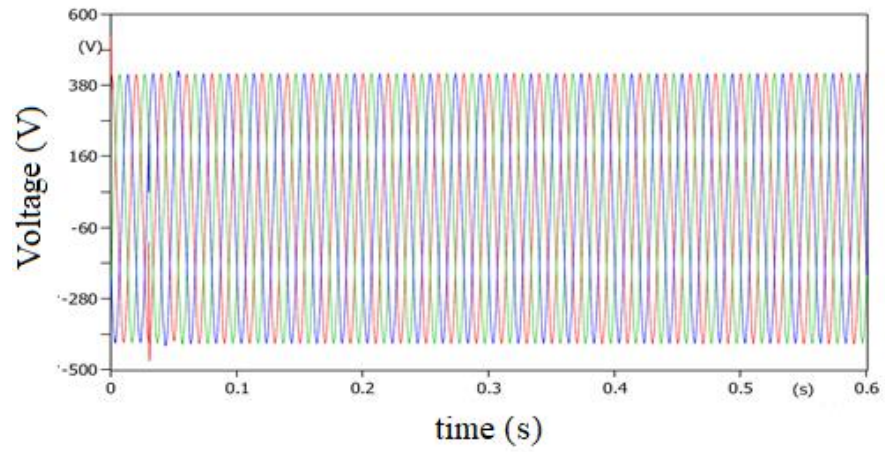

Figure 5.46(c): Using pre-insertion resistor for C-Type filter

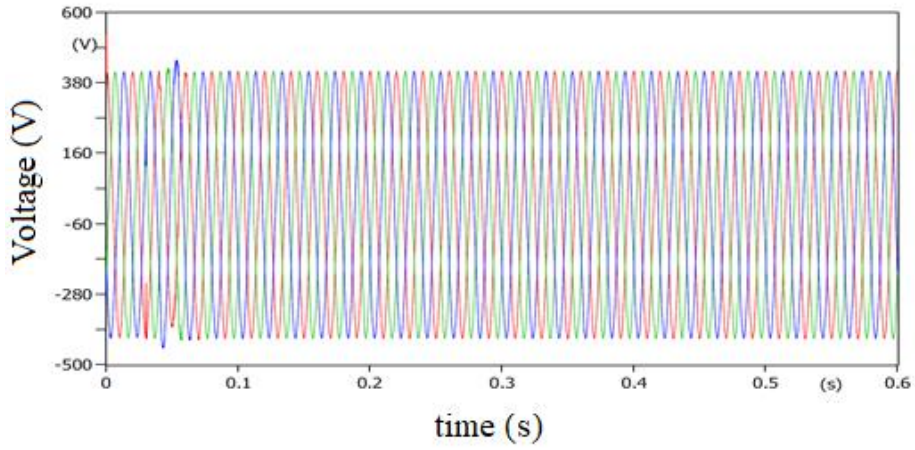

Figure 5.46(d): Using pre-insertion resistor for high pass filter

5.17.2 Controlled Switching

Controlled switching allows for the mechanical closing or opening of circuit breaker contacts at an optimal time. In many studies, it has been proven as a desirable method in reducing switching overvoltages. To mitigate the overvoltage the circuit breaker must close when the voltage across the breaker pole is at its minimum, usually at zero crossing. To determine the effects that the controlled switching would have on the resultant waveform, all four filters were simulated using ATP. The double-tuned filter showed the best results with a reduction of 242 V after using controlled switching. The worst performing filter is the C-Type filter with a reduction of 150 V. The resultant voltage waveforms of the simulations are shown in Figures 5.47(a) to 5.47(d) and the findings are tabulated in Table 5.29.

Table 5. 29: Mitigation using controlled switching

Filters	Overvoltage before	Overvoltage after
Single-tuned filter	963 V	737 V
Double-tuned filter	987 V	745 V
C-Type filter	788 V	638 V
High pass filter	798 V	640 V

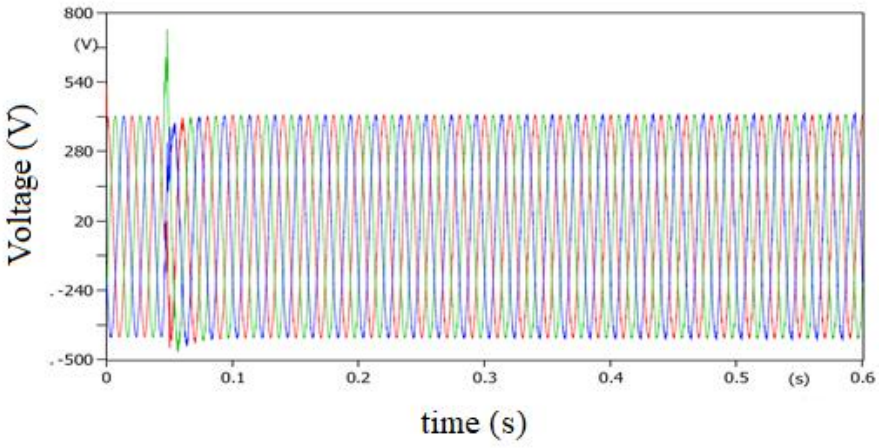

Figure 5.47(a): Using controlled switching for single-tuned filter

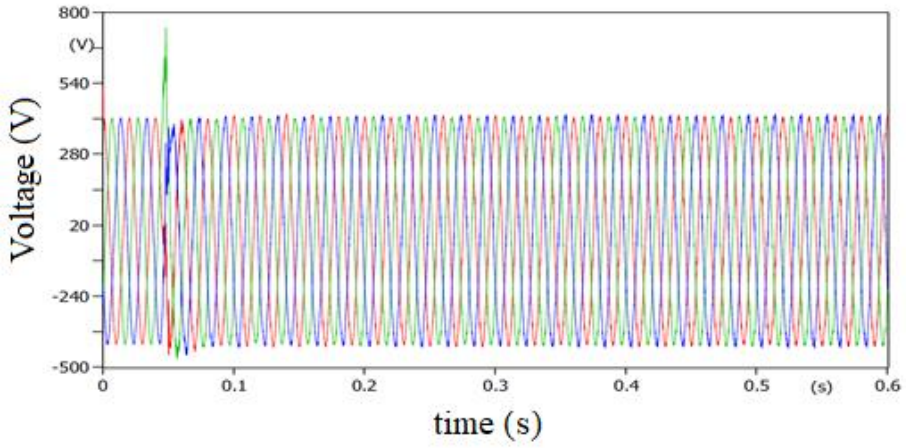

Figure 5.47(b): Using controlled switching for double-tuned filter

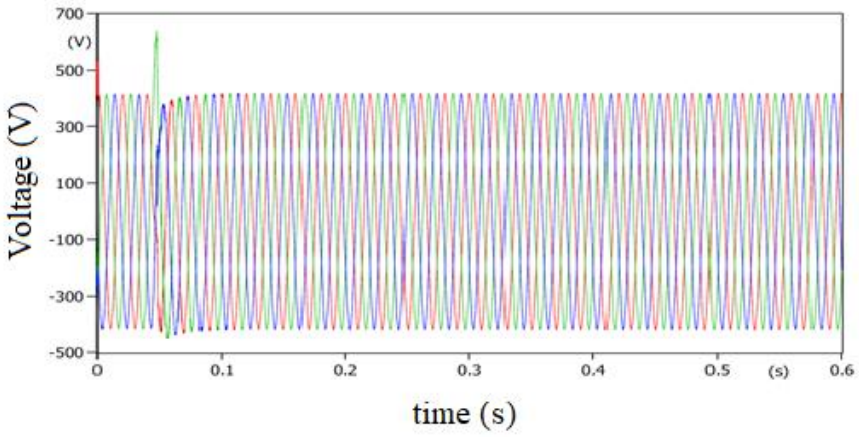

Figure 5.47(c): Using controlled switching for C-Type filter

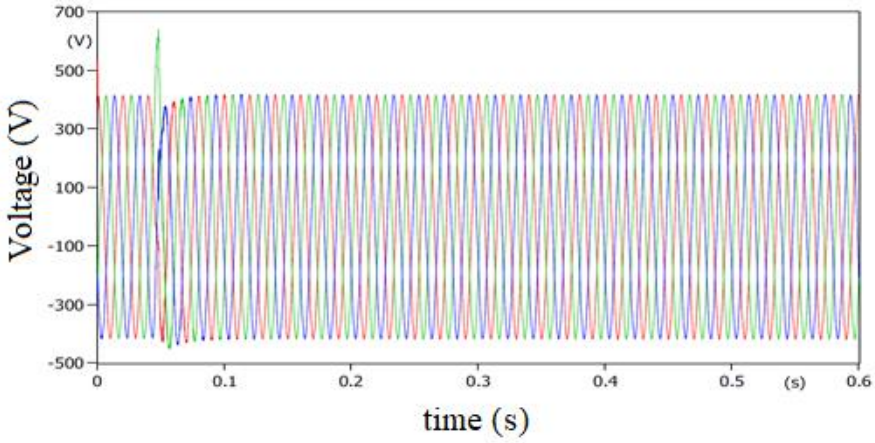

Figure 5.47(d): Using controlled switching for high pass filter

5.17.3 Surge Arrester

There are many models of surge arresters available to represent the behaviour of a metal oxide surge arrester during switching overvoltage. In this study, the surge arrester will be modelled after the IEEE surge arrestor model. The filters are simulated using ATP to determine the effects that the surge arrester would have in reducing overvoltage levels. The results show that the overvoltage of the double-tuned filter is reduced the most by 573 V whilst the C-Type filter experiences the lowest reduction in overvoltage with a value of 367 V. Figures 5.48(a) to 5.48(d), show the resultant voltage waveform of the simulation and the findings are tabulated in Table 5.30.

Table 5.30: Mitigation using surge arrester

Filters	Overvoltage before	Overvoltage after
Single-tuned filter	963 V	413 V
Double-tuned filter	987 V	414 V
C-Type filter	788 V	421 V
High pass filter	798 V	416 V

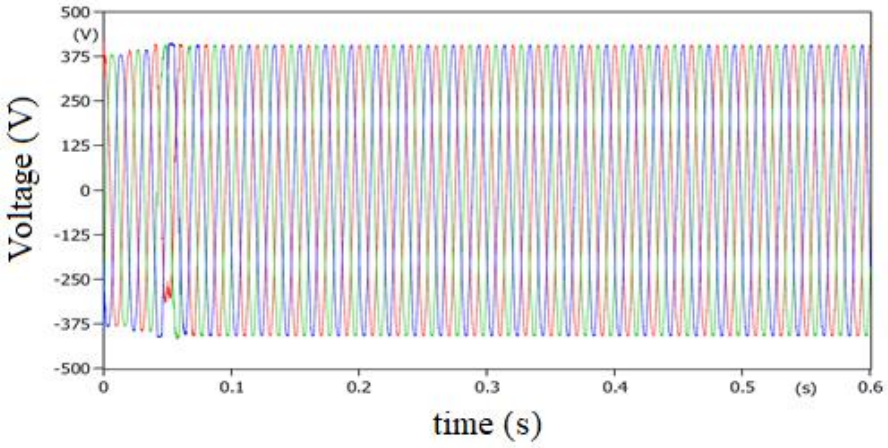

Figure 5.48(a): Using surge arrester for single-tuned filter

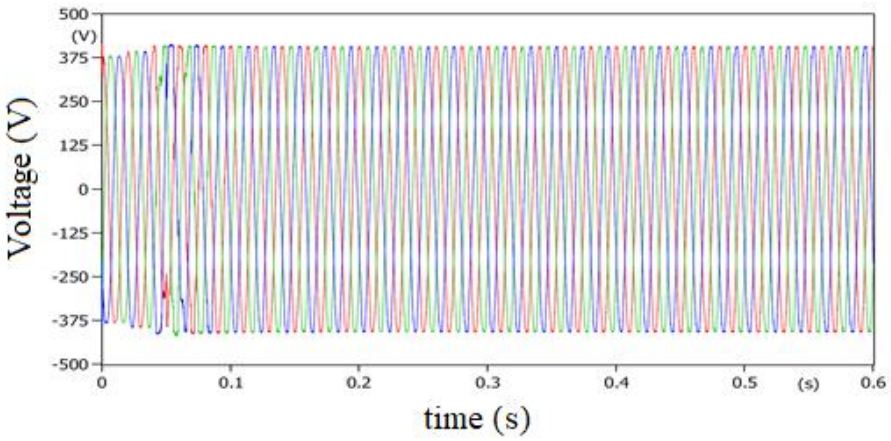

Figure 5.48(b): Using surge arrester for double-tuned filter

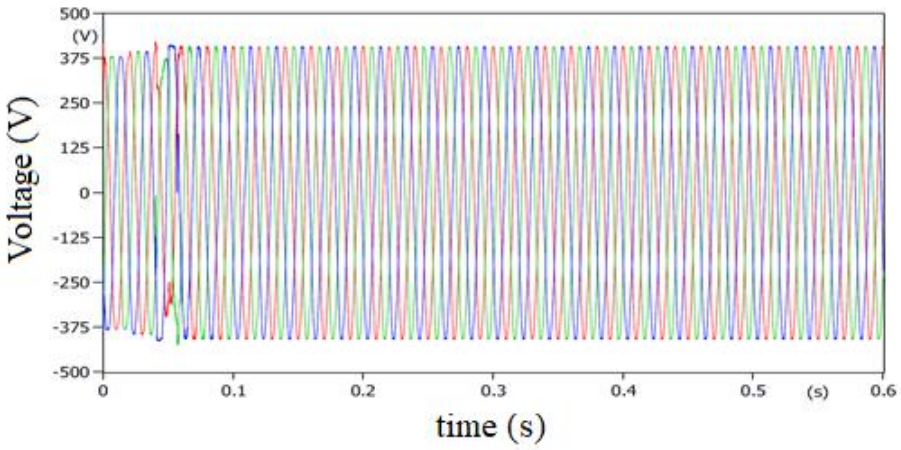

Figure 5.48(c): Using surge arrester for C-Type filter

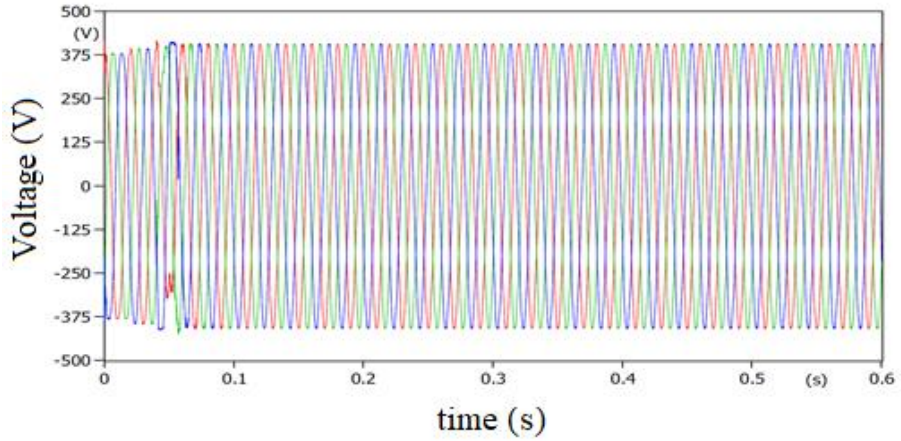

Figure 5.48(d): Using surge arrester for high pass filter

5.17.4 Conclusion on Mitigation Methods for Case Study 2

Upon analysis of the results obtained of the three different mitigation techniques, it was concluded that the surge arrester was most effective in mitigating the overvoltage. The surge arrester has managed to decrease the overvoltage by approximately 61%, making it the best option in limiting excessive voltage in the power system. Mitigation using controlled switching was the least effective in suppressing the overvoltage compared to using a pre-insertion resistor or surge arrester.

5.18 Case Study 3: Harmonics in Stationery Manufacturing Industry

The stationery manufacturing industry produces books, binders, and other paper products for commercial and industrial use. Sophisticated computer software is used to produce large volumes of books that are identical in size and quality. This process of producing books uses several motors and drive systems to operate equipment such as the conveyors, the packaging

machinery, and the printing presses. The motor and drive systems must operate according to the number of books being printed and the demand placed for the finished product. The operation of these high-speed motors can cause harmonic distortion, posing a threat to electronic devices in the system.

5.19 Details of Network Layout

The network shown in Figure 5.49, is made up of a six-drive system, with each drive controlling a single motor. An 11 kV supply is fed from a nearby substation and is stepped down to 415 V by transformer 1. The system is protected by a 1000 A, 11 kV vacuum circuit breaker that will trip if a fault is detected to prevent damage to the main transformer. Circuit breakers 2, 3, 4, 5, 6, and 7 are connected to VSD1, VSD2, VSD3, VSD4, VSD5, and VSD6 respectively. The circuit breaker acts as an electrical switch to protect the VSD's from damage that may be caused by overload or short circuits. The kW rating of each VSD is chosen according to the motor's power rating. The motor is rated at 50 Hz and 1800 rpm with a power factor of 0.83. The ratings of each component in the network are presented in Table 5.31.

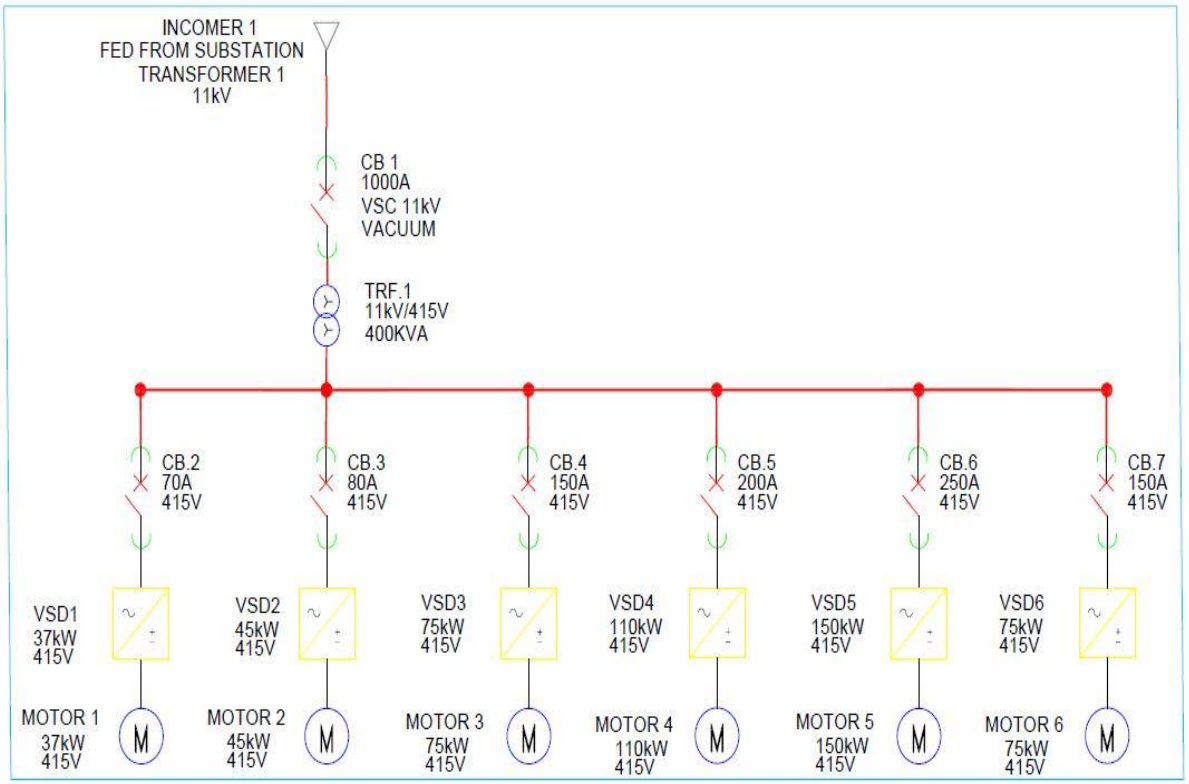

Figure 5.49: Network layout for the stationery manufacturing industry

Table 5.31: Component ratings for the network: case study 3

Components	Ratings
Incomer supply	11 kV
CB 1	1000 A
TRF 1	11 kV/415 V
CB 2	70 A
CB 3	80 A
CB 4	150 A
CB 5	200 A
CB 6	250 A
CB 7	150 A
VSD 1	37 kW
VSD 2	45 kW
VSD 3	75 kW
VSD 4	110 kW
VSD 5	150 kW
VSD 6	75 kW
Motor 1	37 kW
Motor 2	45 kW
Motor 3	75 kW
Motor 4	110 kW
Motor 5	150 kW
Motor 6	75 kW

5.20 Network Analyser Results for Case Study 3

To determine the level and order of harmonic in the system, a harmonic analyser was installed at the main incomer panel for at least 7 days. The device was able to measure and record the frequencies, amplitudes, and various components of the non-sinusoidal waveform. The analyser helps provide a thorough analysis of any power quality issues that may exist in the system. Similar to case studies 1 and 2, the following parameters were measured using the voltage analyser; voltage, current, power, power factor, and harmonics

Voltage: The voltage of the system was measured between a maximum value of 418 V and a minimum value of 387 V as shown in Figure 5.50. The actual voltage used in the plant is 415

V and remains steady during the entire production. The plant runs 24 hours a day and maximum voltage was consumed during off-peak times.

Figure 5.50: Voltage graph

Current: The current of the system was measured between a maximum value of 850 A and a minimum value of 400 A as shown in Figure 5.51. The current was steady during system operation maintaining the continuous running of motors in the system ensuring steady production in the plant.

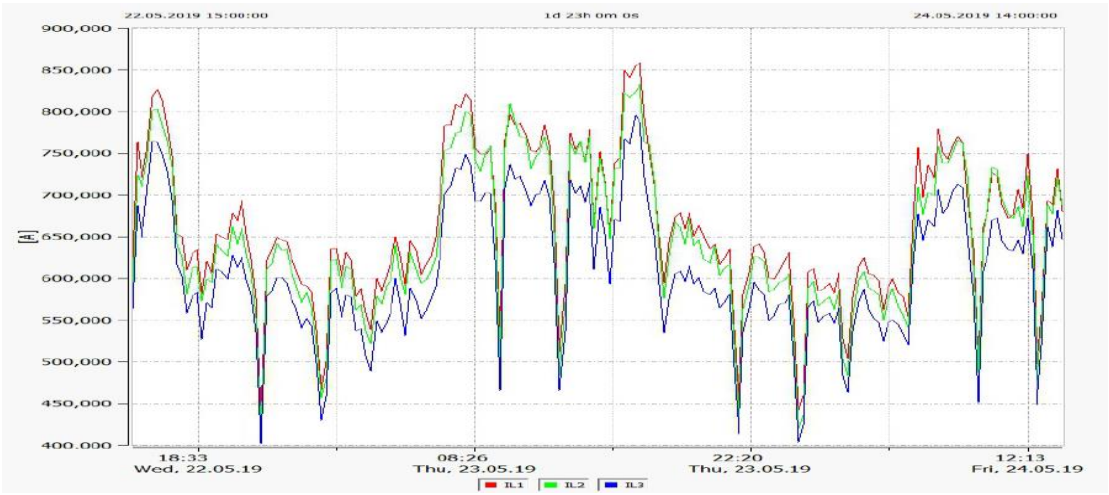

Figure 5.51: Current graph

Power: The power of the system was measured between a maximum value of 500 kW and a minimum value of 280 kW. Similar to case study 2, the industry was billed on a TOU tariff, therefore, the maximum power is consumed during off-peak periods. The waveform for power is presented in Figure 5.52.

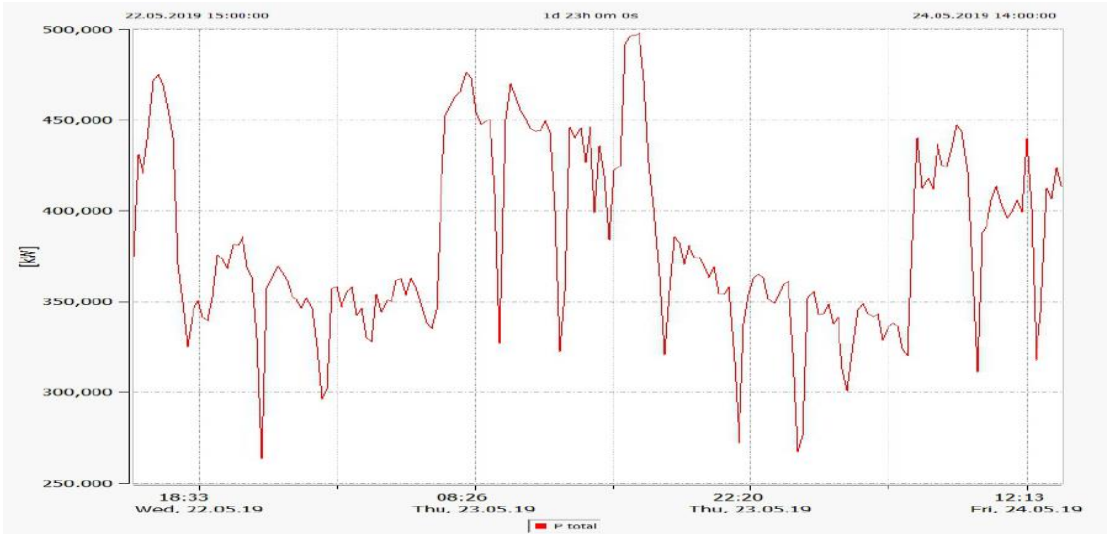

Figure 5.52: Power graph

Power Factor: The power factor of the system reaches a maximum value of 0.94 and a minimum value of 0.782 as shown in Figure 5.53. The average power factor during production was approximately 0.8. This poor factor may result in higher currents required by the equipment and due to which the economic cost of the equipment is increased.

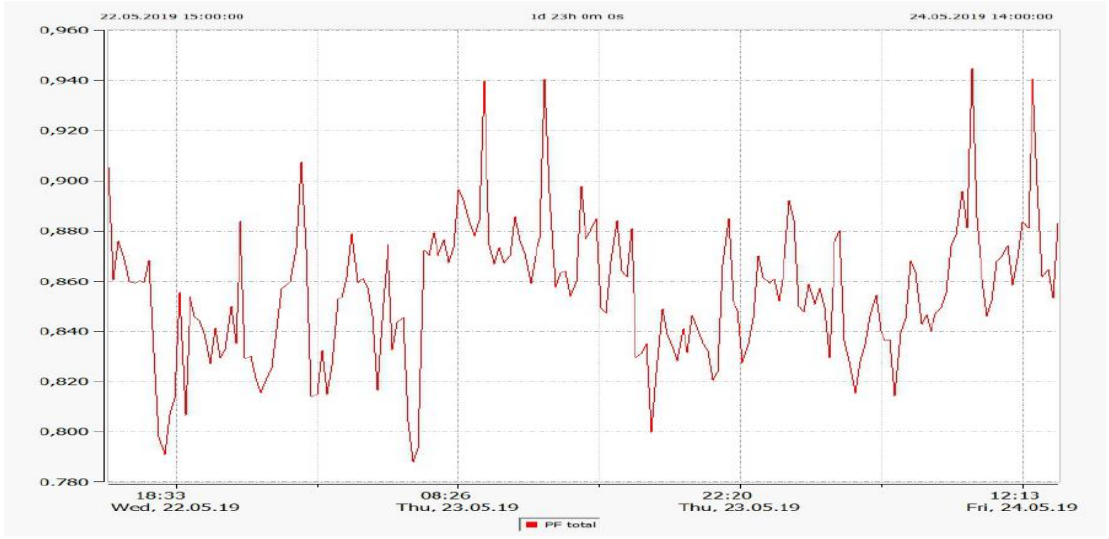

Figure 5.53: Power factor graph

THDV: The voltage harmonics in this system run at an average of 4% but reaches a maximum of 5.35%. This is higher than the limit prescribed by the IEEE 519-1992 standards. The installation of harmonic filters will help reduce the amount of voltage distortion found in the system. The waveform is given in Figure 5.54.

Figure 5.54: Voltage THD graph

THDI: The current harmonics in this system run at an average of 12% but reach a maximum of 18%. Current harmonics are higher when motors run at full load or during peak production times. This causes adverse effects such as overheating and malfunctioning of electronic equipment due to the distortion of the current waveform. The waveform is shown in Figure 5.55.

Figure 5.55: Current THDI graph

5.21 System Modelling in ATP for Case Study 3

The electrical network of the stationery manufacturing industry is shown in Figure 5.56, was modelled using the ATP/EMTP software. Each component was modelled using the ratings as presented in Table 5.31. The transformer was modelled using the BCTRAN model on the ATP. The transformer was connected to the VSD's through an 8 m long single core cable and each

VSD was connected to its respective motor using a 4 m long cable and the cable was modelled using the *PI* model on ATP. To determine the harmonics that the VSD's produce during their operation, each VSD was modelled to operate with a suitably sized motor. The motors were modelled using the single cage rotor model on the ATP software.

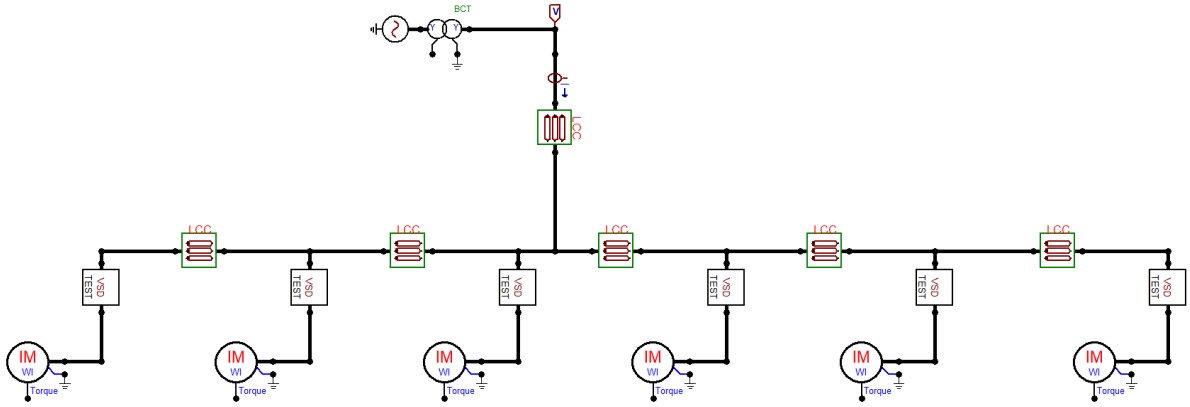

Figure 5.56: ATP simulation model

5.21.1 Modelling of AC Voltage Source

The 3-phase AC voltage source was modelled using the parameters are presented in Table 5.32. The *L-L* voltage was 11 kV with a frequency of 50 Hz. The source is grounded and has a phase shift of 0°.

Table 5.32: Source parameters

Parameter	Value
Amplitude (V)	11000
Frequency (Hz)	50
Start A (sec)	-1
Stop A (sec)	100
Number of phases	3. Phase

5.21.2 Modelling of Transformer

Using the BCTRAN model on ATP, the 3-phase transformer was modelled to step down the incoming voltage from 11 kV to 415 V. The power rating of the transformer is 0.5 MVA with a Yy0 connection. The structure of the transformer has 3-three phase terminals and 1-single phase neutral points common to the primary and secondary windings. The BCTRAN component can be edited and connected to the main circuit. Table 5.33, shows the parameters of the transformer as modelled on ATP.

Table 5.33: Transformer parameters

Parameter	Value
Vector group	Yy0
Rated power	0.5 MVA
Open-circuit voltage (%)	100
Open-circuit current (%)	0.55
Open-circuit losses (kW)	1.6
Short-circuit impedance HV-LV (%)	3.2
Short-circuit impedance losses (kW)	1.56

5.21.3 Modelling of Variable Speed Drives

The variable speed drive was modelled using ATP software with parameters such as switching frequency and DC link capacitor values are required to simulate the operation of the VSD. The switching frequency was used to convert the DC voltage to a simulated AC voltage which leads to harmonic distortion. The DC-link capacitor value is calculated using equation (3.1). The parameters of the VSD are represented in Table 5.34.

Table 5.34: VSD parameters for case study 3

Parameters	VSD 1	VSD 2	VSD 3	VSD 4	VSD 5	VSD 6
Frequency (Hz)	50	50	50	50	50	50
Am ratio	0	0	0	0	0	0
Switching freq (Hz)	3500	2500	2500	3500	3500	2500
Capacitor (µf)	308300	319400	580658	770700	1161271	580658

5.21.4 Modelling of Motors

The motor was modelled on the ATP using the single cage rotor model. The system is made up of six motors that have a rated speed of 1800 rpm. The *L-L* voltage of each of the motors is 415 V and the starting current is 7 times that of the rated current. The motor parameters such as frequency, power, speed, and efficiency are obtained from the name plate details of the individual motors. Table 5.35, shows the parameters for the motor drive.

Table 5.35: Motor drive parameters

Parameters	Motor 1	Motor 2	Motor 3	Motor 4	Motor 5	Motor 6
Frequency (Hz)	50	50	50	50	50	50
Voltage L-L (kVrms)	0.293	0.293	0.293	0.293	0.293	0.293
Power (hp)	49.62	60.35	100.58	147.51	201.15	100.58
Speed (rpm)	1800	1800	1800	1800	1800	1800
Power factor (cos phi)	0.8	0.8	0.8	0.8	0.8	0.8
Efficiency (pu)	0.75	0.75	0.75	0.75	0.75	0.75
Slip (%)	0.72	0.72	0.72	0.72	0.72	0.72
Start current (pu)	7	7	7	7	7	7
Start torque (pu)	0.5	0.5	0.5	0.5	0.5	0.5
Load torque (pu)	1	1	1	1	1	1
Max torque (pu)	1.5	1.5	1.5	1.5	1.5	1.5

5.22 Simulation Results

- **Voltage Graph**

The 3-phase voltage sine wave reaches a maximum value of 415 V at a frequency of 50 Hz. The simulation starts at 0 s and ends at 0.6 s. The sine wave has a periodic time of 0.02 s. Figure 5.57, shows the resultant voltage waveform of the system.

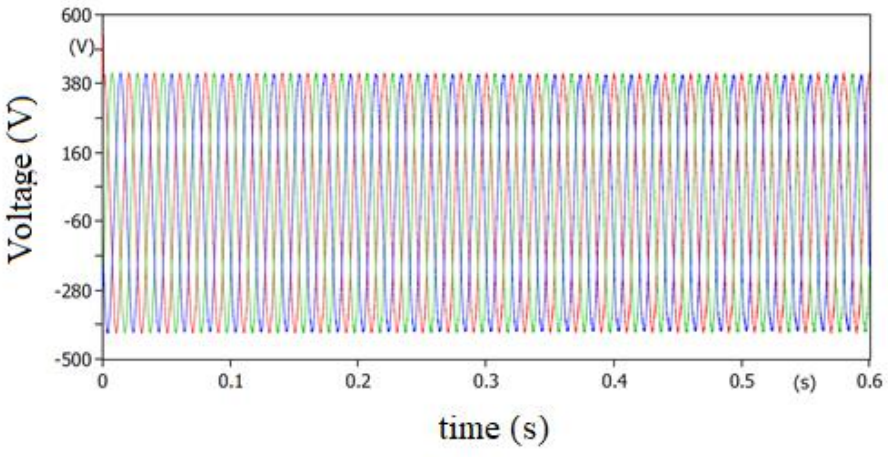

Figure 5.57: Voltage simulation graph

- **Harmonics Graph**

The graph shown in Figure 5.58 presents the harmonic present in the stationary manufacturing industry. The 400 kVA load with a 0.8 power factor produces 3^{rd} and 5^{th} harmonic currents.

The 3rd harmonic reaches a maximum value of 13.174 V and the 5th harmonic reaches a maximum value of 9.943 V. The THD of the system was found to be 5.344 %. This is over the IEEE 519-1992 standards of 5 % or lower for THD. The use of harmonic filters will help in eliminating the harmful harmonics and also will keep the equipment in good working condition for a lot longer.

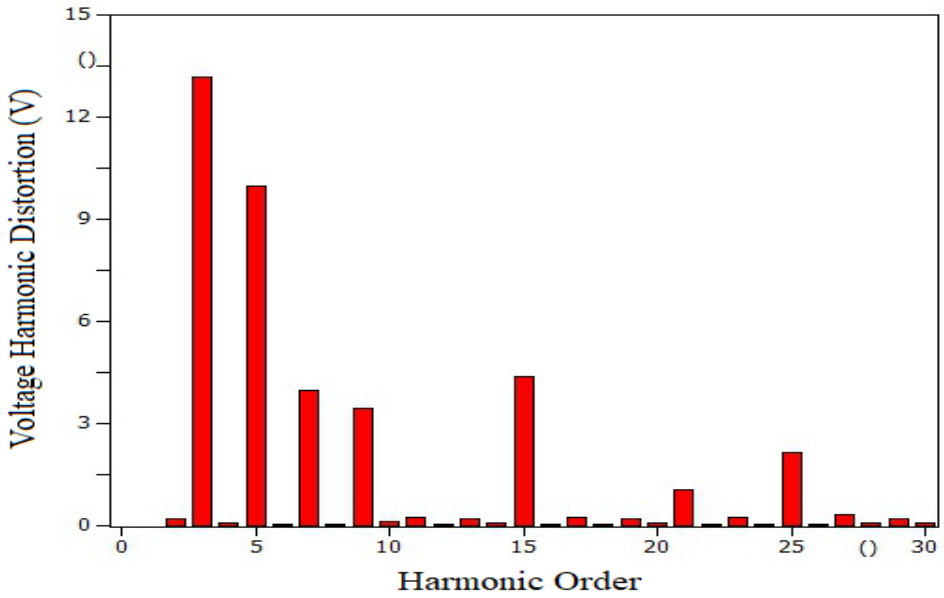

Figure 5.58: Harmonics simulation graph

5.23 Mitigation of Harmonics

5.23.1 Harmonic Filters for Case Study 3

Case study 3 was developed similarly to what was done for case studies 1 and 2, where the four filters were simulated in the ATP software.

5.23.1.2 Simulation of Single-tuned Harmonic Filter

The single-tuned harmonic filter was simulated with the use of ATP/EMTP software. The filter was connected to the main bus to mitigate the harmonics produced during the VSD's operation. Figure 5.59, shows the connection of the single-tuned filter to the network system.

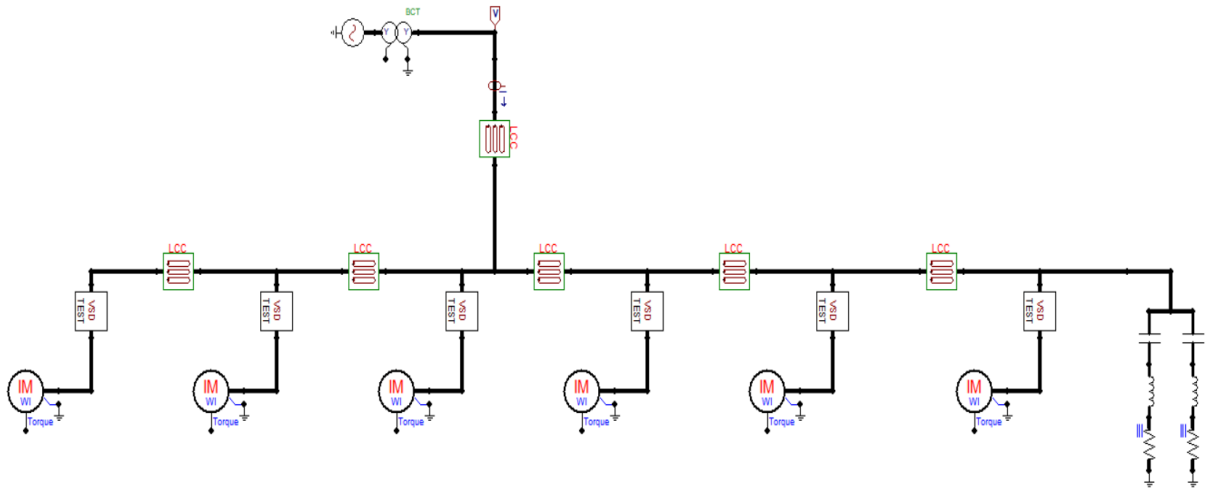

Figure 5.59: Simulation model with single-tuned filter

5.23.1.1 Single-tuned Harmonic Filter

The single-tuned harmonic filter which is a series *RLC* circuit is used to reduce low order harmonics. Table 5.36, presents the parameters of the single-tuned harmonic filter.

Table 5.36: Single-tuned filter parameters

Parameter	Q_f (KVAr)	R_f(Ω)	C_f (µf)	L_f (mH)
3rd	293	0.333	4813.589	0.23387
5th	293	0.6324	5198.68	0.7796

5.23.1.3 Results of Single-tuned Filter Simulation

The single-tuned harmonic filter was able to reduce the THD by 95.9 % compared to filter-less testing results. The 3rd harmonic was reduced from 13.174 V to 0.275 V, while the 5th harmonic was reduced from 9.943 V to 0.779 V. There was a 97.9 % decrease in the 3rd harmonic and 92.16 % decrease in the 5th harmonic. Simulation modelling by using a single-tuned passive filter shows that the filter has the capability of decreasing the THD of the system to fulfill IEEE519-1992 standard requirements. The filter also has the capability of decreasing a desired harmonic order to an acceptable level as shown in Figure 5.60.

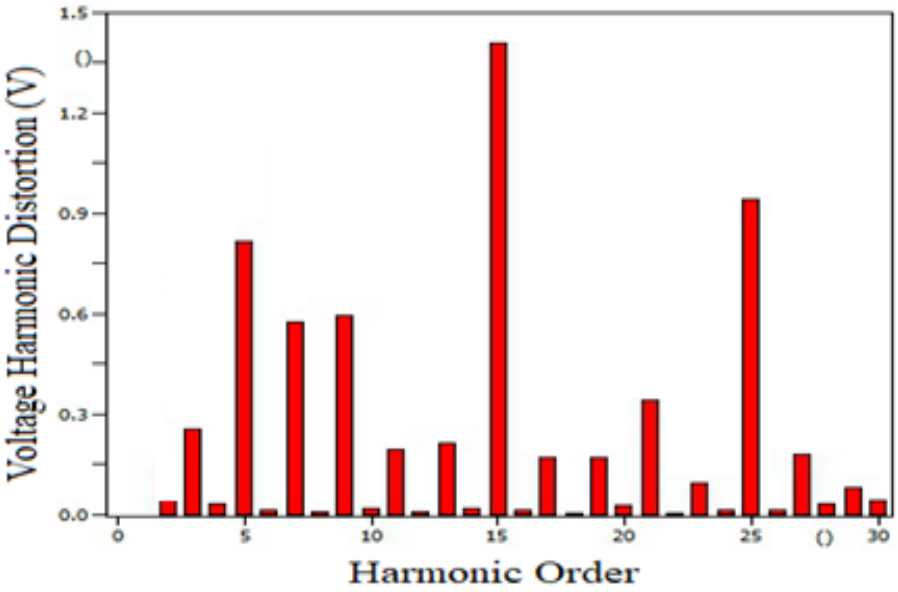

Figure 5.60: Harmonics simulation with single-tuned filter

5.23.2.1 Conventional Double-tuned Harmonic Filter

The double-tuned filter has the same function as the two single-tuned filters connected in parallel. Both filters can attenuate two different frequency harmonics at the same time. The filter has become a point of interest in the past few years for its ability to improve power factor, decrease current harmonic distortion and reduce individual harmonics within IEEE519-1992 limits. Table 5.37 shows the parameters of the double-tuned filter.

Table 5.37: Lumped parameters for double-tuned filter

Parameter	Q_f (KVAr)	C_1(µf)	L_1(mh)	C_2 (µf)	L_2(mh)
3^{rd} and 5^{th}	293	10012.269	0.1799	3003.72	0.08433

5.23.2.2 Simulation of Conventional Double-tuned Filter

The double-tuned filter is connected to the network system as shown in Figure 5.61. The filter is simulated using ATP software to observe the effects it would have in mitigating the harmful harmonics.

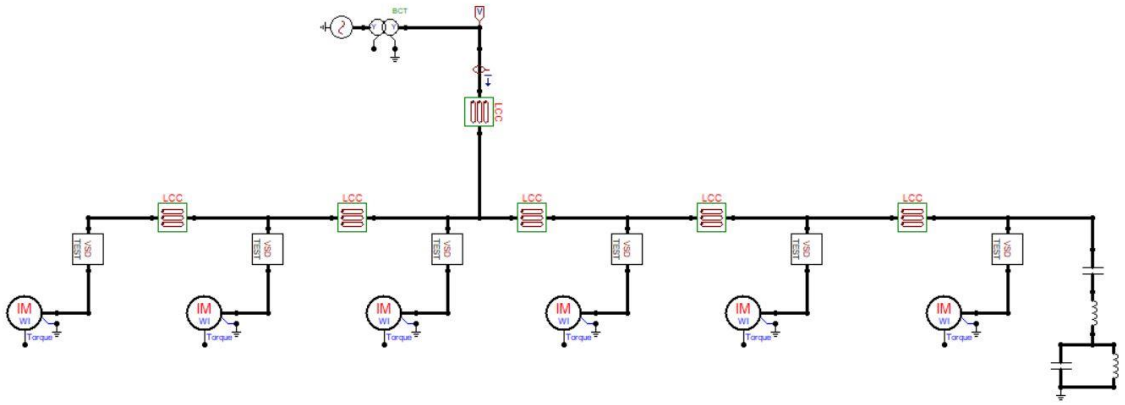

Figure 5.61: Simulation model with double-tuned filter

5.23.2.3 Results of Double-tuned Filter Simulation

When the double-tuned filter was installed in the system the 3rd harmonic decreased from 13.174 V to 0.417 V. The 5th harmonic also decreased from 9.943 V to 1.673 V. This means that there was a 96.83 % decrease in the 3rd harmonic and an 83.17 % decrease in the 5th harmonic. The resultant THD levels have been reduced to 0.406 % due to the operation of the double-tuned filter. Figure 5.62, shows the results of the filter simulation.

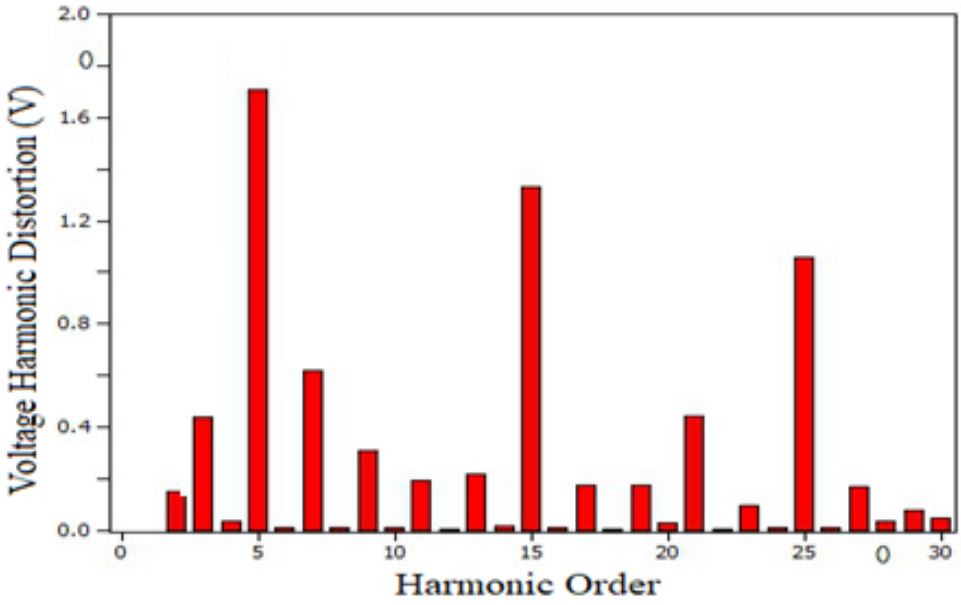

Figure 5.62: Harmonics graph with double-tuned filter

5.23.3.1 C-Type Harmonic Filter

The C-Type harmonic filter is used in many industries to ensure that it complies with harmonic limits specified by the utilities. The filter can reduce lower-order harmonics as well as higher-order harmonics since it is a broadband filter. The parameters to model the filter on ATP are shown in Table 5.38 below.

Table 5.38: Lumped parameters for C-Type filter

Parameter	Q_f Q_f(KVAr)	C_1	C_2(µf)	L (mH)	R(Ω)
3rd	293	5415.29	43322.3	0.23387	0.0152
5th	293	5415.29	129966.9	0.0779	0.0293

5.23.3.2 Simulation of C-Type Harmonic Filter

A simulation study was done and results are obtained using the ATP/EMTP software to show how filtering reduces harmonic distortion. The filter was connected to the network system to suppress the 3rd and 5th order harmonics. Figure 5.63 presents the filter connected to the main bus via a 2 m long cable to improve the power quality.

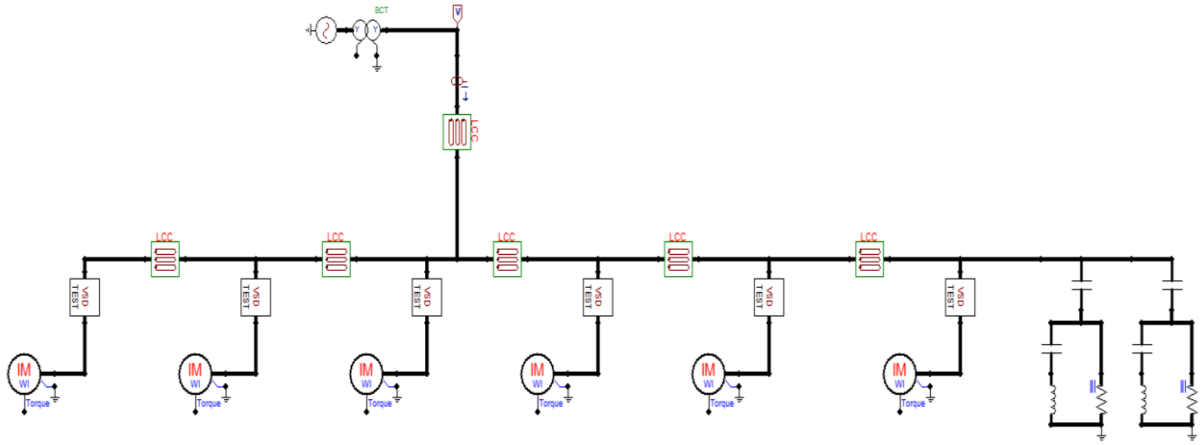

Figure 5.63: Simulation model with C-Type filter

5.23.3.3 Results of C-Type Filter Simulation

The connection of the C-Type harmonic filter to the network system has decreased both the 3rd and 5th order harmonic levels to an acceptable limit specified by the utilities. Figure 5.64, shows that the 3rd harmonic has decreased from 13.174 V to 0.719 V, while the 5th harmonic was decreased from 9.943 V to 1.853 V. This means that there is a 94.5 % decrease of the 3rd harmonic and an 81.36 % decrease of the 5th harmonic. The THD levels were reduced to 0.6384 %. The results obtained mean that the C-Type filter has effectively minimized the harmonic distortion at the point of common coupling.

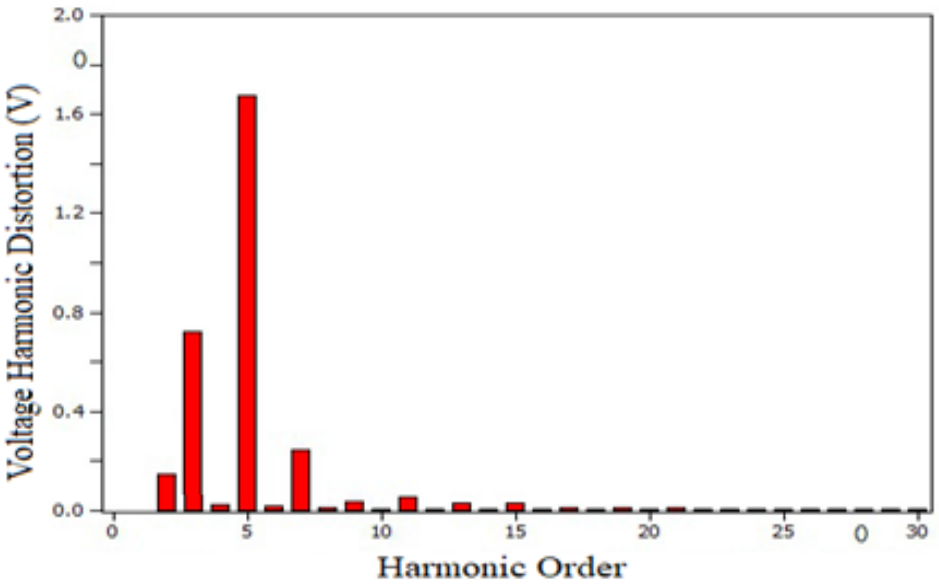

Figure 5.64: Harmonic reduction with C-Type filter

5.23.4.1 Second-order High Pass Filter

The second-order high pass filter is composed of a capacitor and an inductor that affect the response of the filter. The filter can attenuate the output voltage for all frequencies below the cut-off frequency. Above the cut-off frequency, the magnitude of the output voltage is constant. The advantage of this filter is its ability to provide greater roll-off rates between pass band and stop band. The parameters for simulating the filter on ATP are documented in Table 5.39.

Table 5.39: Lumped parameters for second-order high pass filter

Parameter	Q_f (KVAr)	C(µf)	L(mH)	R(Ω)
3^{rd}	293	4813.589	0.23387	0.4858
5^{th}	293	5198.68	0.07795	0.015

5.23.4.2 Simulation of Second-order High Pass Filter

Two second-order high pass filters are connected in parallel to attenuate the 3^{rd} and 5^{th} order harmonics. The operation of the filter was simulated using ATP software to determine if this filter would be a possible option in reducing harmonic distortion in the stationary industry. Figure 5.65 shows the connection of the filter to the existing network.

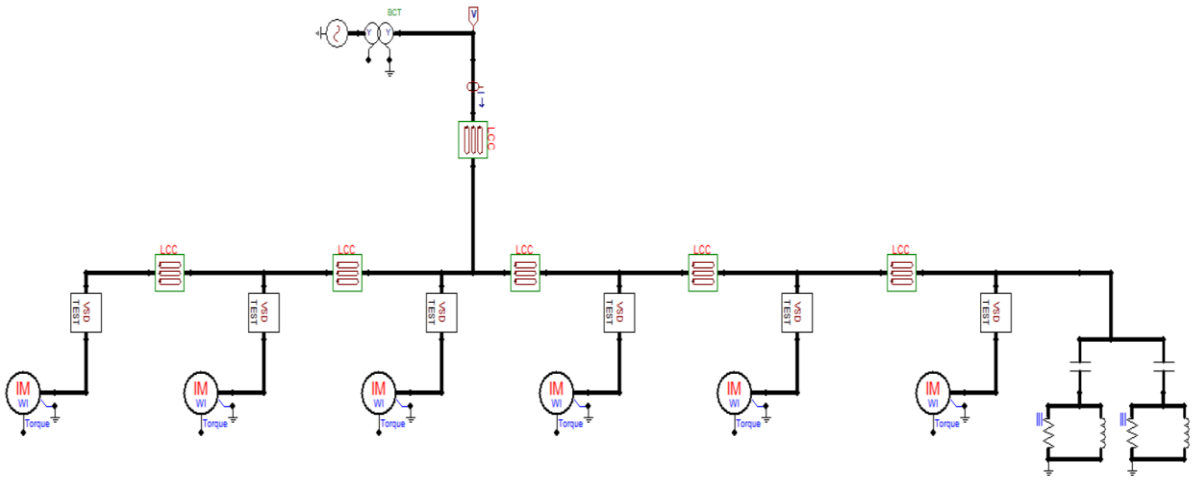

Figure 5.65: Simulation model using second-order high pass filter

5.23.4.3 Results of Second-order High Pass Filter Simulation

Figure 5.66, shows the harmonics present in the system after the installation of the high pass filter. The graph shows a decrease of the 3rd harmonic from 13.174 V to 0.931 V, whilst the 5th harmonic has decreased from 9.943 V to 1.8971 V. This means that there is a 92.9 % reduction in the 3rd harmonic and an 80.92 % reduction in the 5th harmonic. The THD was reduced to 0.6713 %.

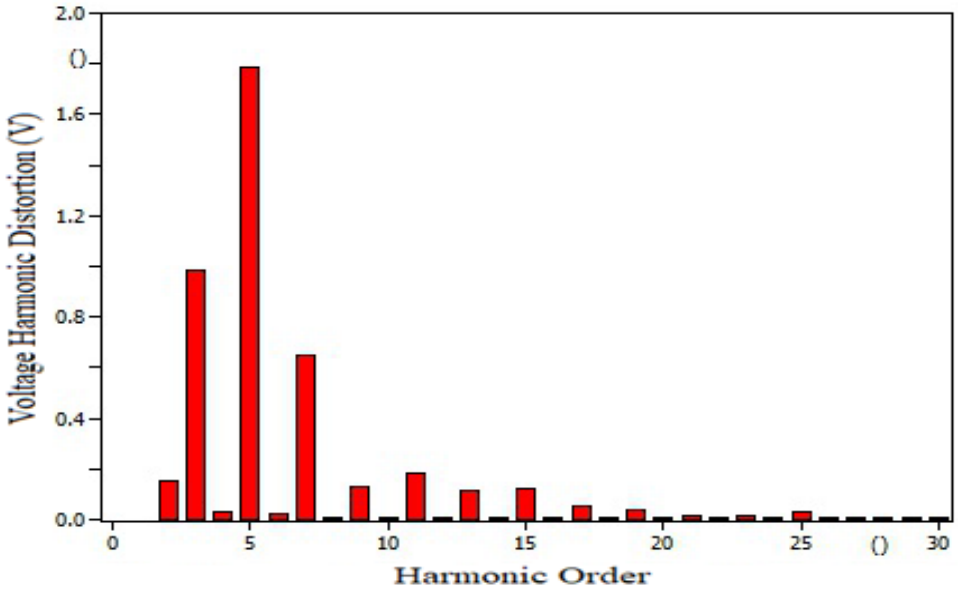

Figure 5.66: Harmonic reduction using second-order high pass filter

5.24 Harmonic Filter Analysis and Results for Case Study 3

With the help of ATP software each harmonic filter was simulated to determine the effects, it would have in mitigating the 3rd and 5th order harmonics. Based on the results compiled in Table 5.40, the best performing filter is the single-tuned filter. The single-tuned filter showed

the greatest improvement in the THD as well as the reduction of the 3rd and 5th harmonics. The worst performing filter was the high pass filter as the reduction of the 3rd and 5th harmonics is the lowest and it has the smallest improvement on THD levels. This is because the high pass filter is designed to have an impedance characteristic that is flat at high frequencies [92]. Therefore, this type of filter can mitigate higher harmonic orders. Whereas the single-tuned filter configuration offers low impedance at the tuning frequency and can be used to attenuate lower order harmonics (3rd, 5th, and 7th) at resonance conditions.

Table 5.40: Result of filter simulations

	Original network	Single-tuned	Double-tuned	C-Type	High pass
3rd harmonic	13.174	0.275	0.417	0.719	0.931
5th harmonic	9.943	0.779	1.673	1.853	1.897
THD (%)	5.344	0.2184	0.4061	0.6384	0.6913

5.24.1 Energization of Harmonic Filters

The energization simulations of all four filters were conducted using ATP software and are shown in Figures 5.67(a) to 5.67(d). Based on the simulation results, the overvoltage experienced was found to be 1050 V for the single-tuned filter, 1120 V for the double-tuned filter, 800 V for the C-Type filter, and 798 V for the high pass filter. The overvoltage observed during energization was highest for the double-tuned filter and the lowest for the high pass filter. The overvoltages exceed the voltage tolerance limit in the power system according to SANS 10142.1. Therefore appropriate mitigation measures need to be taken to meet industry standards. The results of the simulation are tabulated in Table 5.41.

Table 5.41: Overvoltage during energization

Filter	Overvoltage experienced during energization
Single-tuned filter	1050 V
Double-tuned filter	1120 V
C-Type filter	800 V
High pass filter	798 V

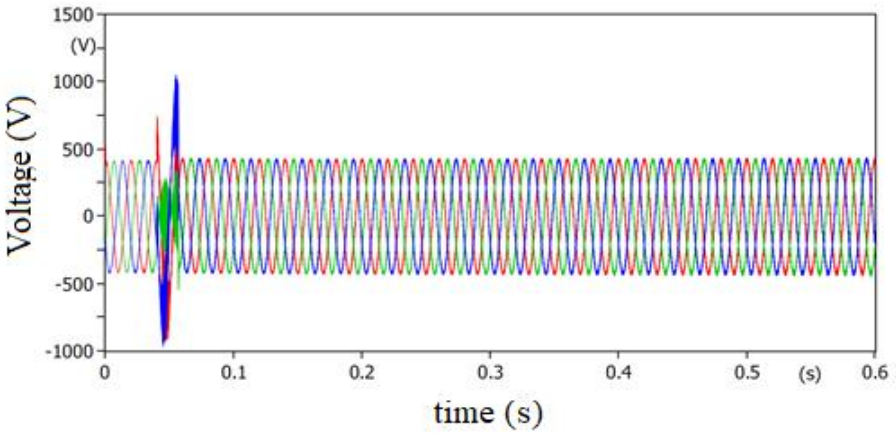

Figure 5.67(a): Energization of single-tuned filter

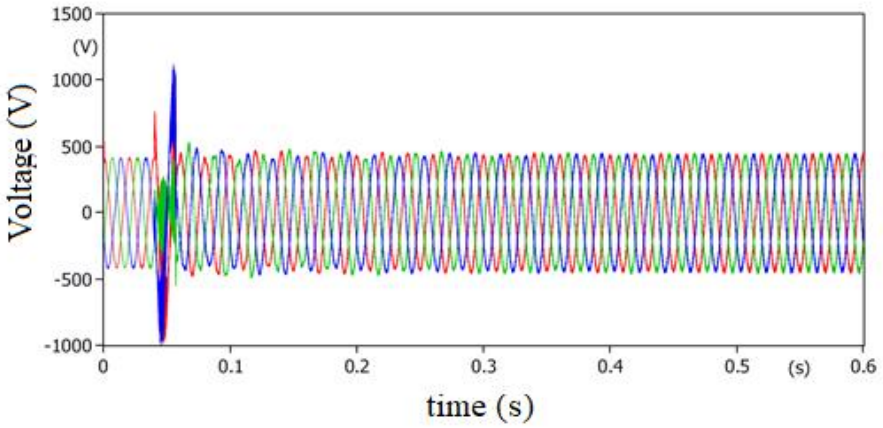

Figure 5. 67(b): Energization of double-tuned filter

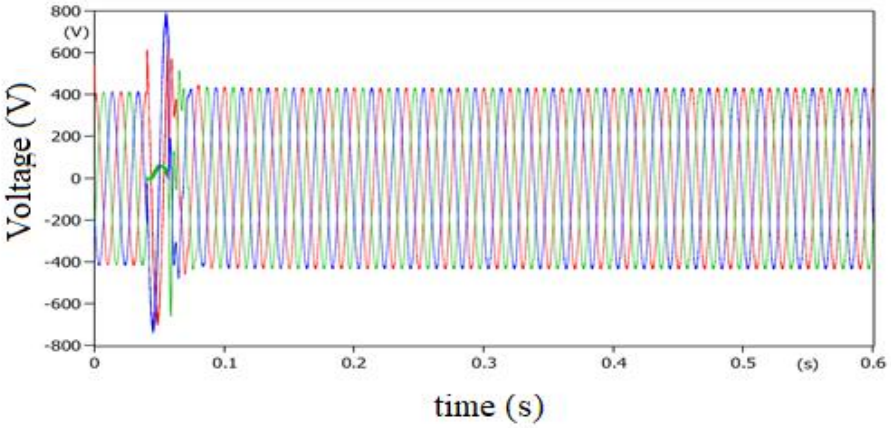

Figure 5. 67(c): Energization of C-Type filter

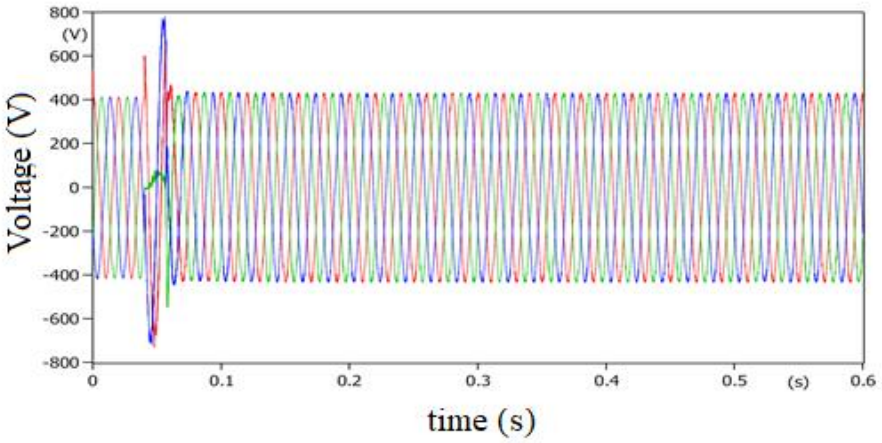

Figure 5. 67(d): Energization of high pass filter

5.24.2 De-Energization of Harmonic Filters

The de-energization simulation for single-tuned, double-tuned, C-Type, and high pass filters, are shown in Figures 5.68(a) to 5.68(d) respectively, were conducted using ATP software. According to the simulation done the overvoltage experienced was found to be 992 V, 1575 V, 905 V, and 1025 V respectively when the circuit breaker was opened at 0.04 s. From the results obtained it is found that the double-tuned filter experienced the highest overvoltage levels, whilst the C-Type filter experienced the lowest overvoltage levels during the de-energization scenario. The results of the simulation are tabulated in Table 5.42.

Table 5.42: Overvoltage during de-energization

Filter	Overvoltage experienced during de-energization
Single-tuned filter	992 V
Double-tuned filter	1575 V
C-Type filter	905 V
High pass filter	1025 V

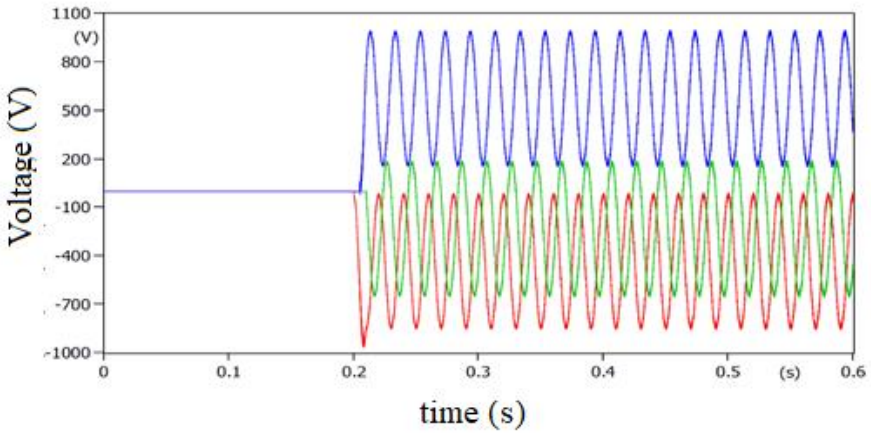

Figure 5.68(a): De-energization of single-tuned filter

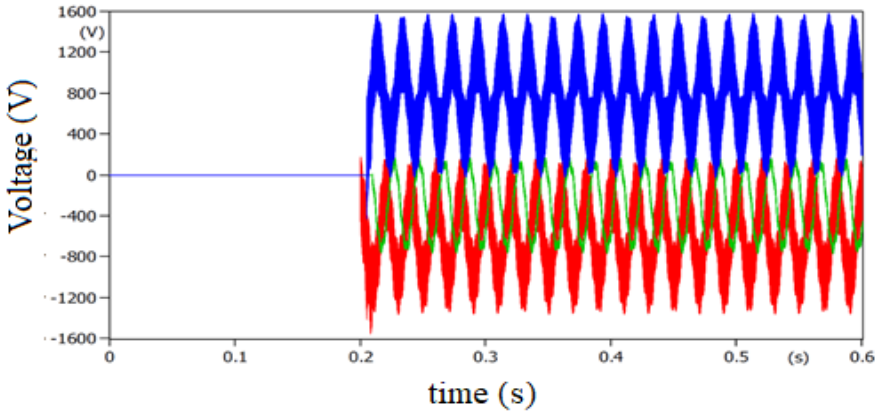

Figure 5. 68(b): De-energization of double-tuned filter

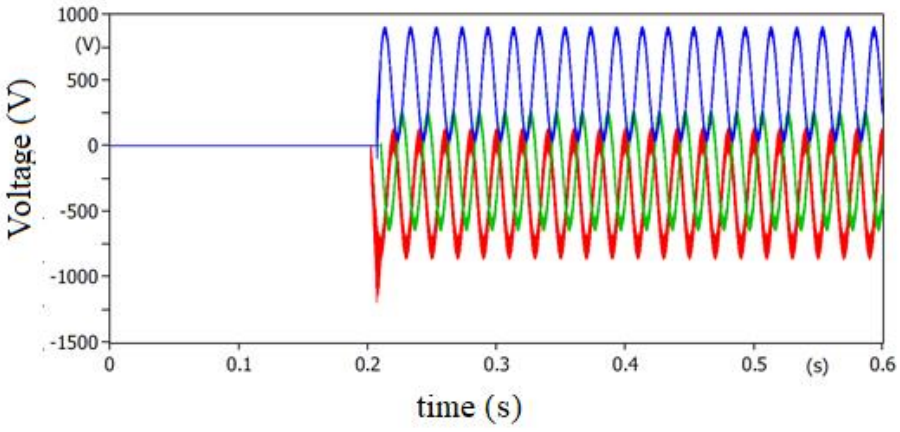

Figure 5. 68(c): De-energization of C-Type filter

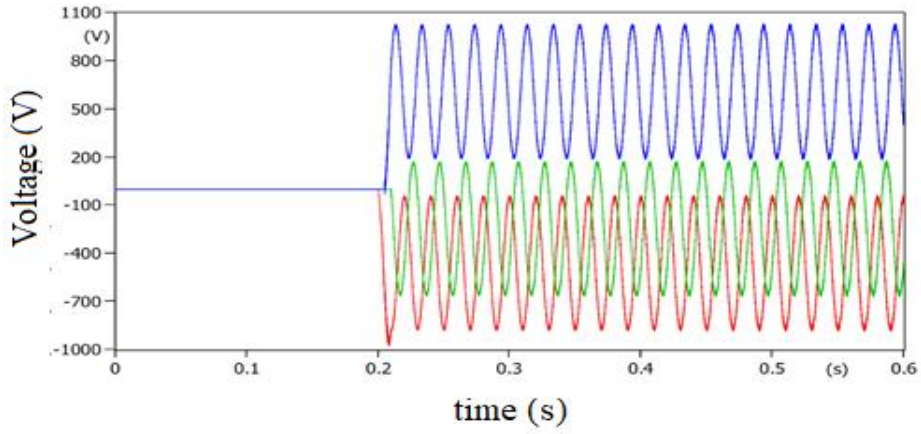

Figure 5. 68(d): De-energization of high pass filter

5.25 Mitigation of Overvoltage for Case Study 3

To protect the electrical equipment from overvoltage caused by the switching activities of harmonic filters, the use of pre-insertion resistors, surge arresters, and controlled switching will be investigated. From the results obtained the best method of mitigation was deduced.

5.25.1 Pre-Insertion Resistor

A pre-insertion resistor consists of a resistor bank connected in parallel to a circuit breaker which acts as a bypass that closes before energization of the filter. The resistor provides damping and reduces surge energy, therefore, acting as an effective countermeasure to overvoltage. To determine the effects that the pre-insertion resistor would have on the resultant waveform, all four filters were simulated using ATP. Figures 5.69(a) to 5.69(d), showed the resultant voltage waveform of the simulation. As presented in Table 5.43, the double-tuned filter has the highest reduction in overvoltage while the high pass filter has the lowest reduction in overvoltage when using a pre-insertion resistor.

Table 5.43: Mitigation using pre-insertion resistor

Filters	Resistor value	Overvoltage before	Overvoltage after
Single-tuned filter	0.159 Ω	1050 V	510 V
Double-tuned filter	0.0712 Ω	1120 V	498 V
C-Type filter	0.0205 Ω	800 V	485 V
High pass filter	0.159 Ω	798 V	501 V

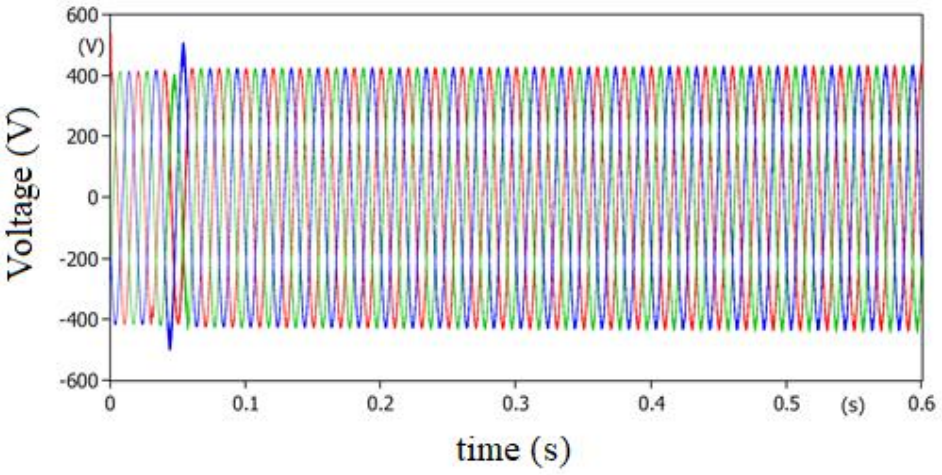

Figure 5.69(a): Using pre-insertion resistor for single-tuned filter

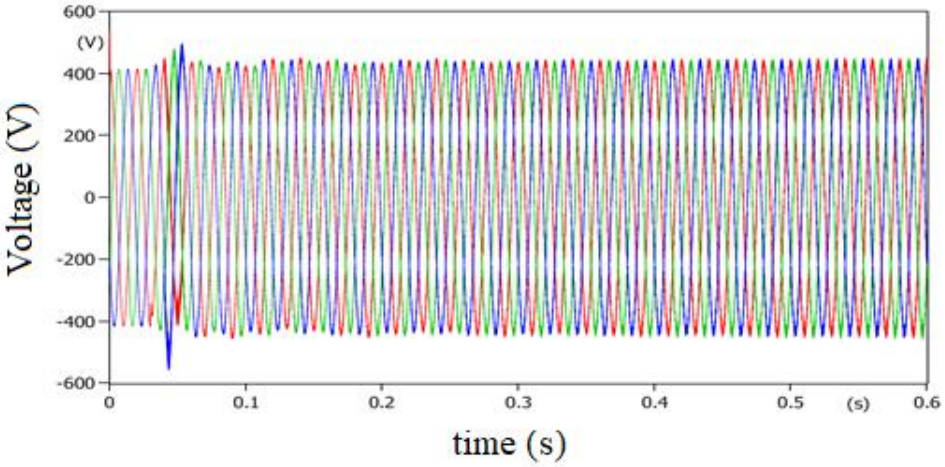

Figure 5.69(b): Using pre-insertion resistor for double-tuned filter

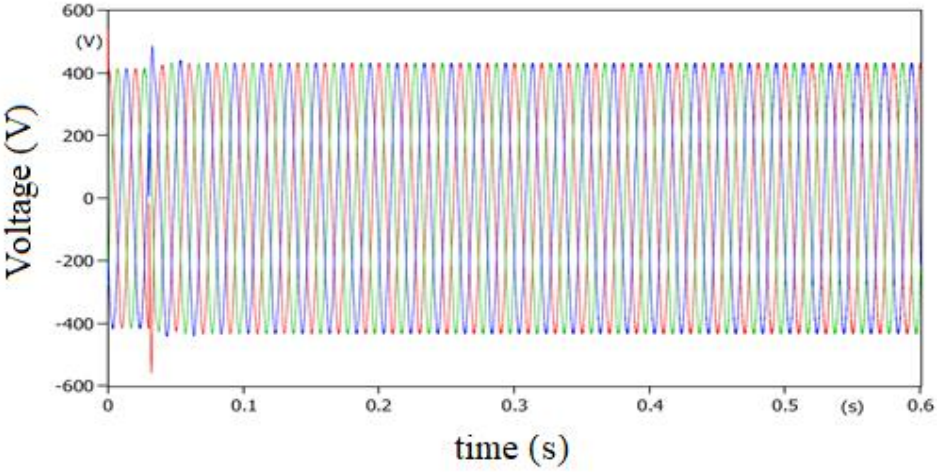

Figure 5.69(c): Using pre-insertion resistor for C-Type filter

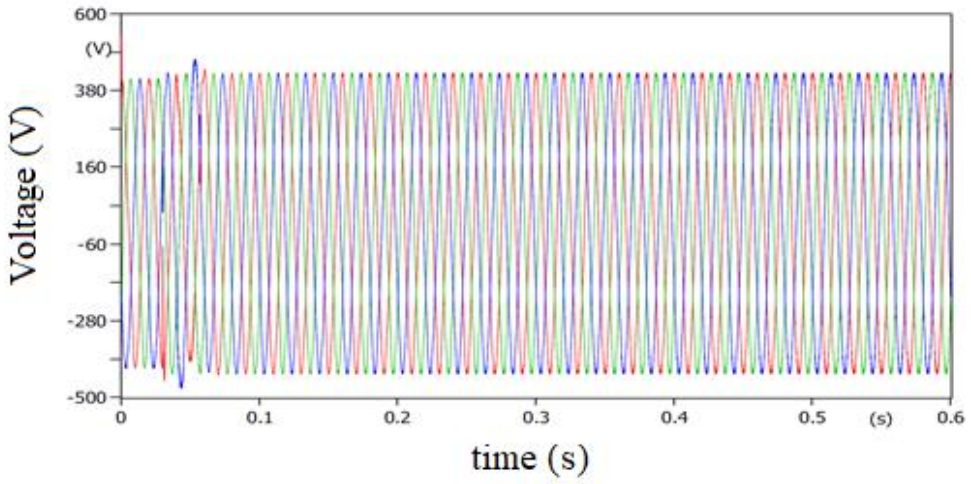

Figure 5.69(d): Using pre-insertion resistor for high pass filter

5.25.2 Controlled Switching

Controlled switching is a method used to eliminate harmful transients using time-controlled switching operations. Closing or opening of the circuit breaker is delayed in such a way that switching occurs at the optimal time, usually at zero crossing. This method is often used to reduce switching overvoltages to improve power quality in power systems. To determine the effects that the controlled switching would have on the resultant waveform, all four filters were simulated using ATP. Figures 5.70(a) to 5.70(d), show the resultant voltage waveform of the simulation. The double-tuned filter showed the best results with a reduction of 169 V after using controlled switching. The worst performing filters are the C-Type filter and the high pass filter with a reduction in overvoltage of 74 V. The results are tabulated in Table 5.44.

Table 5.44: Mitigation using controlled switching

Filters	Overvoltage before	Overvoltage after
Single-tuned filter	1050 V	907 V
Double-tuned filter	1120 V	951 V
C-Type filter	800 V	726 V
High pass filter	798 V	724 V

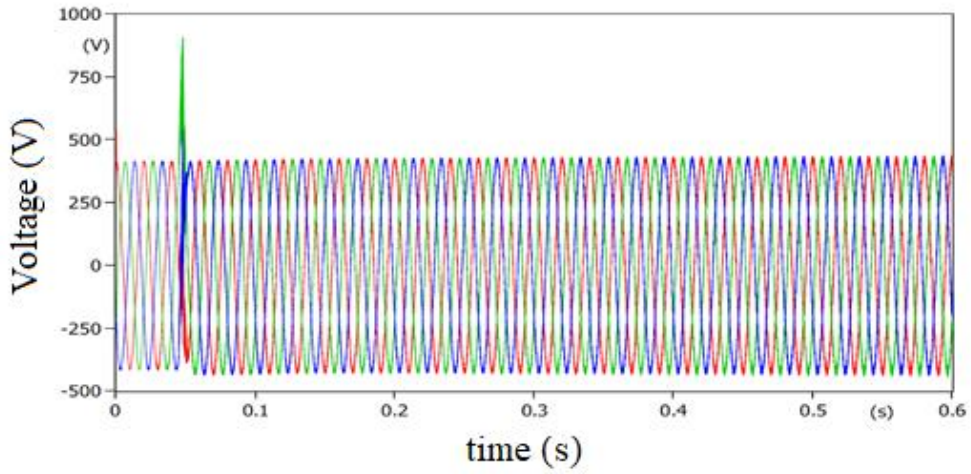

Figure 5.70(a): Using controlled switching for single-tuned filter

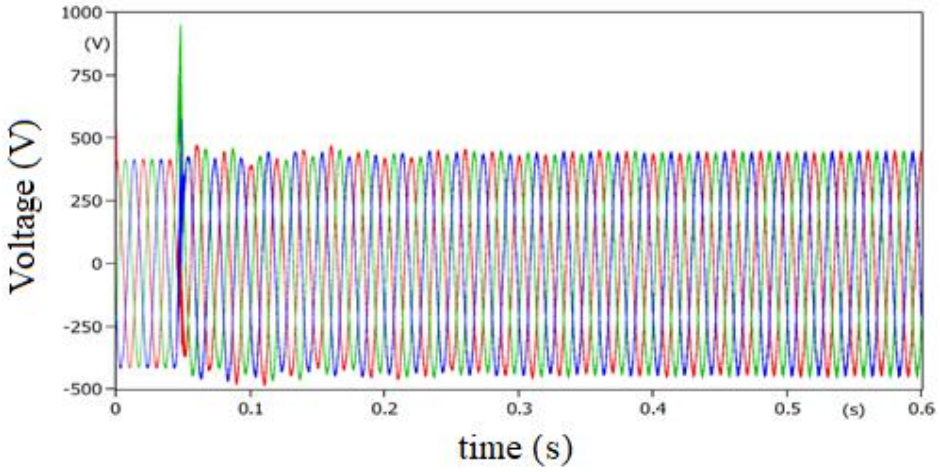

Figure 5.70(b): Using controlled switching for double-tuned filter

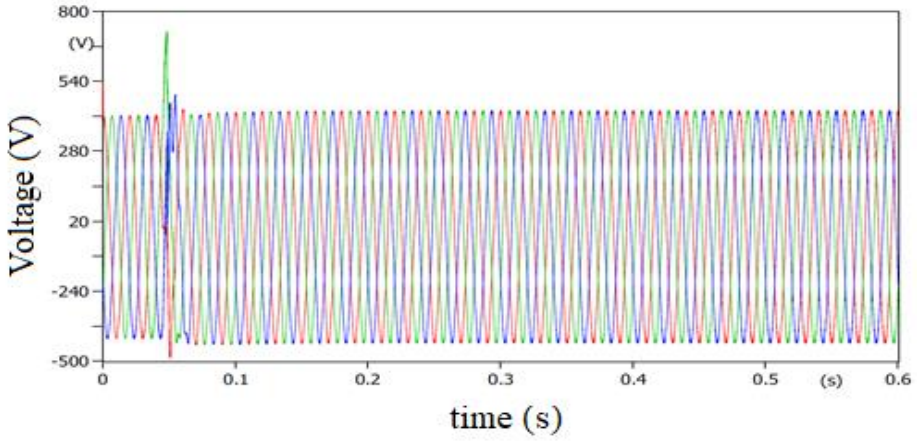

Figure 5.70(c): Using controlled switching for C-Type filter

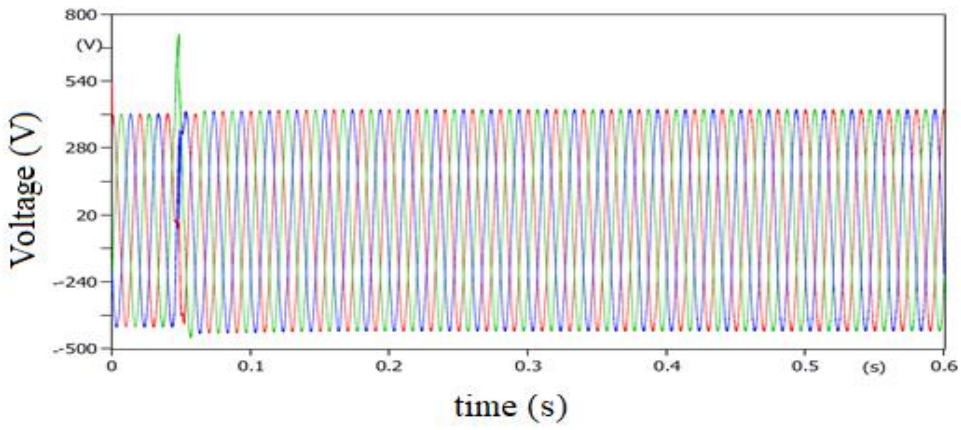

Figure 5.70(d): Using controlled switching for high pass filter

5.25.3 Surge Arrester

Surge arresters act as a protective devices used to limit surge voltage on electrical equipment. Metal oxide surge arresters (MOSA) used in this study were modelled using the IEEE surge arrester model (5). The simulation of the four filters together with the surge arrester was conducted using the ATP and is shown in Figures 5.71(a) to 5.71(d). When the surge arrester was connected to the network during energization, the overvoltage of the double-tuned filter was reduced the most by a 660 V while the high pass filter experiences the lowest reduction in overvoltage with a value of 374 V. The results of the simulations are tabulated in Table 5.45.

Table 5.45: Mitigation using surge arrester

Type of filters	Overvoltage before	Overvoltage after
Single-tuned filter	1050 V	408 V
Double-tuned filter	1120 V	460 V
C-Type filter	800 V	403 V
High pass filter	798 V	424 V

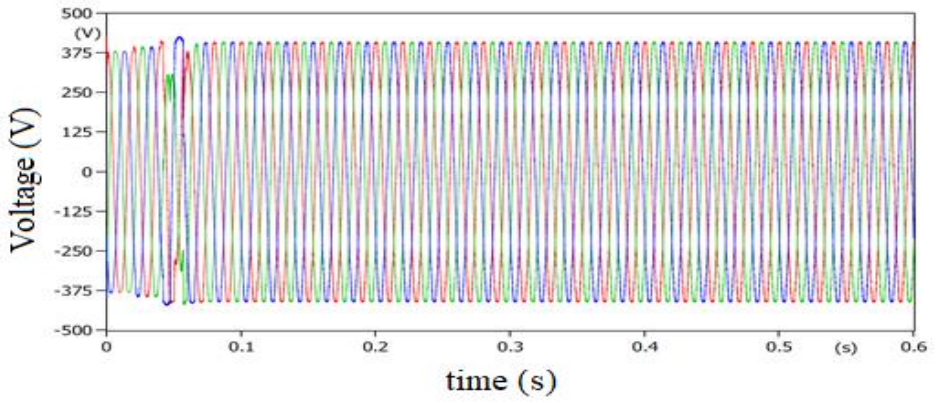

Figure 5.71(a): Using surge arrester for single-tuned filter

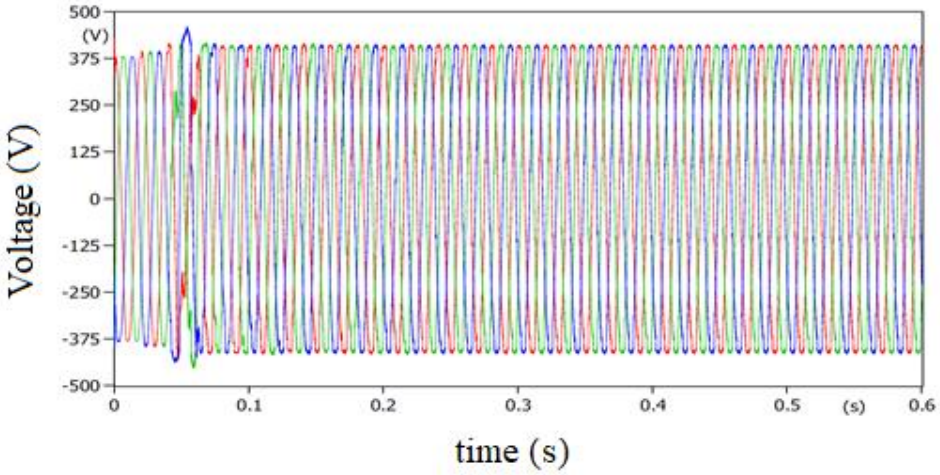

Figure 5.71(b): Using surge arrester for double-tuned filter

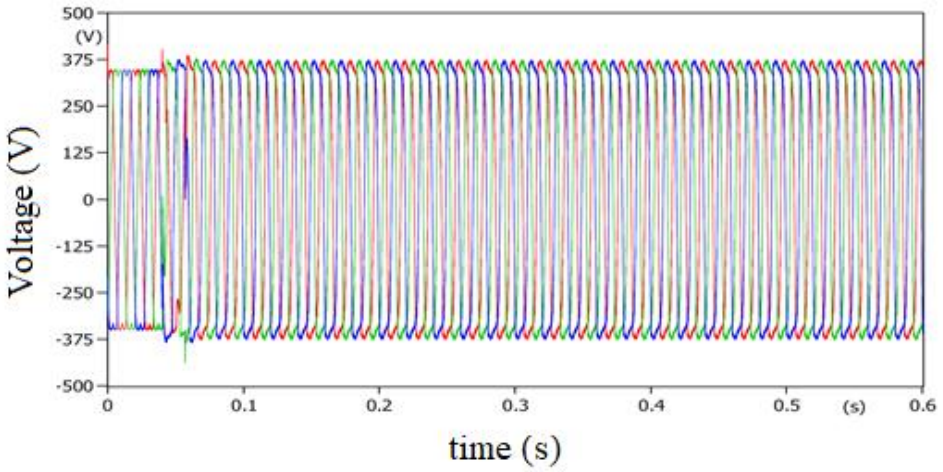

Figure 5.71(c): Using surge arrester for C-Type filter

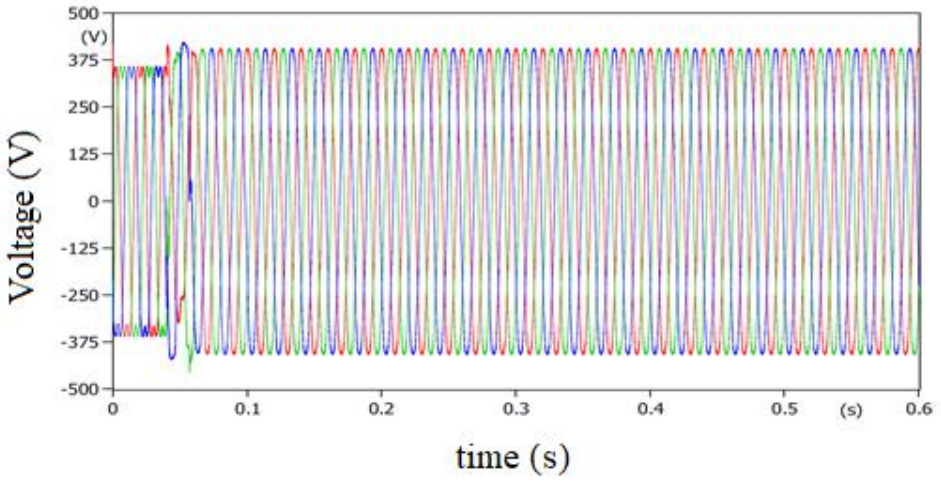

Figure 5.71(d): Using surge arrester for high pass filter

5.25.4 Mitigation Methods Analysis for Case study 3

For mitigation of energization, the surge arrester proved to be most effective while the pre-insertion resistor was found promising. The surge arrester limited the surge voltage produced during energization, therefore, in case study 3 it has proven to be the best method to mitigate temporary overvoltage. This method of mitigation would also reduce overvoltage during de-energization.

5.26 Concluding Remarks on the Case Studies

Harmonic distortions present in all three case studies were observed to be of the 3rd and 5th order of harmonics. To determine the best filter to correct the harmonics, all four filters were simulated using ATP software. The results showed that both the double-tuned and single-tuned filters were the most successful in mitigating both the 3rd and 5th harmonics compared to the C-Type and high pass filters. From the results presented in Table 3.10, the double-tuned filter proved to be the most effective closely followed by the single-tuned filter in case study one, while in case of studies two and three the single-tuned filter proved to be the best performing filters as documented in Table 4.10 and Table 5.10. The performances of both the C-Type and high pass filters in suppressing the individual harmonics were the worst, making it an unsuitable choice.

These results are expected as the single-tuned filter can limit lower-order harmonics below the tuning frequency, whereas the C-Type filter is designed to reduce higher-order harmonics above the tuning frequency. Designing a high pass filter to suppress lower order harmonics leads to high losses at the fundamental frequency due to the presence of a damping resistor. Whereas the absence of a damping resistor in the design of a double-tuned filter allows it to

have negligible losses [93]. The double-tuned filter has a higher quality factor compared to the high pass filter, therefore allowing maximum attenuation of both the 3rd and 5th harmonics.

The use of harmonic filters to attenuate harmonics is important, however, the switching actions of the filter can cause temporary overvoltage that poses a threat to the electrical system. Simulation of the energizing and de-energizing of the harmonic filters were performed using ATP software for all three case studies.

The results of the simulation showed that the overvoltage observed during energization and de-energization was the highest for the double-tuned filter in all three case studies. Simulation of the double-tuned filter during energization yielded an overvoltage of 910 V, 987 V, and 1120 V for case studies 1, 2, and 3 respectively with a switching time of 0.04 s. This is due to the absence of a damping resistor in the configuration of the double-tuned filter. The resistor increases the damping of the system during switching, thus suppressing the overvoltage that occurs. The energy is usually dissipated as heat to reduce the risk of component degradation. The C-Type and high pass filter experienced the lowest overvoltage during energization and de-energization. For case study 1 the overvoltage experienced during energization by the C-Type filter was 732 V and for case studies 2 and 3 the overvoltage experienced by the high pass filter was 788 V and 798 V respectively. The higher resistor values in both these filters helped in reducing the overvoltage during switching.

Mitigation methods of the pre-insertion resistor, controlled switching, and surge arrester were simulated to mitigate the temporary overvoltage caused by the filter switching. The surge arrester was the most effective, whilst the pre-insertion resistor was found promising. The use of a controlled switching device proved to be the least effective method of mitigation. This is due to the surge arresters' ability to withstand increased operating voltage for a period making it ideal to use in situations where temporary overvoltage occurs. The surge arrester has a higher energy absorption capacity compared to using a controlled switching device as the surge arrester may be implemented in different positions to improve suppression of the overvoltage. In all three case studies, the surge arrester was the most successful in reducing the switching overvoltage of the single-tuned filter and least effective in reducing the switching overvoltage of the double-tuned, C-Type, and high pass filters. Hence the implementation of a single-tuned filter to correct the harmonics and a surge arrester to mitigate the temporary overvoltage caused by the switching of the filter has proven to be the most effective solution.

Chapter 6
Conclusion and Recommendation

6.1 Conclusion

The occurrence of harmonics has become more prominent as the use of VSD's increases in various industries. Harmonics flowing in an electrical network can reduce the quality of the electrical supply and affect the integrity of the insulation. Harmonic filters are used to reduce harmonic distortion by diverting harmonic currents in low impedance paths. In doing so the harmonic distortion in a system is reduced to levels detailed in IEEE 519. There are various types of harmonic filters available with their topologies designed to suppress certain harmonic frequencies. To choose the correct filter an assessment of the electrical system is required to determine the harmonics present and to choose the right solution for the particular setup. To allow for computer simulation, an analytical model of each of the components is required. ATP simulation software was used to provide the simulation and allow for the analysis of the network.

The main disadvantages of using harmonic filters are the overvoltage that is produced when the filter is switched on or off. This study focused on identifying temporary overvoltage in three different industries as a problem that could occur frequently and could gradually deteriorate the insulation of the power equipment. This would eventually increase the cost of maintenance and downtime and shorten the lifespan of expensive equipment. However, implementing the mitigation measures reported in this study could counter the effect of these temporary overvoltages, and thereby reduce the problems associated with them. This information is significant in planning and managing any industry to minimize disruptions during the production process. The best harmonic filter, which produced the least overvoltage, as well as the most effective mitigation technique was determined by comparing the simulation results obtained from the ATP software.

From the research study, the following were established from analytical modelling, experimental study, and simulation.

- The single and double-tuned filter works best on systems that experience lower order harmonics as it can filter harmonic orders near the power frequency. The C-type and high pass filters are better suited to attenuate higher-order harmonics due to their wider bandwidth.

- The absence of a damping resistor in the double-tuned filter caused the highest temporary overvoltage during switching operations as compared to the other harmonic filters.
- The use of a surge arrester was the most effective in reducing the temporary overvoltage due to its higher energy absorption capabilities. When the surge arrester is placed correctly in the network, it can reduce the overvoltage by approximately 50 %.

6.2 Recommendations

From the results compiled in this study it could be observed that to improve future research relating to this area, some modifications are needed. Some of these are as follows:

- The effects of overvoltage on other devices such as capacitive voltage transformers (CVT) and inductive voltage transformers (IVT) need to be studied.
- Other types of overvoltage disturbances must be considered and simulated to determine if the mitigation methods proposed are still effective.
- Investigation and mitigation of temporary overvoltage in a high voltage system should be considered to improve the accuracy of the results stipulated in this study.
- The evaluation of interharmonics generated by high-powered VSD's should be considered to determine which harmonic filter would best mitigate these harmonics.

References

[1] D. S. M. Suresh B, C. Yaswanth Reddy, T. B. Isha, N. Krishna Prakash, "Design and Simulation of Passive Filter for an Adjustable Speed Drive," *International journal of electrical electronics and computer systems,* vol. 3, 2015.

[2] E. Matsumoto and M. Anwari, "Impact of multiple adjustable speed drive system to power system harmonics," in *IEEE 2nd International Power and Energy Conference*, 2008, pp. 324-328.

[3] A. B. Nassif, W. Xu, and W. Freitas, "An investigation on the selection of filter topologies for passive filter applications," *IEEE transactions on Power Delivery,* vol. 24, pp. 1710-1718, 2009.

[4] P. X. Help. (June 2018). *Passive filter design (4.46 ed.)*. Available: https://hvdc.ca/webhelp/Master_Library_Models/Passive/Filters/Passive_Filter_Design.html

[5] J. Warecki and M. Gajdzica, "Transients under energizing multiple power filter circuits," *Computer Applications in Electrical Engineering,* vol. 14, 2016.

[6] A. Akinrinde, "Investigation and Analysis of Temporary Overvoltages Caused by Filter Banks at Onshore Wind Farm Substation," *International Journal of Renewable Energy Research,* vol. 7, pp. 770-777, 2017.

[7] W. S. K. M. U. Schmidt, "Transients by switching of filter banks at high-voltage grid," *presented at the XVII International Symposium on High Voltage Engineering, Hannover, Germany, ,* 2011.

[8] I. Arana, "Switching overvoltages in offshore wind power grids. Measurements, modelling and validation in time and frequency domain," Ph. D. Dissertation. Dept. Electrical Engineering, Technical University of Denmark, 2011.

[9] D. Goldsworthy, T. Roseburg, D. Tziouvaras, and J. Pope, "Controlled switching of HVAC circuit breakers: Application examples and benefits," in *Protective Relay Engineers, 2008 61st Annual Conference for*, 2008, pp. 520-535.

[10] J. Guzinski, H. Abu-Rub, and P. Strankowski, *Variable speed AC drives with inverter output filters*: John Wiley & Sons, 2015.

[11] Z. Krzemiński, "Speed observers for sensorless control of AC machines," *Polish Electrical Review,* vol. 5, p. 90, 2014.

[12] K. Pauwels, "Energy savings with variable speed drives," in *Electricity Distribution, 2001. Part 1: Contributions. CIRED. 16th International Conference and Exhibition on (IEE Conf. Publ No. 482)*, 2001, p. 5 pp. vol. 4.

[13] R. G. Ellis and P. Eng, "Power system harmonics–a reference guide to causes, effects and corrective measures," *An Allen-Brandley Series of Issues and Answers-Rockwell Automation,* p. 3, 2001.

[14] S. Haghbin and T. Thiringer, "Impact of Line Current Harmonics on the DC Bus Quality of a Three-Phase PWM Inverter," *International Journal of Electrical Energy (IJOEE),* vol. 2, pp. 184-188, 2014.

[15] A. Elsebaay, M. Ramadan, and M. A. A. Adma, "Studying the effect of non-linear loads harmonics on electric generator power rating selection," *European Scientific Journal,* vol. 13, pp. 1857-7881, 2017.

[16] V. R. P. Ankit M. Patel, Maulik V. Patel, "Harmonic Reduction and Power Factor improvement in three phase three wire system by using Passive Filters," *International Journal of Advance Engineering and Research Development,* vol. 2, 2015.

[17] V. Sousa Santos, H. Hernandez Herrera, E. C. Quispe, P. R. Viego, and J. R. Gómez, "Harmonic distortion evaluation generated by PWM motor drives in electrical industrial

systems," *International Journal of Electrical and Computer Engineering (IJECE),* vol. 7, pp. 3207-3216, 2017.
[18] H. G. Beleiu, V. Maier, S. G. Pavel, I. Birou, C. S. Pică, and P. C. Dărab, "Harmonics Consequences on Drive Systems with Induction Motor," *Applied Sciences,* vol. 10, p. 1528, 2020.
[19] M. Scheidiger, "Power System Harmonics Analysis of High Power Variable Speed Drives," *KTH Electrical Engineering,* 2013.
[20] R. Klempka, Z. Hanzelka, and Y. Varetsky, "Bank harmonic filters operation in power supply system–cases studies," in *Power Quality Issues*, ed: InTech, 2013.
[21] J. A. Martinez-Velasco and F. González-Molina, "Modeling and Analysis of Power Transformers Under Ferroresonance Phenomenon," Doctoral, Electronic, Electric and Automatic Control Engineering, University Rovira I Virgili, Tarragona, 2015.
[22] A. O. Akinrinde, A. Swanson, and R. Tiako, "Transient Analysis and Mitigation of Capacitor Bank Switching on a Standalone Wind Farm," *World Academy of Science, Engineering and Technology, International Journal of Electrical, Computer, Energetic, Electronic and Communication Engineering,* vol. 10, pp. 535-544, 2016.
[23] M. Almutairi and S. Hadjiloucas, "Application of single tuned passive filters in distribution networks at the point of common coupling," *Int J Energy Power Eng,* vol. 11, pp. 177-182, 2017.
[24] Y.-S. Cho and H. Cha, "Single-tuned passive harmonic filter design considering variances of tuning and quality factor," *Journal of International Council on Electrical Engineering,* vol. 1, pp. 7-13, 2011.
[25] K. R. Cheepati, S. Ali, and S. M. Kalavathi, "Overview of Double Tuned Harmonic Filters in Improving Power Quality under Non Linear Load Conditions," *International Journal of Grid And Distributed Computing,* vol. 10, pp. 11-25, 2017.
[26] Y. Mingtao, C. Jianye, W. Weian, and W. Zanji, "A double tuned filter based on controllable reactor," in *Power Electronics, Electrical Drives, Automation and Motion*, 2006, pp. 1232-1235.
[27] G. Mishra, "Design of Passive High Pass Filter for Hybrid Active Power Filter Applications," Master of Technology, Department of Electrical Engineering, National Institute of Technology, Rourkela, 2013.
[28] Y.-P. Chang and C.-J. Wu, "Design of harmonic filters using combined feasible direction method and differential evolution," in *2004 International Conference on Power System Technology, 2004. PowerCon 2004.*, 2004, pp. 812-817.
[29] Y. Xiao, J. Zhao, and S. Mao, "Theory for the design of C-type filter," in *Harmonics and Quality of Power, 2004. 11th International Conference on*, 2004, pp. 11-15.
[30] M. H. R. Centre. *Passive Filter Design*. Available: https://hvdc.ca/webhelp/Master_Library_Models/Passive/Filters/Passive_Filter_Design.htm
[31] T. M. Blooming and D. J. Carnovale, "Application of IEEE Std 519-1992 harmonic limits," in *Pulp and Paper Industry Technical Conference, 2006. Conference Record of Annual*, 2006, pp. 1-9.
[32] N. Othman, M. Rohani, W. Mustafa, C. Wooi, A. Rosmi, N. Shakur, *et al.*, "An Overview on Overvoltage Phenomena in Power Systems," in *IOP Conference Series: Materials Science and Engineering*, 2019, p. 012013.
[33] P. Yang, S. Chen, and J. He, "Effect of different arresters on switching overvoltages in UHV transmission lines," *Tsinghua Science & Technology,* vol. 15, pp. 325-328, 2010.
[34] M. J. Bonner and N. M. Ijumba, "Safety of low voltage switchgear assemblies in South Africa–Part 1," *Energize,* vol. 1, pp. 53-59, 2005.
[35] P. Ferracci, "Ferroresonance Group Schneider: ," *Cahier,* vol. 190, pp. 1-28, 1998.

[36] K. G. King, "Temporary Overvoltage Equipment Limits," K & R Consulting, LLC, USA2004.
[37] M. Beanland, T. Speas, and J. Rostron, "Pre-insertion resistors in high voltage capacitor bank switching," in *Western protective relay conference*, 2004, pp. 1-14.
[38] P. J. R. Delgado, "Harmonic analysis and transient overvoltages due to capacitor switching analysis," Department of Electrical and Electronic Engineering, University of Sevilla, Sevilla, 2015.
[39] R. King, F. Moore, N. Jenkins, A. Haddad, H. Griffiths, and M. Osborne, "Switching transients in offshore wind farms–impact on the offshore and onshore networks," in *International Conference on Power Systems Transients, IPST, Delft, The Netherlands*, 2011.
[40] E. A. Awad, E. A. Badran, and F. M. Youssef, "Mitigation of Temporary Overvoltages in Weak Grids Connected to DFIG-based Wind Farms," *Journal of Electrical Systems,* vol. 10, 2014.
[41] D. Thukaram, H. Khincha, and S. Khandelwal, "Estimation of switching transient peak overvoltages during transmission line energization using artificial neural network," *Electric Power Systems Research,* vol. 76, pp. 259-269, 2006.
[42] M. Kizilcay, K. Teichmann, A. Agdemir, and G. Kaflowski, "Flashovers at a 33-kV filter reactor during energization," *Electric Power Systems Research,* vol. 79, pp. 492-497, 2009.
[43] A. S. Dharmadhikari, "A Review Study on Capacitor Switching Transients of HV Transmission Line With VCB," *International Journal of Innovative Research in Science, Engineering and Technology,* vol. 6, April 2017.
[44] Y. Varetsky, "Transient overvoltages during filter circuit switching-off," in *Modern Electric Power Systems (MEPS), 2010 Proceedings of the International Symposium*, 2010, pp. 1-4.
[45] P. Dimitriadis, "Effects of overvoltage on power consumption," Brunel University London, 2015.
[46] N. F. Gabriel Benmouyal, Douglas Taylor, Mark Talbott-Williams, and Ritwik Chowdhury, "A Unified Approach to Controlled Switching of Power Equipment," *72nd Annual Georgia Tech Protective Relaying Conference,* 2018.
[47] A. Brochure, "Controlled switching, buyer's and application guide," *ABB Ludvika, Schweden Google Scholar*, 2010.
[48] E. A. Awad, E. A. Badran, and F. M. Youssef, "Mitigation of switching overvoltages due to energization procedures in grid-connected offshore wind farms," *Int. J. Adv. Res. Elect. Electron. Instrum. Eng.,* vol. 3, pp. 7020-7028, 2014.
[49] P. C. Fernandez, P. C. Esmeraldo, F. Carvalho, A. Camara, H. Bronzeado, and R. Vaisman, "Mitigation of power system switching transients to improve power quality," in *8th International Conference on Harmonics and Quality of Power. Proceedings (Cat. No. 98EX227)*, 1998, pp. 988-993.
[50] B. Filipović-Grčić, I. Uglešić, S. Bojić, and A. Župan, "Application of Controlled Switching for Limitation of Switching Overvoltages on 400 kV Transmission Line," in *International Conference on Power Systems Transients (IPST 2017)*, 2017.
[51] J. Varetski, R. Pavlyshyn, and M. Gajdzica, "Harmonic current impact on transient overvoltages during filter switching-off," *Przegląd Elektrotechniczny,* vol. 89, pp. 95-98, 2013.
[52] F. Fernandez and R. Diaz, "Metal oxide surge arrester model for fast transient simulations," in *Proceedings of 2001 International conference on power system transients*, 2001, pp. 681-687.

[53] M. Popov, L. Van der Sluis, and G. Paap, "PES Digital Library," *IEEE Power Engineering Review*, vol. 22, pp. 19-19, 2002.
[54] S. Mohammad, C. Gomes, M. AbKadir, J. Jasni, and M. Izadi, "Protection Technique for Transient Overvoltage due to Capacitor Bank Switching in Distribution Systems Using High Pass Filter," *ARPN Journal of Engineering and Applied Sciences*, 2015.
[55] H. Seyedi, M. Sanaye-Pasand, and M. Dadashzadeh, "Application of transmission line surge arresters to reduce switching overvoltages," in *International Conference on Power Systems Transients (IPST'05)*, 2005.
[56] K. Munji, J. Horne, and J. Ribecca, "Design and Validation of Pre-Insertion Resistor Rating for Mitigation of Zero Missing Phenomenon," *International Conference on Power Systems Transients*, pp. 1-6, 2017.
[57] S. Katyara, A. A. Hashmani, and B. S. Chowdhry, "Analysis and mitigation of shunt capacitor bank switching transients on 132 kV Grid station, Qasimabad Hyderabad," *Mehran University Research Journal Of Engineering & Technology*, vol. 34, p. 291, 2015.
[58] M. Fahmi, U. Baafai, A. Hazmi, and T. Nasution, "Harmonic reduction by using single-tuned passive filter in plastic processing industry," in *IOP Conference Series: Materials Science and Engineering*, 2018, p. 012035.
[59] S. Puchalapalli and N. M. Pindoriya, "Harmonics assessment for modern domestic and commercial loads: A survey," in *2016 International Conference on Emerging Trends in Electrical Electronics & Sustainable Energy Systems (ICETEESES)*, 2016, pp. 120-122.
[60] D. M. Soomro and M. M. Almelian, "Optimal design of a single tuned passive filter to mitigate harmonics in power frequency," *ARPN Journal of Engineering and Applied Sciences*, vol. 10, 2015.
[61] M. M. Othman, W. M. F. bin W Mustapha, A. Asyraf, M. Kamaruzaman, A. M. Arriffin, I. Musirin, *et al.*, "Harmonic load mitigation using the optimal double tuned passive filter technique," *Indones. J. Electr. Eng. Comput. Sci.*, vol. 6, pp. 338-48, 2017.
[62] D. Joseph, N. Kalaiarasi, K. Rajan, N. Shanker, and P. Katta, "Surveying the Power Quality in Non-Linear Loads of Tower Block for Performance Assessment Through Optimization and Transformation Filters," *Journal of Computational and Theoretical Nanoscience*, vol. 14, pp. 1931-1947, 2017.
[63] R. Klempka, "Design of C-TYPE passive filter for arc furnaces," *Metalurgija*, vol. 56, pp. 161-163, 2017.
[64] A. Lange and M. Pasko, "Compensation of the reactive power and filtration of high harmonics by means of passive LC filters," *Przeglad Elektrotechniczny*, vol. 86, pp. 126-129, 2010.
[65] J. Das, "Passive filters-potentialities and limitations," *IEEE transactions on industry applications*, vol. 40, pp. 232-241, 2004.
[66] J. Pahl, "Conducted Emissions of Low Power Variable Speed Drives," Electrical and Automation Engineering, Metropolia University of Applied Sciences, 2020.
[67] S. S. Turkel and S. Solomon, "Understanding variable speed drives," *Engineering, Construction and Maintenance*, 1997.
[68] M. H. Bollen, "Understanding power quality problems," in *Voltage sags and Interruptions*, ed: IEEE press, 2000.
[69] E. El-Saadany, "Effectiveness of different filtering methodologies in harmonic distortion mitigation," in *Canadian Conference on Electrical and Computer Engineering 2001. Conference Proceedings (Cat. No. 01TH8555)*, 2001, pp. 1035-1040.

[70] J. M. Mushagala, "Harmonic analysis and effectiveness of mitigation techniques applied to a bipolar HVDC system," *International conference on Engineering technology*, 2017.
[71] D. Ismail, A. Rosnazri, and T. Soib, "Design of a single-phase rectifier with improved power factor and low THD using boost converter technique," *American Journal of Applied Sciences*, vol. 37, 2006.
[72] J. A. B. Moreno, "Design and Specification of Harmonic Filters for Variable Frequency Drives," *IEEE Applied Power Electronics Conference and Exposition*, 2016.
[73] H. K. Høidalen, L. Prikler, and J. Hall, "ATPDraw-Graphical preprocessor to ATP, Windows version," in *Proceedings of International Conference on Power Systems Transients, IPST*, 1999, pp. 20-24.
[74] H. K. Høidalen, "ATP-Draw," *PC software for windows, version*, vol. 5, 2012.
[75] Nersa. (2008). *The South African Grid Code*. Available: https://www.nersa.org.za/electricity-overview/electricity-grid-code/
[76] S. D. Cho, "Parameter estimation for transformer modeling," *IEEE Transactions on Power Delivery*, vol. 1, pp. 140 - 146, 2002.
[77] V. Dhote, P. Asutkar, and S. Dutt, "Modeling and simulation of three-phase power transformer," *Int. J. Eng. Res. Appl*, vol. 3, pp. 2498-2502, 2013.
[78] G. Ala and M. Inzerillo, "An Improved Circuit-Breaker Model in MODELS Language," *International Conference on Power System Transients*, 1999.
[79] X. Liang and W. Xu, "Modeling variable frequency drive and motor systems in power systems dynamic studies," in *2013 IEEE Industry Applications Society Annual Meeting*, 2013, pp. 1-11.
[80] S. K. Jain, F. Sharma, and M. K. Baliwal, "Modeling and Simulation of an Induction Motor," *International Journal of Engineering Research and Development*, vol. 10, pp. 57-61, 2014.
[81] C. A. Christodoulou, F. A. Assimakopoulou, I. F. Gonos, and I. A. Stathopulos, "Simulation of metal oxide surge arresters behavior," in *2008 IEEE Power Electronics Specialists Conference*, 2008, pp. 1862-1866.
[82] Masterflex. (02/05/2020). *Fluke 435 Logging Power Quality Analyzer Three-Phase*. Available: https://www.masterflex.com/i/fluke-435-logging-power-quality-analyzer-three-phase/2002016
[83] M. Jamil, G. M. Hashmi, Z. A. Syed, and Q. Awais, "Harmonics in Adjustable Speed Drives: Causes, Effects, and Solutions," in *2007 International Conference on Information and Emerging Technologies*, 2007, pp. 1-6.
[84] M. F. McGranaghan and D. R. Mueller, "Designing harmonic filters for adjustable-speed drives to comply with IEEE-519 harmonic limits," *IEEE transactions on industry applications*, vol. 35, pp. 312-318, 1999.
[85] V. Sousa, H. Hernández, E. C. Quispe, J. R. Gómez, and P. R. Viego, "Analysis of harmonic distortion generated by PWM motor drives," in *2017 IEEE Workshop on Power Electronics and Power Quality Applications (PEPQA)*, 2017, pp. 1-6.
[86] ABB. (2016, August). *Reducing harmonics caused by adjustable frequency drives*. Available: https://www.ee.co.za/article/reducing-harmonics-caused-by-adjustable-frequncy-drives.html
[87] A. Abraham, "Power quality analysis of variable speed drives," University of Witwatersrand, Johannesburg, 2014.
[88] F. C. Dezza and H. K. Høidalen, "Power Transformer Modelling Advanced Core Model," Department of Electrical Engineering, University of Milan, Milan, 2004.
[89] R. Klempka, "A new method for the C-type passive filter design," *Electrotechnical Review*, vol. 21, p. 22, 2012.

[90] J. Bickford and A. Heaton, "Transient overvoltages on power systems," in *IEE Proceedings C (Generation, Transmission and Distribution)*, 1986, pp. 201-225.
[91] Y.-h. HE and S. Heng, "A new method of designing double-tuned filter," in *Proceedings of the 2nd International Conference on Computer Science and Electronics Engineering*, 2013.
[92] Elprocus. (20/10). *What is a High Pass Filter? Circuit Diagram, Characteristics, and Applications*. Available: https://www.elprocus.com/what-is-a-high-pass-filter-circuit-diagram-characteristics-and-applications/
[93] S. Modi and P. Sevantilal, "An Investigation on Harmonics and Active/Reactive Power of Asymmetrical Operation of 12-Pulse Converter and Mitigation of Harmonics," The Maharaja Sayajirao University of Baroda, 2017.